

LCOE reduction for the next generation offshore wind turbines

OUTCOMES FROM THE INNWIND.EU PROJECT

October 2017



Funded by the European
Community's Seventh
Framework Programme



LCOE reduction for the next generation offshore wind turbines

OUTCOMES FROM THE INNWIND.EU PROJECT

October 2017



www.innwind.eu

PRINCIPAL AUTHORS:

Peter Hjuler Jensen (DTU)
Takis Chaviaropoulos (NTUA)
Anand Natarajan (DTU)

AUTHORS (PROJECT PARTNERS):

Flemming Rasmussen (DTU)
Helge Aagaard Madsen (DTU)
Peter Jamieson (Univ. of Strathclyde)
Jan-Willem Van Wingerden (TU Delft)
Vasilis Riziotis (NTUA)
Athanasios Barlas (DTU)
Henk Polinder (TU Delft)
Asger Abrahamsen (DTU)
David Powell (Magnomatics)
Gerrit Jan Van Zinderen (DNV GL)
Daniel Kaufer (Rambøll)
Rasoul Shirzadeh (Univ. of Oldenburg)
Jose Azcona Armendariz (CENER)
Spyros Voutsinas (NTUA)
Andreas Manjock (DNV GL)
Uwe Schmidt Paulsen (DTU)
James Dobbin (DNV GL)
Sabina Potestio (WindEurope)

PROJECT COORDINATION:

Peter Hjuler Jensen (DTU)

PUBLICATION COORDINATION:

Sabina Potestio (Wind Europe)

ACKNOWLEDGEMENTS:

Ervin Bossanyi (DNV GL), Kais Atallah (Univ. of Sheffield), Paul Weaver (Univ. of Bristol), Arno Van Wingerde (Fraunhofer IWES), Martin Kuhn (university of Oldenburg), Stoyan Kanev (ECN), Bernard Bulder (ECN), Detlev Heinemann (Univ. of Oldenburg), John Dalsgaard Sørensen (AAU), Zhe Chen (AAU), Po Wen Cheng (Univ. of Stuttgart), Frank Lemmer (Univ. of Stuttgart), Ole Petersen (DHI), Ben Hendriks (WMC), Kimon Argyriadis (DNV GL), Raimund Rolfes (Univ. of Hannover), Dimitris Saravanos (Univ Patras), Andreas Makris (CRES), Niklas Magnusson (SINTEF), William Leithead (Univ. of Strathclyde), Carlos Pizarro De La Fuente (Gamesa), Per H. Lauritsen (Siemens), Harald Bersee (SE Blades), Carlo Bottasso (Politecnico di Milano), Alessandro Croce (Politecnico di Milano), Jason Jonkman (NREL), Antonio Ugarte (CENER), Paul Todd (Magnomatics).

COORDINATOR



PARTNERS



LEGAL DISCLAIMER

The sole responsibility for the content of this publication lies with the INNWIND.EU consortium. It does not necessarily reflect the opinion of the European Union.

CONTENTS

GLOSSARY OF TERMS	10
EXECUTIVE SUMMARY	11
1. INTRODUCTION	14
2. DESIGN CHALLENGES AT 10 MW TO 20 MW	16
2.1 Cost drivers in Offshore Wind Development	16
2.1.1 The European Wind Initiative	16
2.1.2 Size of commercial offshore turbines	17
2.1.3 OPEX and turbine size	18
2.1.4 Effect of upscaling on LCOE	19
2.2 Technical challenges, concept and innovation selections made	21
2.2.1 Upwind vs downwind rotor	21
2.2.2 Three-bladed vs two-bladed rotors	21
2.2.3 Kingpin vs traditional drive train support	21
2.2.4 Direct Drive versus geared concepts	22
2.2.5 Jackets versus other bottom-fixed support structures	22
2.2.6 Challenges in floating designs	23
2.3 New Requirements for Wind Turbine Design Standards	24
2.3.1 External conditions for designing 10-20 MW offshore wind turbines	26
3. SELECTED PLATFORMS AT THE SYSTEM LEVELS	28
3.1 Reference and Evolutionary Designs	28
3.1.1 Reference Turbines	28
3.1.2 Evolutionary Architectures	29
3.2 New Platforms	31
3.2.1 Two-bladed upwind/downwind rotors with semi-floater	32
3.2.2 Three-bladed upwind rotors with non-conventional direct drive, bottom-fixed or floating	32
3.2.3 Support Structures	34
3.3 Revolutionary Platforms	35

3.3.1 20 MW Multirotor System	35
3.3.2 10 MW Floating VAWT	36
4. INNOVATIONS NEEDED AT COMPONENT LEVEL	38
4.1 Blades	38
4.1.1 State of the art in blade design for large offshore turbines	38
4.1.2 Validation of the design tools used in the project against experimental data / benchmark	39
4.1.3 Validation of structural design tools	42
4.1.4 Innovative concepts researched regarding aerodynamic design	42
4.1.5 Innovative concepts researched in structural design	45
4.1.6 Active control using flaps	47
4.1.7 Demonstration in the wind tunnel and on a rotating test rig in the presence of wind turbulence	47
4.1.8 Manufacturing and testing of a morphing trailing edge flap	49
4.1.9 Integrated blade design	50
4.1.10 Main scientific and technological accomplishments	52
4.2 Electromechanical Conversion	53
4.2.1 State of the art in drive train design for large offshore turbines	53
4.2.2 Superconducting generators (SC)	53
4.2.3 Magnetic Pseudo-Direct Drives (PDD)	58
4.2.4 Power electronics for Superconductor Direct Drive (SCDD) and Pseudo Direct Drive (PDD) generators	64
4.2.5 Integrating SC and PDD generators in 10-20 MW turbines Nacelle Designs ..	65
4.2.6 Main scientific and technological accomplishments	67
4.3 Support Structures	70
4.3.3 Designs for 10 MW wind turbine class	74
4.3.4 Designs for 20 MW wind turbine class	77
4.3.5 Main scientific and technological accomplishments	78
4.4 Road to market	80
4.4.1 Technology Roadmaps – overall principle	80

4.4.2 Technology Roadmaps – example.....	81
5. CONTROLS AND INTEGRATIONS OF INNOVATIONS AT THE SYSTEM LEVEL	82
5.1.1 Introduction of the State of the art in controllers for large offshore turbines ...	82
5.1.2 New sensors for turbine control	83
5.2 Innovative wind turbine control concepts	84
5.2.1 Individual Pitch and Flap control.....	84
5.2.2 Blade independent active flap control	87
5.3 Innovative turbines with advanced control-Appreciation of LCOE reduction potential	89
6. REVOLUTIONARY PLATFORMS	91
6.1 A 20 MW Multirotor System.....	91
6.1.1 Why multirotor?	91
6.1.2 The INNWIND.EU 20 MW multirotor	91
6.1.3 LCOE evaluation	93
6.1.4 Lessons learnt	93
6.2 A 10 MW Floating Vertical Axis Wind Turbine	93
7. IMPACT OF INNOVATION ON LCOE AT COMPONENT AND PLATFORM LEVEL	97
8. CONCLUSIONS	101
Rotors.....	101
Drivetrain.....	101
Substructure	102
9. FURTHER READING	103

GLOSSARY OF TERMS

- **Aeroelastic** – Coupling between aerodynamics and elastic structural properties
- **BTC** – Bend twist Coupling in a blade, i.e. as the blade bends, by design, it also twists
- **Cp-max** – A normalized specification that relates to the maximum electrical/mechanical power and usually specified with respect to a tip-speed ratio (ratio of linear speed of the rotor tip to mean wind speed)
- **CPT - Cone penetration tests for identifying soil properties**
- **Guyed substructure** – Catenary type cables attached from the seabed to the substructure that is also attached to the seabed, but able to articulate about a joint on the seabed
- **HAWT** – Horizontal axis wind turbine - the axis of rotor rotation is horizontal
- **Jacket** – fixed frame based offshore sub- structure
- **LiDAR** – (Light detection and ranging) uses pulsed or continuous laser light to measure wind speed based on the reflected light from particles in the air
- **MRL** – Manufacturing readiness level – The maturity level of the technology for manufacturing or production
- **Pseudo** – Magnetic Direct drive (PDD) – use of a permanent magnet gearbox (no mechanical gears) combined with a ring generator
- **Reynolds number** – dimensionless number relating to the ratio of inertial force to viscous force on a fluid taken at a reference length scale
- **RNA** – Rotor Nacelle Assembly
- **RWT** – Reference Wind Turbine
- **Semi floater** – structure that is anchored to the seabed using an articulated joint and uses buoyancy to stay upright in combination with guy cables also attached to the seabed
- **Spar buoy** – Tubular floating foundation that has ballast in the lower section and buoyancy in the upper section, hence floats in a vertical orientation
- **Spinner** – The outer cover of the rotor hub
- **Superconductor** – A material that below a critical temperature conducts electricity with negligible resistance. High, medium and low refers to the relative temperature at which the material becomes superconducting.
- **TRL** – Technology Readiness Level – The maturity level of the technology for exploitation
- **VAWT** – Vertical axis wind turbine – the axis of rotor rotation is vertical

EXECUTIVE SUMMARY

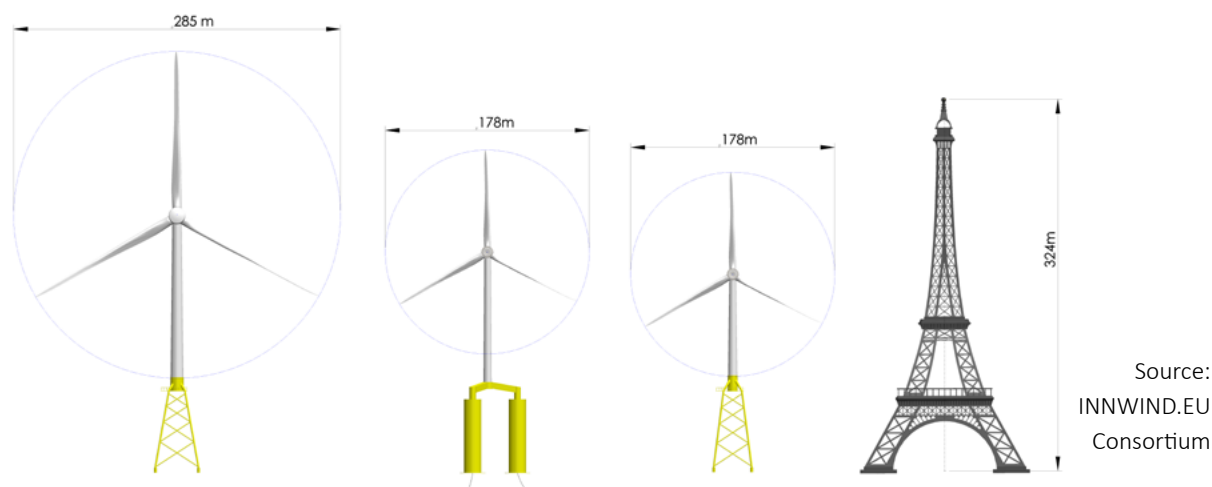
INNWIND.EU is a project with a budget of nearly €20 million and with 28 partners. Its objectives include the conceptual design of beyond-state-of-the-art 10-20 MW offshore wind turbines and hardware demonstrators of their critical components. Thus far, the project has developed several innovative rotor designs, drivetrain components, and fixed and floating substructures that greatly reduce the Levelized Cost of Energy (LCOE) for 10-20 MW offshore wind turbines. No technological “show-stoppers” for the development of wind turbines between 10-20 MW wind turbines are seen, but manufacturing processes for critical components such as the hub and blade bearings are not fully developed and need to be matured.

Large integrating projects such as INNWIND.EU facilitate effective consortia working on multi-disciplinary innovations. The INNWIND.EU consortium consists of large wind turbine manufacturers, certification bodies, consulting companies, research institutions and leading universities.

An assessment of the entire wind turbine with different innovations has been made at the 10 MW and 20 MW scales by applying performance indicators and a comprehensive cost model developed in the project. Moving from conventional 5 MW offshore turbines to lightweight 10 MW-20 MW scale allows a reduction in LCOE due to the larger turbine size along with the use of an efficient lightweight rotor and the shift from traditional three-stage geared drive trains to a medium speed drive. Significantly further reduction of LCOE can be expected for both 10 MW and 20 MW designs, due to the advanced concepts researched in INNWIND.EU, getting LCOE close to 80 €/MWh for 20MW turbines and 85 €/MWh for 10MW turbines. This corresponds to an overall reduction of more than 30% in LCOE compared to the reference value of 106.9 €/MWh corresponding to 5 MW turbine sizes, thus bringing 20 MW offshore wind turbines closer to the market.

FIGURE 0.1:

(left to right), 20 MW with 285m rotor diameter, 10 MW with 178m rotor diameter floating, 10 MW with 178m rotor diameter.



Some of the key promising innovations as developed in the project that reduce LCOE and increase efficiency include:

- The Low Induction Rotor (LIR), which constrains the extreme loads at the blade root and allows large rotor diameters with increased energy capture;
- Optimized aerodynamic and structural platforms of blades for reduced blade root fatigue and tower base fatigue;
- Active control with a focus on blade trailing edge flaps and blade trailing edge section morphing for load alleviation;
- High temperature superconducting generators to increase efficiency;
- Pseudo-Magnetic Direct drives (PDD) that also significantly increase transmission efficiency;
- Advanced optimal jacket designs at 50 m water depths to support wind turbines at 10 MW and 20 MW capacities;
- Guyed articulated sub structure at 50 m water depth that avoids resonant excitation for 2-bladed and 3-bladed rotors;
- Novel triple-spar semi-submersible floating wind turbine for 10 MW wind turbines.

To develop and validate the design basis of floating wind turbines, several wave tank tests have been made in the project that test semi-submersible and tension leg platforms. The floater response and parameters of waves measured in the tests are available to the public upon request. Met-ocean conditions required for the design of future large wind turbines up to 300 m in height, with wind velocity profiles and associated wave climate have been constructed using advanced models and validated with data from the FINO3 platform. This met-ocean database allows the set-up of an external conditions design basis for 10-20 MW wind turbines. All the above are available on request.

Future research in moving the Technology Readiness Levels (TRL) of the new 20 MW wind turbine designs which

are presently around TRL 4 to TRL 6 is recommended by large scale testing of its components, improved manufacturing processes and improved structural properties. Fundamental research is also recommended in new methods, materials and technologies that enable digitalization of very large offshore wind turbines, thus opening up for new design and development opportunities.

SCIENTIFIC SUMMARY

The innovations developed for significantly reducing LCOE at the 10 MW and 20 MW capacities have been classified as Evolutionary (implying traditional designs), Radical (implying new types of designs) and Revolutionary (implying a complete change in design philosophy). A brief scientific description of the key innovations is given below.

The low induction rotor was developed with dedicated airfoils for the outer part of the blade which are designed for operation at a low lift coefficient of around 0.8 and whose aerodynamic characteristics were validated against wind tunnel measurements. Tools for the integrated design of aeroelastic tailoring with passive blade deflection couplings have been developed along with numerous solutions for an optimum combination of passive and active control. The TRL level of these rotor innovations have been moved from around 3 at the start of the project to TRL 5 at its closure. Innovative wind sensors such as a spinner anemometer and spinner LiDAR that measure high frequency wind time series either at a point on the spinner (anemometer) or at many points in front of the turbine (LiDAR) have been demonstrated. The Spinner anemometer allows ease of wind turbulence measurements as an input to controls enabling load mitigation or increasing energy capture.

Medium temperature superconducting generators with Magnesium DiBoride (MgB_2) coils were investigated, along with coil testing which showed that the reliability of the coil windings had to improve to ensure low resistivity. The superconducting coil Yttrium Barium Copper Oxide (YBCO) was also tested, which though showing great potential, requires significant reductions in cost to enable commercial usage at 10-20 MW scales. Reducing the cost of medium temperature superconducting wire by a factor of 4 and simultaneously increasing the critical current density by a factor of 4 is required for cost-effective gen-

eration for fixed base offshore wind turbines. The status of these superconducting generators is at a TRL of 4. This is because, even though the tower top weight may be reduced by 30% compared to a conventional drivetrain, this reduction in weight translates to insignificant benefits in LCOE due to the large cost fraction of the substructure, which remains relatively unchanged.

The PDD provides for magnetic gearing with a permanent magnet generator and has been tested in a lab at different scales of 5 kNm, 16 kNm and 200 kNm max torque values. It provides for high generation efficiencies of at least 95% at the small scales and is expected to reach 98% for the large generators. This increase in efficiency, along with moderate cost, is expected to contribute to about 4% lower LCOE. Its current status is at a TRL 4.

Fixed Substructure design at 50 m water depth is highly challenging for 10 MW wind turbines due to the 3P (3 times rotor speed) excitation of the sub structure for 3-bladed rotors and 2P (2 times rotor speed) excitation for 2-bladed rotors. An advanced optimal jacket was designed with a fatigue life of 25 years for the 10 MW turbine for 3-bladed rotors, while an innovative articulated joint sub structure was designed for the 2-bladed rotor. The TRL level of the jacket solution is relatively high, since jackets are already commercially used, while the TRL level of the articulated joint structure is at 3. At the 20 MW scale, it was found to be relatively easy to avoid rotor harmonic excitation, thereby enabling jacket substructure designs. Vertical axis (VAWT) and horizontal axis (HAWT) floating wind turbines have been designed for 10 MW capacities.

Technology roadmaps depicting the path to market for these innovations have been developed along with necessary standards to certify such wind turbines.

The project has very successfully addressed all its objectives and also put forth recommendations for future focus in the development of the 20 MW offshore wind turbine. The consortium would like to thank the EU commission for their support of this project and making possible such a cross-European research initiative whereby the European research capacity is utilized to develop innovations.

1.

INTRODUCTION

The European Union has set ambitious objectives for energy and climate change policy. It aims at increasing the share of renewable energy to 20% by 2020 and at least 27% of its final energy consumption by 2030.¹ The Renewable Energy Directive mandates that these 2020 targets are to be fulfilled through national targets.² In contrast, the 2030 targets do not contemplate national targets, but a common EU target fulfilled by the contribution of all Member States. This will be done through National Energy and Climate Action Plans set by each country. Measures could include supporting investments in renewables in line with European State Aid Guidelines, facilitating permitting and planning procedures and investing in Research and Innovation (R & I).

The European Strategic Energy Technology Plan (SET-Plan) aims at responding to the investment challenges in R & I through the development of low-carbon technology and its deployment.³ It promotes cooperation between dif-

ferent stakeholders, EU countries, companies, research centres, etc.⁴

The European Technology and Innovation Platform (ETIP Wind) is a forum to support the SET-Plan and to bring together EU Member States, industry and research to promote the market uptake of wind energy.⁵ Furthermore, the EU funds renewable energy projects through Horizon 2020, the programme that allocates more than €80 billion to R & I over the 7 year period from 2014 to 2020.

Wind power plays a crucial role in reaching the EU's renewable goals. It has grown exponentially in recent years and is expected to cover up to 23% of EU's electricity demand to 2030.⁶ Today, wind energy already meets 11% of the EU's power demand with high penetration levels in several countries (Denmark 42%; Spain 20%; Germany 13%; UK 11%) and represents over 300,000 jobs and generates €72 billion in annual turnover.⁷

1 EEA (2009). Europe's onshore and offshore wind energy potential. An assessment of environmental and economic constraints; European Commission, Climate Action (2017). 2030 climate and energy framework.

2 European Commission (2009). Directive 2009/28/EC of the European Parliament and of the Council of 23 April 2009. Available at <http://eur-lex.europa.eu/legal-content/EN/TXT/PDF/?uri=CELEX:32009L0028&from=EN>

3 European Commission (2014). Strategic energy technology plan.

4 Ibid.

5 JRC (2016). JRC Wind energy status report 2016 Edition. Available at <http://publications.jrc.ec.europa.eu/repository/bitstream/JRC105720/kjna28530enn.pdf>

6 EEA (2009). Europe's onshore and offshore wind energy potential.

7 WindEurope (2017). Wind energy today.

Whilst other regions have started to develop offshore sites, Europe has been harnessing wind energy at sea for over two decades⁸.

Europe has immense offshore wind energy potential, looking toward 2030.⁹ However, when assessing future energy potential it is imperative to make projections with respect to the developments of wind turbines both in terms of technology advancement and economic development.¹⁰

Well-aligned to the above policy framework, the overall objectives of INNWIND.EU are the high performance innovative design of beyond-state-of-the-art 10-20MW offshore wind turbines and hardware demonstrators of some of their critical sub-components. The progress beyond the state of the art is envisaged as an integrated wind turbine concept with 1) a light weight rotor having a combination of adaptive characteristics from passive built-in geometrical and structural couplings between deformations and active distributed smart sensing and control, and 2) an innovative, low-weight direct drive generator and 3) a standard mass-produced integrated tower and substructure that simplifies and unifies turbine structural dynamic characteristics at different water depths.

The results obtained and the lessons learned are summarized in the following Sections of the report.

Section 2 presents the driving EU SET-Plan targets and market expectations for LCOE reduction targets. It describes the evolution of state-of-the-art in offshore turbine design from 6 MW in 2012 to 10 MW in 2017. It introduces LCOE as an overarching Key Performance Indicator (KPI) and the cost models developed for calculating it. It also demonstrates the benefits of very large turbines in deep offshore in terms of LCOE and its different constituents AEP, CAPEX and OPEX. In the same section we address the technical challenges in designing for 10-20 MW turbines and the relevant pre-selection made regarding the turbine architectures considered in the project. Needs for new standards and external conditions at high atmospheres are also discussed.

Section 3 introduces the selected wind turbine design platforms and innovations around which the project

work is organized. These design platforms are classified in three categories: Evolutionary, Radically New and Revolutionary. Evolutionary refers to technology at the system level and component level where the TRL level is near to market. Radically new technology refers to technologies that still need lab testing and proof of concept for acceptance by the industry. Two- and three-bladed upwind and downwind rotors with non-conventional drive trains and offshore substructures are considered here. Revolutionary platforms are those of very low TRL (1 or 2).

Section 4 details the researched performed at the main components level (rotor, drive train and offshore substructure). For each research theme the state-of-the-art technology is presented first, followed by the innovative concepts researched in the project. This section comprises the core part of the present research project. Main scientific results and technological accomplishments are presented and discussed along with lessons learnt. Technology roadmaps are finally presented for selected, more promising, innovations with the aim to facilitating their road to market.

Section 5 presents the project accomplishments in advanced control and the role it can play in loads and, therefore, LCOE reduction. Advanced control algorithms combined with innovative control sensors (LiDAR or spinner anemometer-based) are presented and discussed. Individual flap control gets particular attention in this part of the report.

Section 6 provides details on the work done for the revolutionary platforms. Two concepts have been researched: a 20 MW MultiRotor system and a 10 MW floating Vertical Axis Wind Turbine (VAWT).

Section 7 assesses the most promising 10 and 20 MW innovative concepts researched in the project with regard to their impact on LCOE and other critical performance indicators such as components, turbine mass and cost, as well as turbine and wind farm capacity factor, along with some rough considerations for OPEX. Dedicated cost models developed in the project have been used to quantify the results and demonstrate the cost reduction potential of each individual innovation and their combinations.

⁸ WindEurope (2017). Offshore wind energy.

⁹ EEA (2009). Europe's onshore and offshore wind energy potential. An assessment of environmental and economic constraints.

¹⁰ Ibid.

2.

DESIGN CHALLENGES AT 10 MW TO 20 MW

This section introduces LCOE as an overarching Key Performance Indicator (KPI) and describes the corresponding cost models. The benefits of very large turbines in deep offshore in terms of LCOE and its different constituents AEP, CAPEX and OPEX are highlighted. The technical challenges in designing 10-20 MW turbines, the relevant turbine architectures considered in the project and the needs for new standards and external conditions at high atmospheres are presented in the following sections.

2.1 COST DRIVERS IN OFFSHORE WIND DEVELOPMENT

2.1.1 THE EUROPEAN WIND INITIATIVE

In 2011, the European Wind Industrial Initiative (EWII) introduced a single overarching KPI in order to monitor the impact of the Wind Energy Roadmap (2010-2020) on the sector¹¹. This overarching Key Performance Indicator (KPI) is the Levelised Cost of Electricity (LCOE) produced by wind power and it is expressed in Euro per Mega-

watt-hour (€/MWh). The LCOE represents the sum of all costs over the lifetime of a given wind project, discounted to the present time, and levelised based on annual energy production. The basic parameters necessary for the calculation of the LCOE are listed in Table 2.1, along with the adopted reference values.

TABLE 2.1
Reference case values for the LCOE in EWII ¹¹

PARAMETERS	OFFSHORE
Capital investment cost – CAPEX (€/kW)	3,500
O&M costs including insurance(€/kW/yr)	106(*)
Balancing costs (€/MWh)	3
Capacity factor (%)	40
Project lifetime (years)	25
Real discount rate (%)	5.39
Total plant capacity (MW)	300
Size of wind turbines (MW)	5-7

As seen in the table, the main LCOE drivers for an offshore wind farm are its CAPEX, OPEX (O & M costs) and Capacity Factor (CF). CAPEX is often split into two parts, one addressing the turbine itself and another for the balance

¹¹ SETIS-TPWIND (2011). Key Performance Indicators for the European wind industrial initiative, Version: 3.

of plant (BoP) where the cost of the offshore foundation system is accounted for. For a typical deep water offshore wind plant, the following contributions to LCOE are expected: CAPEX Turbine 30%, CAPEX BoP 40% and OPEX 30%.

Note that O & M costs are significantly underestimated in the original EWII LCOE model. As an example, we refer to a 2013 study of RolandBerger¹² where the current O & M cost for a typical offshore wind farm at that time was taken at 140 €/kW/yr (significantly more than the 106 €/kW/yr of the table).

EWII set a target for a 20% RTDI driven reduction in offshore wind LCOE until 2020 compared to 2010 levels. This is in line with the target that the wind energy market has also set. There are several publications and press releases by major offshore wind farm developers and operators such as DONG¹³ and E.ON¹⁴ stating that they aim to cut the cost of wind energy in the North Sea to less than 90 €/MWh by 2020 compared with the 160 €/MWh of 2012. In order to get this 60% cost reduction DONG has plans to radically increase the size of the offshore turbines it will install, from 3 to 4 megawatts in 2012 to 8 to 10 MW in 2016 through 2020. In a recent publication, Siemens unveiled a new turbine platform in the next five years, hinting at a 10 MW+ turbine as it targets €80/MWh by 2025¹⁵.

for blade length at 88.4 metres. The turbine has been selected for three of France's first six offshore projects, all of around 500 MW. Siemens has twice since upgraded its direct-drive offshore turbine to a power rating of 8 MW with an extended rotor diameter of 154 metres.

Increasing the turbine rating and size has an important impact on all main three LCOE drivers, CAPEX, OPEX and CF. A 2012 study conducted by BVG associates¹⁶ provided insight to the scaling laws ruling the different CAPEX contributors but also DECEX (decommissioning expenditure). The study considered a 500 MW offshore wind farm located at several distances from the nearest construction and operation port, comprising turbines of 4, 6 and 8 MW at different average water depths of between 25 and 45 m. The type C site of the BVG study is located 40 km from the port and has an average water depth of 45 m and average wind speed 9.7 m/s at 100 m above mean sea level. This is the site type closest to the external conditions of INN-WIND.EU assumptions. The turbines at this site are supported by four-legged piled jackets with a separate tower. The results¹⁶ for a baseline wind farm are summarized in Table 2.2.

2.1.2 SIZE OF COMMERCIAL OFFSHORE TURBINES

When INNWIND.EU started in 2012, the maximum size of the commercial offshore turbines available in the market was 5-6 MW. Two characteristic members of this family were the GE 6 MW / 150.8m diameter Class IB Haliade and the Siemens 6 MW / 120m diameter turbines. Originally announced by Vestas as a 7 MW unit in 2011, the V164's has in the meantime been upgraded to 9+ MW. The first project using the V164, DONG Energy's Burbo Bank extension is currently under construction. In the meantime two additional 8MW turbines were put on the market, the ADWEN AD-180 is setting a new benchmark

12 RolandBerger (2013). Offshore wind towards 2020. On the pathway to cost competitiveness. Available at http://www.rolandberger.com/media/publications/2013-05-06-rb-sc-pub-Offshore_wind_toward_2020.html

13 E&E News (2013). Renewable energy, mammoth wind turbines will cut offshore costs by 40% in 7 years, developer says. Available at <http://www.eenews.net/stories/1059978057>

14 Available at http://www.windpoweroffshore.com/2013/02/21/eon_focuses_on_95mw_goal/#.UZtdAbVmh8E

15 Available at <http://www.windpowermonthly.com/article/1399841/siemens-teases-10mw-turbine>

16 BVG associates (2012). Offshore Wind Cost Reduction Pathways. Technology work stream.

TABLE 2.2

CAPEX and DECEX dependence on the turbine rated power¹⁶

TYPE	PARAMETER	UNITS	4MW-C	6MW-C	8MW-C		4MW-C	6MW-C	8MW-C
CAPEX	Project up to WCD incl construction phase insurance	k€/MW	163	155	150	%	4	5	4
	Contingency		324	304	303		9	9	9
	Turbine nacelle		790	839	916		22	24	27
	Turbine rotor		491	581	648		13	17	19
	Support structure incl tower		994	865	831		27	25	24
	Array cables		104	103	98		3	3	3
	Installation		788	580	478		22	17	14
	Total		3,653	3,426	3,423		100	100	100
DECEX	Decommissioning	k€/MW	473	348	287				

From the individual CAPEX categories, turbine costs per MW are increasing with rated power while there is a decrease in the costs of support structure along with installation costs. This is in line with the project's early finding that classical upscaling of a given turbine technology increases the turbine CAPEX by $p^{3/2}$ while the BoP CAPEX by p^1 , where p is the nominal power ratio. Learning curve effect and innovation reduce both CAPEX exponents ($3/2$ and 1) considerably. Array cable costs seem turbine size independent. Decommissioning costs are also reducing for larger turbines, staying proportional to the installation costs (with a fixed ratio of 60%). Although decommissioning costs are quite high in absolute values, their contribution to LCOE is limited, since they are annualized with a small factor representing the fact that DECEX will not occur until the end of the project's lifetime.

2.1.3 OPEX AND TURBINE SIZE

Increasing the turbine size reduces the OPEX per installed MW. Evidently, the OPEX part which is simply proportional to the number of turbines in the farm is decreasing when larger turbines are used. Further OPEX reduction can be expected from innovative operation and maintenance schemes. Roland Berger¹² assumes a 14% reduction of annual OPEX cost only by shifting from the 3 MW to the

6 MW turbines. The Crown Estate¹⁷ estimates in a similar study a reduction of 10-15%.

INNWIND.EU performed parametric calculations for the 500 MW wind farm placed in the metocean zone 2B11 using the O2M-Plus tool of DNV-GL. Introducing as free parameters the turbine rated power and reliability level we calculated direct O & M cost per MWh produced and the related wind farm availability losses. The through-life turbine reliability was modelled by means of a typical "bathtub" curve which addresses the three phases of the turbine service life: the early-life "bedding-in" period, the high reliability intermediate period and the end-of-the-design-life period where failures due to wear and tear occur more frequently. Failures were classified into four categories depending on the severity of the required repair. A reference reliability level is that of a turbine suffering a typical number of failures per year (of all four categories mentioned above) where more than 60% of them simply require a visit for a manual restart. Better or worse reliability levels in our investigation are introduced by assuming a multiplier of the reference number of failures.

¹⁷ The Crown Estate (2012). Offshore Wind Cost Reduction. Pathways study.

FIGURE 2.1

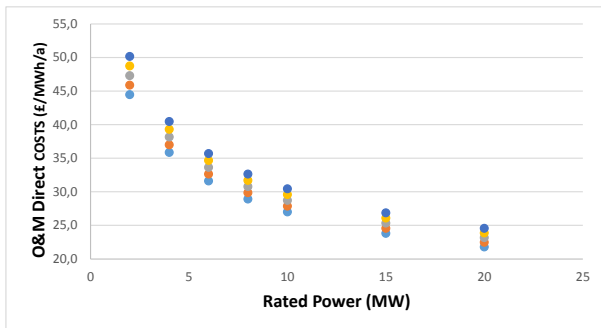
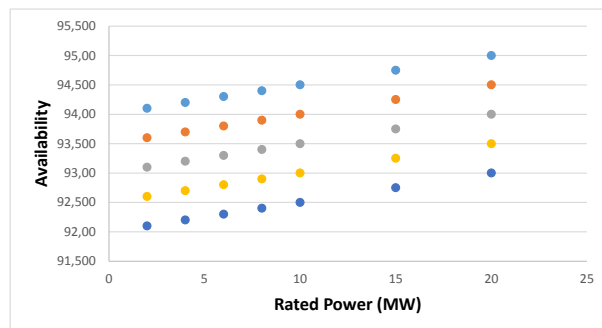
Sensitivity of energy availability and O&M costs to the turbine rated power and reliability.

PLANT ENERGY AVAILABILITY

Turbine Rated Power (MW)	RELIABILITY LEVEL				
	-10	0	10	20	30
2	94.1	93.6	93.1	92.6	92.1
4	94.2	93.7	93.2	92.7	92.2
6	94.3	93.8	93.3	92.8	92.3
8	94.4	93.9	93.4	92.9	92.4
10	94.5	94.0	93.5	93.0	92.5
15	94.8	94.3	93.8	93.3	92.8
20	95.0	94.5	94.0	93.5	93.0

O&M DIRECT COSTS (£/MWh/a)

Turbine Rated Power (MW)	RELIABILITY LEVEL				
	-10	0	10	20	30
2	44.4	45.9	47.3	48.7	50.1
4	35.9	37.0	38.2	39.3	40.5
6	31.6	32.6	33.6	34.7	35.7
8	28.9	29.8	30.8	31.7	32.6
10	27.0	27.9	28.7	29.6	30.4
15	23.8	24.6	25.3	26.1	26.9
20	21.8	22.5	23.2	23.9	24.6



The results of the O & M study are presented in Figure 2.1. It is seen that using larger turbines not only significantly reduces the O & M direct costs but also slightly increases the wind farm availability in benefit of the annual energy production. As expected, the increasing reliability of the wind turbines (the different colours of dots) has positive effects on both availability and direct O & M costs.

2.1.4 EFFECT OF UPSCALING ON LCOE

Even classical up-scaling has a positive effect on the capacity factor of a large offshore wind farm. This effect was studied in the UPWIND Project¹⁸ where the (aerodynamic) wind farm capacity factor was calculated as a function of the WT rated power. The mean wind speed distribution used at the hub height of all designs was a Rayleigh with

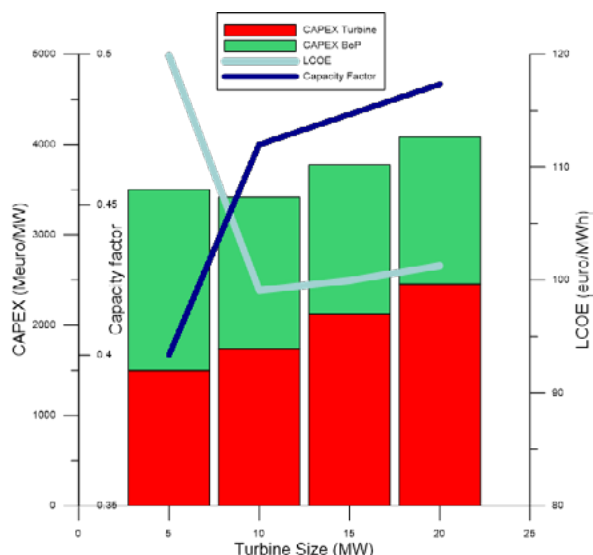
mean 10 m/s while the wind rose was assumed uniform direction-wise. Two wind farm sizes were considered, with 500 and 1000 MW installed capacity. The spacing of the turbines was 7D X 7D, leading to similar offshore area requirements for all turbine sizes.

The wind farm aerodynamic capacity factor (the production of all turbines including the wake effects) increases with the size of the single turbine. Going from 5 to 10 MW, we have a nearly linear increase of almost 2.5 percentage units, with an additional increase of 2.5 units from 10 to 20 MW. This effect is attributed to the reduction of wake effects due to the smaller number of turbines in the wind farm when the rated power of the individuals increases. This capacity factor improvement is not related to better wind resource available at larger distances from the shore (and deeper waters) or going at larger hub heights. These are additional factors that might further increase

18 E.S. Politis and P.K. Chaviaropoulos (2008). Integrated Wind Turbine Design, UpWind Project (SES6-CT-2005-019945), Workshop on Cost Functions Stuttgart.

the farm capacity and are (indirectly) linked to the single turbine size.

FIGURE 2.2
Turbine size influence to LCOE and its main drivers



The synthesis of the above suggests that larger turbines increase the turbine CAPEX and the wind farm capacity factor while decreasing the BoP CAPEX, the OPEX and the

DECEX. Given the state of the technology and the wind resource, there will always be an optimal turbine size that minimizes LCOE and which is water depth dependent. This optimal size increases with the depth. This is further illustrated in Figure 2.2. Note that the optimal size of 10 MW suggested by the figure is only indicative.

Clearly, a quantitative decision on the optimal turbine size for a specific offshore site which also accounts for the technology evolution and the potential that innovation adds to LCOE reduction should be based on a proper cost model integrated to the LCOE calculator. Such a cost (and mass) model has been developed in INNWIND.EU to assess the innovative designs at the components and system level researched in the project. The model: i) is developed at the sub-components level, ii) is based on key turbine design parameters (Rated Power, Diameter, Hub-height, Rated Torque etc.) and operating conditions, (wind class, etc.), iii) is suitable and flexible enough for up-scaling studies too, taking account of technology learning curves, iv) account of variations in raw materials pricing, inflation and currency fluctuations so that cost data from different periods and markets can be synchronized, v) explores previous experience from earlier cost modelling works in WINDPACT (USA) and UPWIND (EU). The Input / Output section of the cost model is shown in Figure 2.3.

FIGURE 2.3
The I/O section of the INNWIND.EU cost model

TURBINE INPUT PARAMETERS		INTERMEDIATE TURBINE RESULTS		RESULTS	
10000	Power (kW)	1.01	Omega (rad/s)	WF Capacity Factor	0.425
178.0	Diameter (m)	9.66	RPM max	Turbine Cost (M€2012/MW)	1.372
90.0	Max Tip Speed (m/s)	105.20	Rated Torque (kNm)	BoP Cost (M€2012/MW)	1.695
119.0	Hub height (m)	24885	Rotor swept area (m ²)	CAPEX (M€2012/MW)	3.066
11.4	Rated speed (m/s)	0.478	Rotor Cp_max (-)	O&M Direct Costs (€/MWh)	34.81
10.0	Design speed (m/s)	0.940	Drive Train Efficiency @ full load (100%)	LCOE (€/MWh)	98.56
1: Innwind.EU 10MW RWT Blade - scaled	Blade Model	0.830	Drive Train Efficiency @ partial load (10%)		
2: Medium Speed (40:1) Innwind.EU RWT - Sca	Drive Train Model	0.507	Turbine Capacity Factor		
1: RWT 10MW Standard - Scaled	Tower Model				
1: Jacket 10 MW RWT - Scaled	Offshore Support Structure				
0%	Reliability Surcharge (%)				
WIND FARM DATA		SITE CONDITIONS		OTHER DATA	
500	Total Capacity (MW)	9.20	Mean Annual Wind Speed (m/s)	€/€ (2012)	1.250
9.0%	Wake Losses (%)	2.00	Weibull shape factor k (-)	\$/€ (2012)	1.320
2.0%	Electrical Losses (%)		O&M Class 2b or 2c	WT Price/Cost of components	1.400
6.0%	Availability Losses (%)			BoP Price/Cost Multiplier	1.000

2.2 TECHNICAL CHALLENGES, CONCEPT AND INNOVATION SELECTIONS MADE

When the project kicked-off, a 10 MW onshore turbine paper design was already available which, complemented with a 10 MW jacket, formed the 10 MW Reference Wind Turbine (RWT) of the project, serving as the initial basis for further comparisons. A 20 MW RWT was introduced at a later stage. These reference designs revealed many of the technical challenges a designer would face at the rated power scale of interest. Some of these challenges are identified and discussed below along with the selections made for their confrontation.

2.2.1 UPWIND VS DOWNWIND ROTOR

Market selection of the standard three-bladed upwind concept occurred in the early 1980s after a very short concept competition phase, and the main focus thereafter in industrial development has been the upscaling of this successful concept rather than challenging conceptual characteristics like upwind vs downwind. The upwind rotor was chosen mainly in order to reduce the impact of the tower wake (on loads and noise), even though it was known that the downwind configuration offered some potential benefits related to better centrifugal de-loading by coning and unrestricted flapwise downwind blade bending, as well as the possibility for free yawing and application of negative tilt, which might give more axial flow for wind turbines in complex terrain.

With the upscaling to multi-MW turbines that require more lightweight and thus more flexible blades, the main design requirement became the avoidance of tower strike, and forward pre-coning and blade pre-bending was introduced. However, these two blade characteristics are subject to limitations. Apart from being important parameters in the blade optimization, they are also a key factor in determining the blade operational aeroelastic behaviour, where the main constraint is still to avoid tower strike.

Downwind operation offers some options for further weight reduction by allowing the blade to be more flexible

at the cost of more tower wake interaction and the risk of blade vortex lock-in with increased blade passage noise.

2.2.2 THREE-BLADED VS TWO-BLADED ROTORS

For three-bladed designs, critical n-P value appears to be the 3-P while 1-P and 6-P are normally outside the critical range for resonance. The 3-P excitation can be alleviated through an exclusion zone in the variable speed controller, which however compromises the power performance of the turbine and does not totally prevent the problem. If resonance is not avoided, the turbine will suffer from higher fatigue loads in the wind speed range where 3-P excitation takes place. With or without exclusion zone in control it is beneficial to translate the excitation zone at lower wind speeds which, for offshore sites of economic interest, have less probability of occurrence and, thus, contribute less to the AEP and the lifetime fatigue loads. For a given rotor diameter and power curve, moving the 3-P resonance to lower wind speeds can be accomplished through i) increasing the design TSR which also increases the design tip-speed (increasing erosion as long as noise is not a problem) and calls for slenderer blades or ii) reducing the system's first global frequency, which is more effectively done by increasing the tower height and consequently the support structure loading.

If the three-bladed / jacket design is challenging, the two-bladed / jacket seems impossible since one has to prevent 1-P, 2-P and 4-P excitation. In this case, an alternative soft support structure has to be adopted. It has been shown that a semi-floater support structure can do the job.

2.2.3 KINGPIN VS TRADITIONAL DRIVE TRAIN SUPPORT

The main function of the nacelle is to support the rotational motion of the hub holding the turbine blades and to transmit the mechanical power from the blades into the shaft and finally into the drive train. Thus the shaft must be supported by either one or two main bearings. These bearings should have a high reliability, because they are difficult and expensive to replace at sea. Traditional drive

trains have two main bearings holding the shaft and then a gearbox and generator sitting behind the main bearings. This concept, however, is not believed to be viable for turbines much larger than 10 MW, because the two main bearings will be loaded differently and to a level beyond the current capacity of main bearings. In order to distribute the turbine rotor loads more evenly between two main bearings, then, it has been proposed to place the two bearings on a static pin going through the hub and on each side of the hub. This concept has been termed the King-Pin concept and is used for the INNWIND.EU nacelle.

2.2.4 DIRECT DRIVE VERSUS GEARED CONCEPTS

The function of the drive train in large offshore wind turbines is to convert the mechanical power provided by the turbine blades into electrical power flowing out through the cable that connects the turbine to the power grid on land. For this purpose, a generator where rotating magnetic fields can induce a voltage in the windings of the generator is used. If the generator is loaded then there will also be a current running in the cable and the generator will provide a torque on the turbine shaft keeping the rotation speed of the turbine blades at the optimal rotation speed compared to the incoming wind speed. The electrical loading of the generator is provided by an electrical circuit connected to a transformer stepping up between the generator voltage of a few kilo volts to 36-66 kilo volt of the wind farm collection cables. The collection cables from each turbine in the wind farm is connected to a transformer platform that brings the power to land through the main power cable at a voltage of 100-200 kilo volts.

The major design trends within drive trains for large offshore wind turbine can be categorized into two main types:

GEARED

A gearbox is placed between the turbine shaft and the generator in order to convert high torque and slow speed of the turbine shaft to low torque and high speed of a generator, which can be small and cheap.

- **Pros:** Standard gearboxes and generators can be used and are therefore cheap.

- **Cons:** There are many moving parts, which tend to break more often than what they are designed for. It is expensive to replace gearboxes offshore.

DIRECT DRIVE

The high torque and slow speed of the turbine shaft is connected directly to a large generator, which is larger and more expensive than the generator sitting after the gearbox.

- **Pros:** Few moving parts and, therefore, higher expected reliability.
- **Cons:** Direct drive generators are often large and heavy, as they must be designed as part of the turbine.

State of the art within drive trains for large offshore wind turbines is to reduce the number of gear stages in the gearboxes and connect a medium speed generator to the gearbox. This reduces the complexity of the drive train, but still allows for a reduced torque of the generator. Examples of this approach is found with the 9 MW MHI Vestas Offshore Wind V-164 turbine and the 8 MW Adwen AD-8-180. Another trend is to use a permanent magnet direct drive generator as has been done by Siemens Wind Power for the 8 MW SWT-8.0-154 turbine and the 6 MW GE Haliade turbine. Drive trains based on a 3 stage gearbox are, however, still used for large offshore turbines such as the Senvion 6.2M152.

2.2.5 JACKETS VERSUS OTHER BOTTOM-FIXED SUPPORT STRUCTURES

The water depth range at the site under consideration is usually the most important criteria for the type of support structure. But soil conditions, wind turbine size and experience from the designer also have major influence. As a rule of thumb, monopile-like structures are most suitable for shallow waters and jacket like structures are suitable for deeper waters. Unfortunately, it is not possible to define these limits exactly. In recent years the transition was approximately around 35-40 m. The allowable range for each support structure concept regarding the water depth

is changing because technology advances continuously and further influential parameters such as soil conditions, met-ocean conditions and the size of the wind turbine result in variable limits. For example, a site with 50 m water depth and very stiff soil and small wave heights might still allow a competitive monopile design for 10 MW wind turbines, but shallow waters with soil in loose sand with extreme occurrence of scour and large wave heights will require solutions beyond a monopile. The design of the foundation always needs to follow an integrated approach considering many influential parameters of the site and the wind turbine appropriately. The most prevalent foundation design today is either the monopile or the jacket support structures, which are by far the most developed concepts. Innovative solutions such as suction buckets in combination with a monopile or jacket are currently being developed and are also being addressed in INNWIND.EU. One should keep in mind the logistics for manufacturing – and especially installation – of very tall structures. For water depths beyond 60 m, it can be problematic to handle the overall dimensions, e.g. required width and total height of the jacket. The total height of bottom-fixed support structures could exceed the capacity of cranes with respect to possible lifting height and lifting distance.

Another aspect is the clustering due to water depth variations within the wind farm. Here the jacket support structure shows high flexibility as the overall stiffness (thus natural frequency) of the jacket is less affected than for monopiles. That finally means that the resulting wind turbine fatigue loads on the support structure are comparable for different jackets in the wind farm. The support structure frequency usually lies within the 1p and 3p frequency range of the wind turbine, whereas monopiles tend to reach the lower end (1p) and jackets tend to reach the upper end (3p) currently. This indirectly opens up easier realization for jackets in deep waters than for using monopiles.

In this project the water depth is 50 m and a large number of innovations of the wind turbine are addressed. The dynamic interaction of wind turbine loads and a monopile response is generally more problematic than for a wind turbine with a jacket. This is mainly a consequence of the hydrodynamic induced loading on the super structure. In order to allow innovations of the wind turbine being developed parallel to the support structure, the jacket concept is chosen as the reference design in INNWIND.EU. It is a robust support structure which allows development

of wind turbine innovations “quasi”-independently from the foundation, but of course not the other way round (no matter which support structure is designed).

2.2.6 CHALLENGES IN FLOATING DESIGNS

In floating configurations, as in bottom-fixed platforms, the rotational speed of the wind turbine rotor can excite the tower’s natural frequency. In consequence, the accurate computation of the tower’s natural frequencies coupled with the floating platform has particular importance. In addition, the platform’s natural periods as a rigid body have to be located sufficiently far from the central frequencies of the wave spectrum. For platforms using catenary mooring lines, these periods are low and typically avoid significant excitation from waves, with an exception during the natural periods of the heave motion for semisubmersible floating concepts. This period tends to be located inside the wave spectrum, around 15 s - 20 s. The use of heave plates to damp the vertical motion can improve the behaviour of these platforms.

The evaluation of the global damping of the platform for the different degrees of freedom is also an important challenge, because it embodies complex physical effects related to viscosity that not all simulation tools can capture. Detailed CFD simulations and experimental scale testing in wave tanks are required to accurately characterize the damping level including viscous effects that greatly influence the global platform dynamics.

The simulation of floating wind turbines requires integrated tools because physical effects such as rotor aerodynamics and platform hydrodynamics are strongly coupled. A great effort to develop these tools has been undertaken in the last few years, although further research is still needed. An effect of particular importance for floating wind turbines is non-linear hydrodynamics. The inclusion of these non-linearities can imply a high computational cost. These effects produce high frequency and low frequency excitation as result of the interaction between different wave components of the spectrum. The low frequencies can excite the natural periods of the platform in the case of catenary moored platforms and can have particular importance in the design of the mooring system. For TLPs, the high frequency compo-

nents caused by non-linearities can also excite the platform's natural frequencies.

A particular effect that can have importance in the design of TLP is the excitation of the tension lines by vortex-induced vibration (VIV) phenomena. This effect requires complex simulations with structural models of the lines coupled with hydrodynamic models taking into consideration the fluid viscosity.

Specific control strategies for the floating wind turbines have to be developed to optimize designs. The dynamics of these systems are very different from onshore or bottom fixed systems. Floating wind turbines present low natural periods that increase the complexity of the control strategy.

Finally, more effort has to be made during the design phase regarding aspects such as manufacturing, installation, operation and maintenance of the floater. These aspects can have a great impact on the final energy cost.

2.3 NEW REQUIREMENTS FOR WIND TURBINE DESIGN STANDARDS

Besides the evaluation of suitable concepts for reducing LCOE of 10-20 MW offshore wind turbines, as discussed above, a number of innovative designs on component and system level have been developed by INNWIND.EU partners. Many of these developments have a realistic potential to reduce future LCOE of offshore wind of the 10-20 MW class of offshore wind turbines.

In order to estimate the technology-readiness level (TRL) and the potential time-to-market of these INNWIND.EU innovations, we have analysed the existing state-of-the-art guidelines and standards and their applicability. Certification by third party expertise according to established standards is an appropriate measure for estimating the TRL of an innovation. For instance: with a prototype certification, a TRL of level 6 to 7 can be documented and confirmed. This milestone within the development of an innovation serves as a 'door opener' for achieving

authority building permissions and/or support by financial investors.

Six promising examples of INNWIND.EU innovations have been selected within the project for a detailed review:

- Flaps and active control for smart blades
- Passive control of flexible blades and structural optimisation for lightweight rotors
- Superconducting generators
- Pseudo-direct drive generators
- Low-cost bottom-mounted support structures
- Cost-effective floating support structures

In cooperation with the INNWIND.EU partners an analysis of the TRL and applicable guidelines and standards have been performed according to Horizon 2020¹⁹; the technology readiness levels are presented in section 4.4. The result for the rating of six selected INNWIND.EU innovations is shown in the following table:

TABLE 2.3:
TRL for 6 selected INNWIND.EU innovations

NO	WORK PACKAGE TASK	TR LEVEL
1	Task 2.1: WP2 Advanced smart control systems	TRL 3 - 4
2	Task 2.3: Lightweight rotor, Innovative materials	TRL 3 - 7
3	Task 3.1: Superconducting generator	TRL 4
4	Task 3.2: Magnetic Pseudo-Direct Drive	TRL 4
5	Task 4.1: Bottom-mounted Offshore structure design	TRL 5
6	Task 4.2: Floating foundation design	TRL 4

One conclusion of this analysis was that many of the INNWIND.EU innovations can already be certified with existing guidelines and standards. Certification levels such as "Prototype Certification" or "Type Certification" are found to be achievable. As described above, the wind industry will introduce commercial 10 MW wind turbines in the near future. To this end, international standardisation institutions and certification bodies, such as IEC or DNV GL, have been updating their guidelines and stand-

¹⁹ European Commission (2013). Horizon 2020 – work programme 2014-2015. 19 general annexes revised. Available at http://ec.europa.eu/research/participants/data/ref/h2020/wp/2014_2015/annexes/h2020-wp1415-annex-ga_v2.1_en.pdf

ards to cope with the requirements of this generation of wind turbines.

INNWIND.EU innovations covered by existing standards:

- T2.1 High-speed aerodynamics
- T2.2 Lightweight blade design
- T3.3 Power Electronics
- T3.4 Drive train design
- T4.3 Low-cost bottom-fixed structures
 - Jacket 10-20 MW
 - Full-Truss jacket
 - Semi-floating pile

On the other hand, gaps and missing guidelines and standards have been detected for selected INNWIND.EU innovations. The following innovations require extended guidelines and standards to achieve higher TRL's and respective certification levels:

- T2.3 Active and passive control
 - T2.31 Morphing flaps and blade sections
- T3.1 Superconducting generator
- T3.2 Magnetic Pseudo-Direct Drives

T4.32 Suction bucket design

T4.13 Composite components

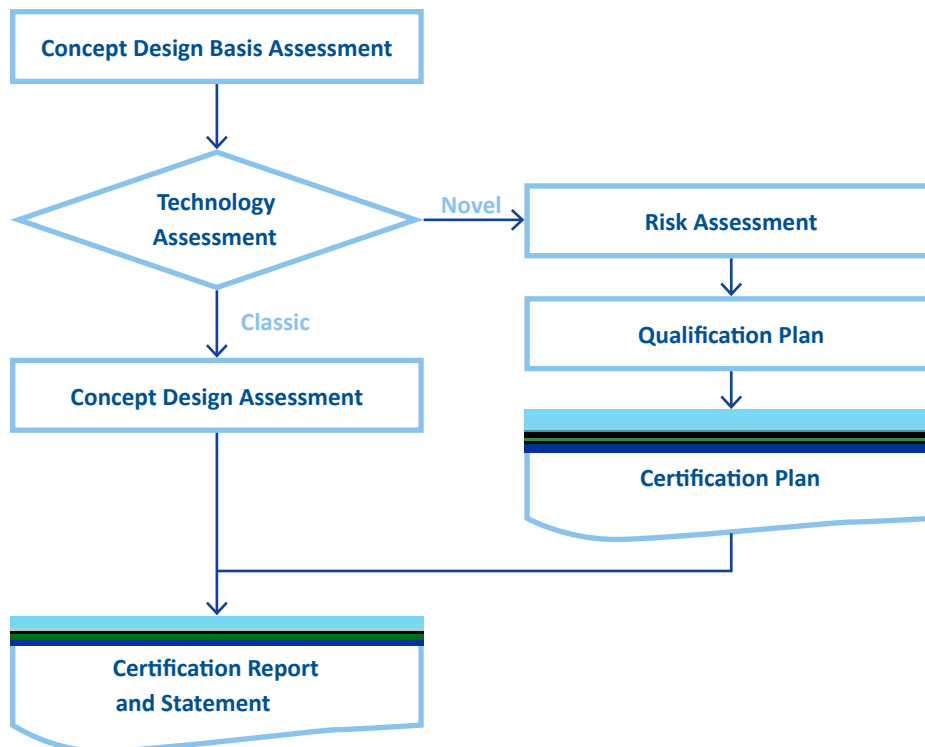
T4.2 Validation of integrated floating simulation tools

An alternative approach has been proposed for the INNWIND.EU innovations which are not covered by the existing guidelines and standards. Originally developed by the oil and gas sector, the Technology Qualification (TQ) is a profound method of evaluating an innovative component or system by deconstructing the design into its sub-units. Each unit is then analysed with respect to its failure modes and risk classes and finally summarised to an overall risk assessment evaluation and certification plan for the next certification level. Within INNWIND.EU, this approach has been exemplarily applied to the two INNWIND.EU innovations: active flap control and superconducting generator.

The following graph gives an overview on this alternative certification approach.

Further details for this certification approach can be found in the standards DNVGL-SE-0160 and DNV-RP-A203

FIGURE 2.4:
Technology Qualification process

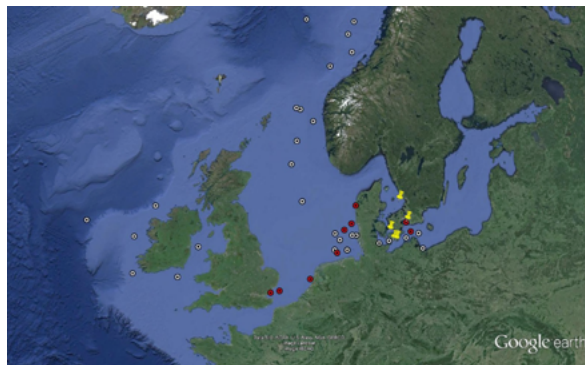


2.3.1 EXTERNAL CONDITIONS FOR DESIGNING 10-20 MW OFFSHORE WIND TURBINES

The establishment of a database that provides information on the wind speed and turbulence at higher atmospheres (above 150 m) and its connection with wave conditions is essential for designing large offshore wind turbines in the 10-20 MW range. There are several databases which contain wind parameter measurements for various near- and offshore sites across Europe. The locations of buoy measurements (black/white points) and met masts (red and yellow markers) in the North and Baltic Seas are shown in Figure 2.5

FIGURE 2.5

Map of measurement locations in the North and Baltic seas.



One of the available datasets, the FINO 3, has been further analysed to suit the project needs. The main argument for selecting FINO 3 is that both met mast and LiDAR data was available for the same time period. So, the LiDAR measurements can be evaluated up to a height of 100 m with reference to the data of the meteorological mast. This allows for a reliable investigation of wind conditions in tall atmospheres up to the maximum measuring height of the LiDAR system at 160 m. Furthermore, at FINO 3 there are available measurements of wave parameters from 2009.

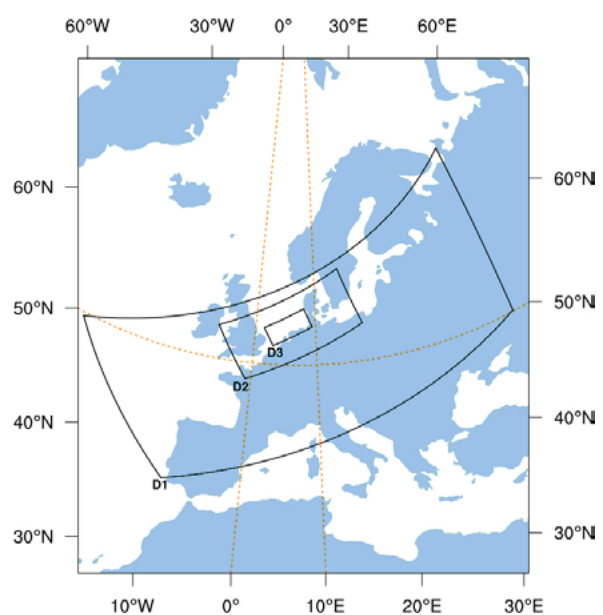
In parallel to the FINO 3 dataset analysis, the project derived wind profile data up to 310 m height above mean sea level from high-resolution mesoscale simulations performed with the Weather Research and Forecasting (WRF) model. Simulations for 2007 and 2011 have been carried out for three nested domains with a grid resolution in the finest domain of $2 \times 2 \text{ km}^2$ (Figure 2.6). The

values of eight parameters – wind speed, wind direction, thermal stability parameters (inverse Obukhov length), pressure, temperature, humidity, turbulent kinetic energy and turbulence intensity – are given in the delivered data set for different heights (every 20 m from 30 m up to 310 m) as 10 minute time series'. Additionally, the time series for the following variables are given: the planetary boundary layer height, the sea surface roughness height, the wind shear parameter alpha and the sea surface skin temperature. To optimize the accuracy, test simulations with four different parameterization schemes for the planetary boundary layer have been carried out and have been compared to measured data of the met masts FINO 1 and FINO 3. The results underline the importance of atmospheric thermal stratification for the vertical profiles of the turbine design parameters.

Furthermore, a novel gust model based on 3D Fourier methods has been developed which allows for the generation of any kind of wind event described by a set of constraints and which can be used in probabilistic design. The model makes it possible to specify gusts that only cover part of the rotor disk, which is a realistic scenario for 10–20 MW turbines.

FIGURE 2.6

WRF domain sizes for this simulation with the southern North Sea. The inner domain D3, which covers the southern North Sea, has grid resolution of $2 \times 2 \text{ km}^2$



In order to produce mesoscale wind and wave data as external conditions, a one month period was selected for simulation of the North Sea met-ocean conditions by combining a wind model (WRF) and wave model (MIKE 21 SW). Five wave stations were used for model validation: Sleipner, Ekofisk, K-13, FINO1 and FINO3, providing a good spatial and temporal coverage. The wave-modelling focused on assessing the benefit of a high resolution atmospheric model versus the use of the “standard approach” of using global re-analysis (CFSR) as atmospheric forcing for the waves. An implementation of a wave-age-dependent surface roughness in the wave model was also assessed. Model output data at Horns Rev, FINO1 and FINO3 were made available to the project partners. The data include wind speed and direction at different altitudes, integrated wave parameters (significant height, mean period, Wave direction) and 2D energy spectra (frequency and direction) with half-hourly time resolution.

3.

SELECTED PLATFORMS AT THE SYSTEM LEVELS

Setting the range of interest to 10-20 MW turbines, the design platforms are classified according to three categories: Evolutionary, Radically New and Revolutionary.

Evolutionary architectures are considered those based on technologies (at both the system and component levels) with TRL levels near to market, i.e. TRL5 and greater. The radically new platforms are engaging technologies that still need lab testing and proof of concept for acceptance by the industry, while revolutionary denotes those design platforms with present TRL levels 1 or 2.

The project focuses on the two first categories, further researching suitable innovative concepts at the components level (rotor, drive-train, offshore support structure) and controls.

3.1 REFERENCE AND EVOLUTIONARY DESIGNS

3.1.1 REFERENCE TURBINES

Typical examples of evolutionary architecture are the 10 and 20 MW Reference turbines. Here the main issue was

the upscaling to larger turbine size using mature technologies, taking advantage of the larger size whenever possible. As discussed earlier, the size of the turbine in itself is an important parameter for minimizing LCOE in deep offshore.

The two reference turbines have a classical 3-bladed, up-wind, max power coefficient (C_{pmax})-driven rotor design of high specific power (W/m^2). Their all-glass blades are pre-bent, using thicker than usual profiles for improved structural efficiency without compromising their aerodynamic efficiency. This is a Reynolds-driven benefit which comes with very large turbines, as thicker airfoils operating at very high Reynolds can have similar performance with thinner operating at lower Reynolds levels.

The 10 MW RWT was designed as an IEC Class IA turbine to withstand increased fatigue loads mainly due to wake effects, since ambient turbulence offshore is well below subclass C. Fatigue is the design driver of some of the expensive subcomponents of offshore turbines, such as the supporting jacket. Given the fact that wake effects are reduced when larger turbines are deployed for a fixed wind farm capacity, we decided to design the 20 MW RWT as an IEC Class IC turbine.

The two reference turbines have a medium-speed drive train with gearing ratio $\sim 1:50$ and a medium speed permanent magnets generator. For multi-MW turbines this selection performs well in terms of reliability and cost. Full range power conversion is possible.

A standard PI variable speed collective pitch controller is used in both turbines. Due to the 3-P resonance discussed above, the 10 MW RWT variable speed controller applies an exclusion zone at relatively low wind speeds. This has been avoided for the 20 MW RWT by slightly increasing its tip-speed-ratio and by using a taller tower that softens the first system's global eigen-frequency.

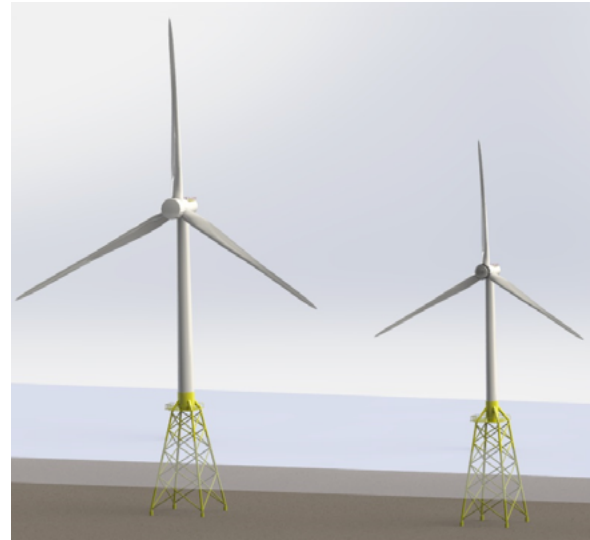
The reference jackets are assumed classical designs in terms of architecture, materials used and manufacturing procedures. Their legs are piled to the seabed.

Basic data and technical specifications for the 10 and 20 MW Reference Wind Turbines are given in Table 3.1.

TABLE 3.1
Basic turbine data for the 10 and 20 MW RWT

REFERENCE WIND TURBINES		
Rated Power [MW]	10	20
TEC Class	IA	IC
Number of blades [-]	3	3
Rotor Placement (Upwind-Downwind)	U	U
Rotor Diameter [m]	178.3	252.2
Hub Height from m.s.l. [m]	119	167.9
Blade Length [m]	86.4	122.1
Rated Wind Speed [m/s]	11.4	11.4
Minimum Rotor Speed [RPM]	6	4.2
Rated Rotor Speed [RPM]	9.6	7.13
Optimal TSR [-]	7.5	7.5
Gear Ratio [-]	50	48
Blade mass [Tons]	41.7	118
Hub mass [Tons]	105.5	278
Nacelle mass [Tons]	446	1098
Tower mass [Tons]	628.4	1600-1780
Tower Top mass, RNA [Tons]	676.7	1730
Water depth (mean sea level - m.s.l.) [m]	50	50

Acces Platform a.m.s.l. [m]	25	25
Jacket Mass [Tons]	1210	1670
Transition piece mass [Tons]	330	450



3.1.2 EVOLUTIONARY ARCHITECTURES

The main features of the reference designs are maintained along with the reference drive trains. Innovative solutions are sought for the 3-bladed upwind rotors to improve their energy capture and structural efficiency. Given the fact that the rotors are shaping the AEP while their contribution to the overall offshore turbine CAPEX is relatively small, it appears that a larger (and more expensive) rotor than the reference may significantly reduce LCOE by increasing energy capture. Nevertheless, the extra yield has to come without overloading the downstream components, increasing the overall turbine CAPEX.

The project explores several ways for increasing the rotor size (lower specific power designs) while maintaining the system's loads at their reference levels. One way is by optimizing the induction level in the aerodynamic design, aiming to achieve the best trade-off between power production and hub-loading. The optimization leads to a Low Induction Rotor (LIR) which can be best realized through a low solidity blade platform combined with low lift airfoils. Another, complementary, way is to apply passive or active load mitigation techniques, possibly combined with advanced control. Regarding passive loads alleviation, INNWIND.EU put a lot of effort in bend-twist coupling (BTC)

technology. In BTC designs, when the blade bends out of plane, it simultaneously twists passively nose down, reducing aerodynamic loading. This is accomplished either geometrically, by back sweeping the blades, or through the structural design by exploring the anisotropic properties of the composite materials or properly placing the shear-centre of the blade sections in respect to the twisting axis. Advanced turbine control based combining cyclic and individual pitch control is also sought in evolutionary designs. Innovative blade structure designs are sought, using full carbon or hybrid glass-carbon elements, for increasing the stiffness and adjusting the natural frequencies of the longer blades as well as enhancing their local buckling resistance properties.

Advanced jacket designs for 10 MW wind turbines require that the support structure fundamental frequencies are away from rotation excitation, that is for a 3-blade rotor, away from 3P and 6P excitations. Such a design is often very difficult to achieve due to the stiff nature of the jacket structure. The reference jacket for the 10 MW reference wind turbine is a traditional design which has 3P excitation and therefore low fatigue life. The advanced jacket designs created in this project allow for an integrated design approach so that correct tubular member diameter and thickness is applied at joints so as to possess sufficient fatigue resistance. This provides a jacket design as given in Table 3.2. Furthermore, an effective optimization of the jacket structure to reduce the natural frequencies below the 3P excitation zone has also been made so that the design meets a target lifetime while still being cost-effective. The optimal jacket design configuration is provided in Table 3.3

TABLE 3.2
Advanced Detailed Design Jacket parameters for the 10 MW RWT

JACKET GENERAL	DIMENSIONS	VALUE
Base Width	[m]	33
Top Width	[m]	16
Interface elevation	[mMSL]	26
Transition Piece height	[m]	8
Number of horizontal braces		none
NUMBER OF LEGS		4
Jacket legs outer diameter (upper / lower leg)	[mm]	1422/ 1828

Jacket legs maximum wall thickness	[mm]	108
Jacket legs minimum wall thickness	[mm]	38.1
NUMBER OF X-BRACES LEVELS		4
Max. Upper x-braces diameters (outer)	[mm]	610
Max. Upper x-braces wall thicknesses	[mm]	31.8
Max. Middle upper x-braces diameters (outer)	[mm]	711
Max. Middle upper x-braces wall thicknesses	[mm]	34.9
Max. Middle lower x-braces diameters (outer)	[mm]	812
Max. Middle lower x-braces wall thicknesses	[mm]	31.8
Max. Lower x-braces diameters (outer)	[mm]	914 / 1168
Max. Lower x-braces wall thicknesses	[mm]	41.3
NUMBER OF PILES	[-]	4
Pile penetration	[m]	38
Pile diameter	[mm]	2540
Pile wall thicknesses	[mm]	25.4 - 44.5
Pile top elevation above mudline (Stick-out length)	[m]	1.50
Overlap length (grout length)	[m]	7.5
MASS		
Jacket structure (primary steel)	[t]	1093
Transition Piece	[t]	258
Steel Appurtenances (estimation)	[t]	48
Piles (all)	[t]	342
Grout (estimation)	[t]	125
Total	[t]	1866
NATURAL FREQUENCY OVERALL STRUCTURE		
1st eigenfrequency (1st bending mode)	[Hz]	0.2635

TABLE 3.3

Optimized modular jacket parameters for the 10 MW RWT

DESCRIPTION	UNIT	FOUR X-BRACE LEVELS
Half base width	[m]	12.0
Half top width	[m]	7.25
Transition piece height	[m]	10.0
Jacket legs max inner radius	[mm]	297
Jacket legs max wall thickness	[mm]	74
Jacket legs min wall thickness	[mm]	45
Jacket mass (excl. transition)	[tons]	654
Transition jacket mass	[tons]	171
Total legs mass	[tons]	197
Total X-braces mass	[tons]	457
NATURAL FREQUENCY OVERALL STRUCTURE		
1st eigenfrequency (1st bending mode)	[Hz]	0.2267

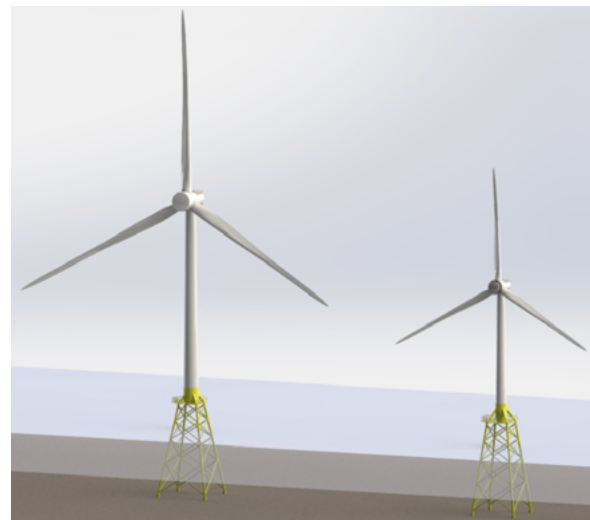
Basic data and technical specifications for the 10 and 20 MW evolutionary designs are given in Table 3.4

TABLE 3.4

Basic turbine data for the 10 and 20 MW evolutionary designs: 285 m 20 MW (left), 178 m 10 MW (right)

EVOLUTIONARY ARCHITECTURES		
Rated Power [MW]	10	20
TEC Class	IA	IC
Number of blades [-]	3	3
Rotor Placement (Upwind-Downwind)	U	U
Rotor Diameter [m]	178-202	252-285
Hub Height from m.s.l. [m]	119-131	168-173
Blade Length [m]	86-98	122-138
Rated Wind Speed [m/s]	11.4-11.0	11.4-11.0
Minimum Rotor Speed [RPM]	6	4,2
Rated Rotor Speed [RPM]	9.6	7.13
Optimal TSR [-]	7.5	7.5
Gear Ratio [-]	50	48

Blade mass [Tons]	37-49	100-132
Hub mass [Tons]	105.5	278
Nacelle mass [Tons]	446	1098
Tower mass [Tons]	628.4	1600-1780
Tower Top mass, RNA [Tons]	676.7	1730
Water depth (mean sea level - m.s.l.) [m]	50	50
Access Platform a.m.s.l. [m]	25	25
Jacket Mass [Tons]	1210	1670
Transition piece mass [Tons]	330	450



3.2 NEW PLATFORMS

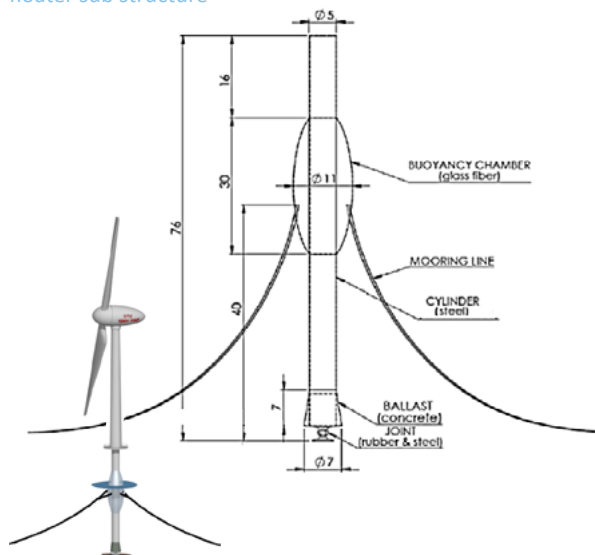
Two platforms are discussed in this section. The first includes two-bladed designs, upwind and downwind, combined with a soft semi-floater in order to circumvent 2P-4P excitation consequences. The second platform addresses three-bladed upwind designs which, further to the innovations introduced earlier, explore possibilities for weight and cost reduction offered by non-conventional direct drive generators, superconducting and magnetic pseudo-direct drive (PDD), for bottom-fixed and floating designs.

3.2.1 TWO-BLADED UPWIND/ DOWNWIND ROTORS WITH SEMI-FLOATER

For two-bladed rotors, it is very important that there is no excitation of the support structure from 2P and 4P harmonics. Given that the 10 MW wind turbine has a rated RPM close to 9.6, the 2P frequency region is from 0.2 Hz. To 0.32 Hz, which band will result in resonant excitations for the jacket designs shown in Table 3.2 and Table 3.3. To avoid such excitation, a support structure with drastically reduced eigen-frequency is needed without moving to a floating solution since the water depth is still 50 m.

FIGURE 3.1

A two-bladed upwind 10 MW turbine placed on a semi-floater sub structure



The semi-floater concept provides such a viable solution for a 2-bladed rotor. It is a combination of the classic monopile substructure and the traditional spar-buoy floater. It is illustrated in Figure 3.1, where the concept consists of three main constituents: an articulated joint at the soil bed, the mooring system, and the floating system. The floating system is made of a buoyant chamber and the main cylindrical substructure. The buoyant chamber was developed as an ellipsoid of 30.0 m height and 11.0 m diameter cast out of glass fibre. The buoyant force for platform stability is provided by the buoyant chamber placed near sea level and from the buoyant force generated by the cylinder. Concrete ballast is attached to the base of the cylinder to lower its centre of gravity and the

weight of the ballast is calibrated to ensure that the net steady vertical force is in equilibrium.

The substructure is connected to the sea-bed using an articulated (or universal) joint embedded into a reinforced concrete base. The reinforced concrete base is a short cylinder whose upper face has a hemispherical cavity. The reinforced concrete base works like a gravity based foundation providing fixity to the platform. The other contact points to the soil are the mooring lines anchorages. The catenary mooring lines are connected to the sub structure with delta connections, which have their fairleads attached to the buoyant chamber. The delta connection aims at providing torsion resistant effect to counter the turbine yaw motions.

TABLE 3.5

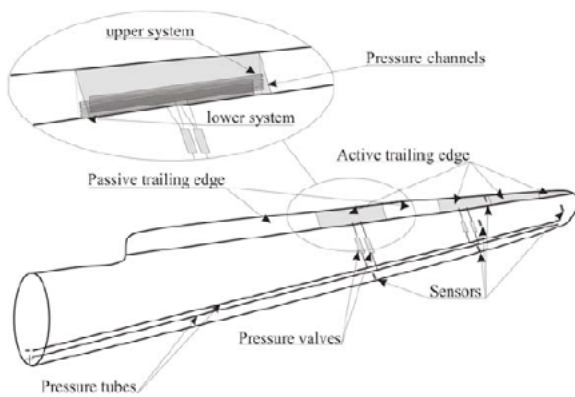
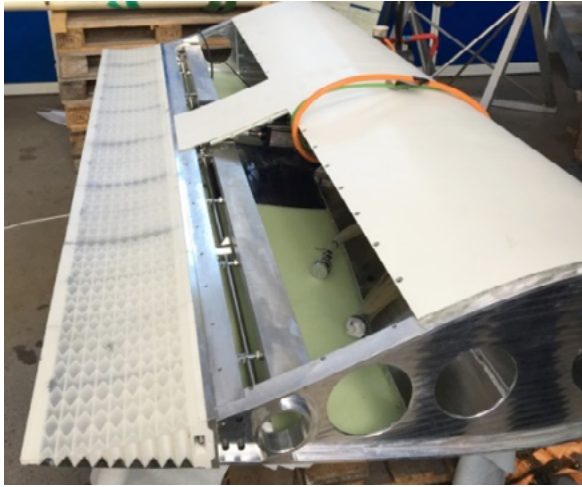
System level frequencies of the 2-bladed rotor on a semi-floater

MODE	NATURAL FREQUENCY [HZ]	LOGARITHMIC DAMPING [%]
1st Tower side-side mode	0.0679	12.713
1st Tower fore-aft mode	0.0680	12.734
1st Tower yaw mode	0.1516	0.0544

3.2.2 THREE-BLADED UPWIND ROTORS WITH NON-CONVENTIONAL DIRECT DRIVE, BOTTOM-FIXED OR FLOATING

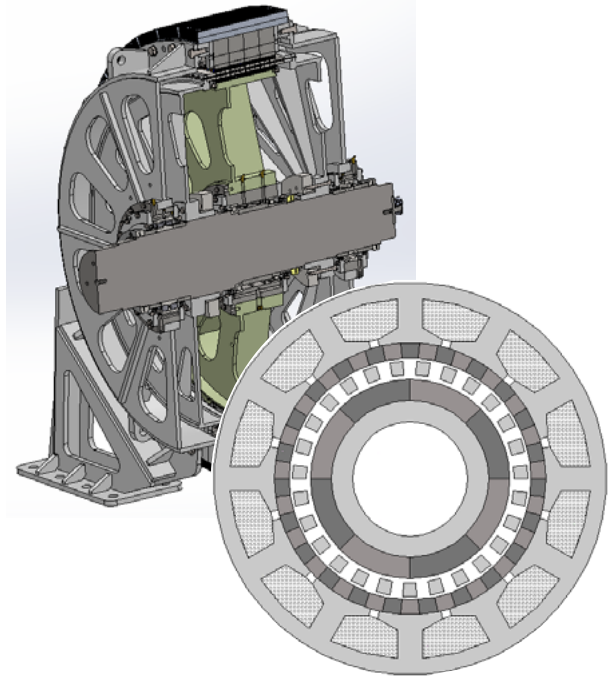
Further to the evolutionary innovations introduced earlier, we here exploit possibilities for further loads reduction by deploying distributed flaps along the blades span. The optimal position and size, the integration in the blade structure, the activation techniques and the distributed control of such flaps are researched in the project. We also seek combination with advanced feedforward control concepts, fed by wind data from LiDAR or spinner anemometer.

FIGURE 3.2
Deploying flaps along the blade span



Magnetic and superconducting drives are researched, along with dedicated power electronics that allow full range power conversion and their integration into the nacelle design. The magnetic pseudo direct-drive (PDD) generator is realizing the possibility of applying magnetic gears in wind turbines. In a PDD generator, the magnetic gear and the electrical generator are mechanically as well as magnetically integrated. Prototypes of PDD machines with a continuous torque output of 4 kNm to ~16 kNm have been designed, manufactured and tested. A 200kNm wind turbine generator is currently being manufactured and will be tested in Q1 2018.

FIGURE 3.3
The PDD concept and 0.5 MW PDD generator.



Superconducting coils in wind generators is a promising technology, because the high magnetic flux and current densities compared to conventional generators enable a considerable reduction of the generator weight and volume at large power levels which might be of particular importance for floating turbines. Additionally superconducting direct drive generators will have no or a 100 times smaller dependence on Rare Earth element metals compared to permanent magnet direct drive generators. In INNWIND.EU the use of different superconducting materials, with main focus on MgB_2 and $\text{YBa}_2\text{Cu}_3\text{O}_7$, along with their cryogenic cooling systems, has been considered and tested.

FIGURE 3.4
Integrating non-conventional direct drives in the nacelle through the king-pin concept

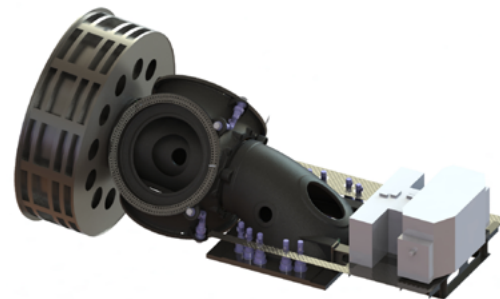
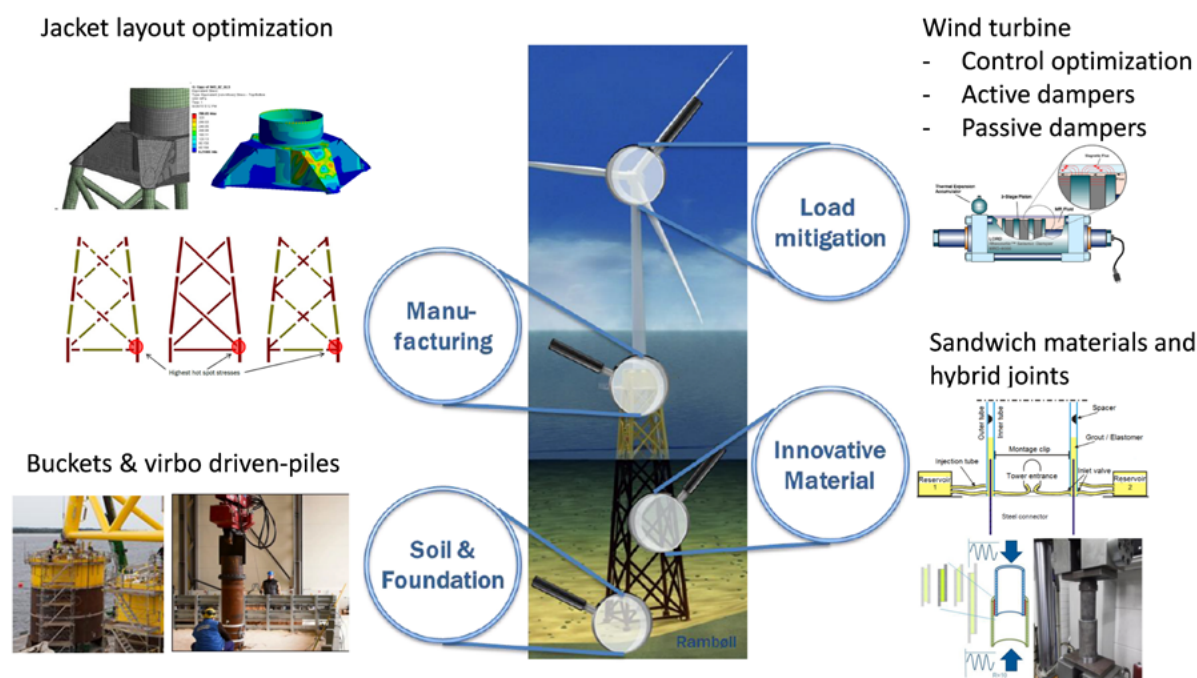


FIGURE 3.5

Overview of components' innovation in jacket design



3.2.3 SUPPORT STRUCTURES

Different innovations at the components level for the advanced jacket sub structure have been developed and tested under laboratory conditions in the project. A schematic of the different innovations is depicted in Figure 3.5. Adhesive joints were tested as an alternative for welded connections in jacket members and further developments needed to develop this technology have been proposed. Sandwich tubes for jackets were also tested to determine the performance of composite materials in jackets. These are rod-like structural components consisting of three components: two relatively thin steel tubes and a core made of ultra-high performance concrete (UHPC).

Different types of damping mechanisms on jacket members have been proposed for 20 MW wind turbines. This includes a torsional damper to dissipate the first torsional mode of the tower to alleviate jacket member loads from this component. Another innovative proposal is the use of Magneto Rheological (MR) dampers inside the braces of the jackets to significantly increase their damping and local stiffness to reduce fatigue damage. Such concepts are today at a TRL level 2 or 3 and need further studies to

implement practically, but are very essential to design a 20 MW jacket cost-effectively. A concept at a much higher TRL level is suction buckets for jacket piles. These are near commercialization today and have the potential to reduce installation time and reduce the need for long piles.

Optimization of the jacket with respect to its manufacturing needs to consider all four main manufacturing cost contributors – namely material, welding, coating and assembly costs have been made to quantify the impact of manufacturing, transportation and installation costs. Further soil tests to determine the effectiveness of vibro-driving of jacket piles were made with promising results that indicate the potential of this type of installation for 10 MW jackets.

The construction of a fully floating platform for 10 MW wind turbines is proposed as a hybrid concept between a semi-submersible floater and a spar, aiming to take advantage from both concepts to increase stability. The design is called “Triple Spar.” The three concrete columns are connected by a steel tripod which supports the tower of the 10 MW INNWIND.EU reference wind turbine, as shown in Figure 3.6. The use of concrete allows for a decrease in the platform cost in comparison with conventional steel substructures.

FIGURE 3.6
Reference 10 MW floater



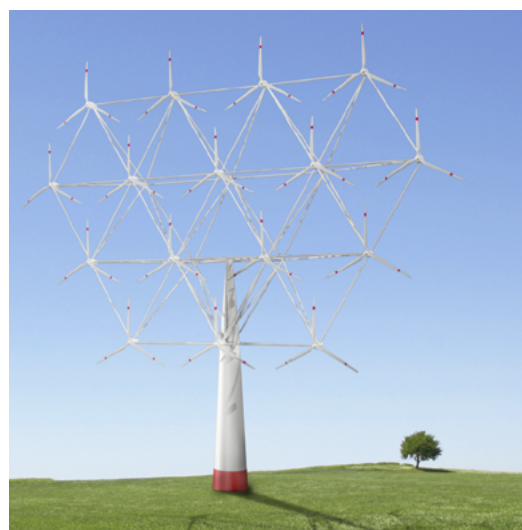
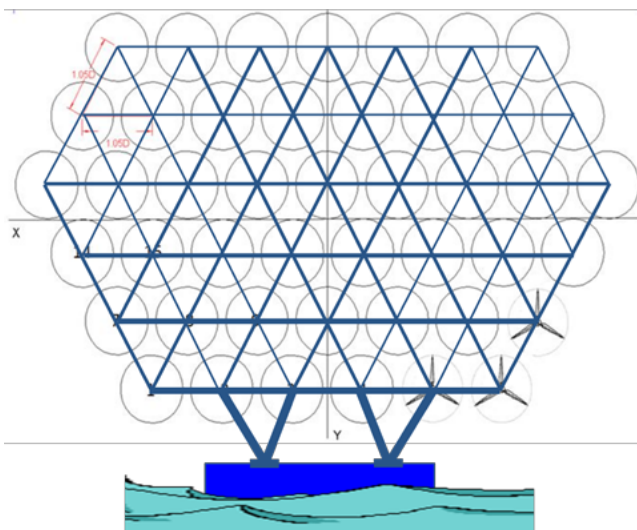
3.3 REVOLUTIONARY PLATFORMS

Two revolutionary platforms have been researched: a 20 MW multirotor floating system and a 10 MW Vertical Axis Wind Turbine (VAWT) floating turbine.

3.3.1 20 MW MULTIROTOR SYSTEM

Multirotor technology has a long history and the multirotor concept persists in a variety of modern innovative systems. However, the concept had generally fallen out of consideration in mainstream design due to a perception that it is complex and unnecessary, given the technical feasibility of very large single wind turbine units. The multirotor concept of having many rotors on a single support structure avoids the upscaling disadvantages of the unit turbine and facilitates the benefits of large unit capacity (potentially much larger than will be economically feasible for the single turbine) at a single location. This design uses 45 horizontal axis rotors, each rated at 444 kW, in a planar arrangement supported by an interlocking space frame. An optimisation of the supporting structure for minimum weight was performed, leading to a solution using standardised tubular steel sections with an overall weight of ~ 3750 t.

FIGURE 3.7
20 MW floating MRS concept comprising 45/444 kW wind turbines



Interestingly, during April 2016 VESTAS announced the erection, testing and validation of a 900 kW MRS concept turbine (4/225 kW) which has been installed at the RISØE DTU Wind Campus.

3.3.2 10 MW FLOATING VAWT

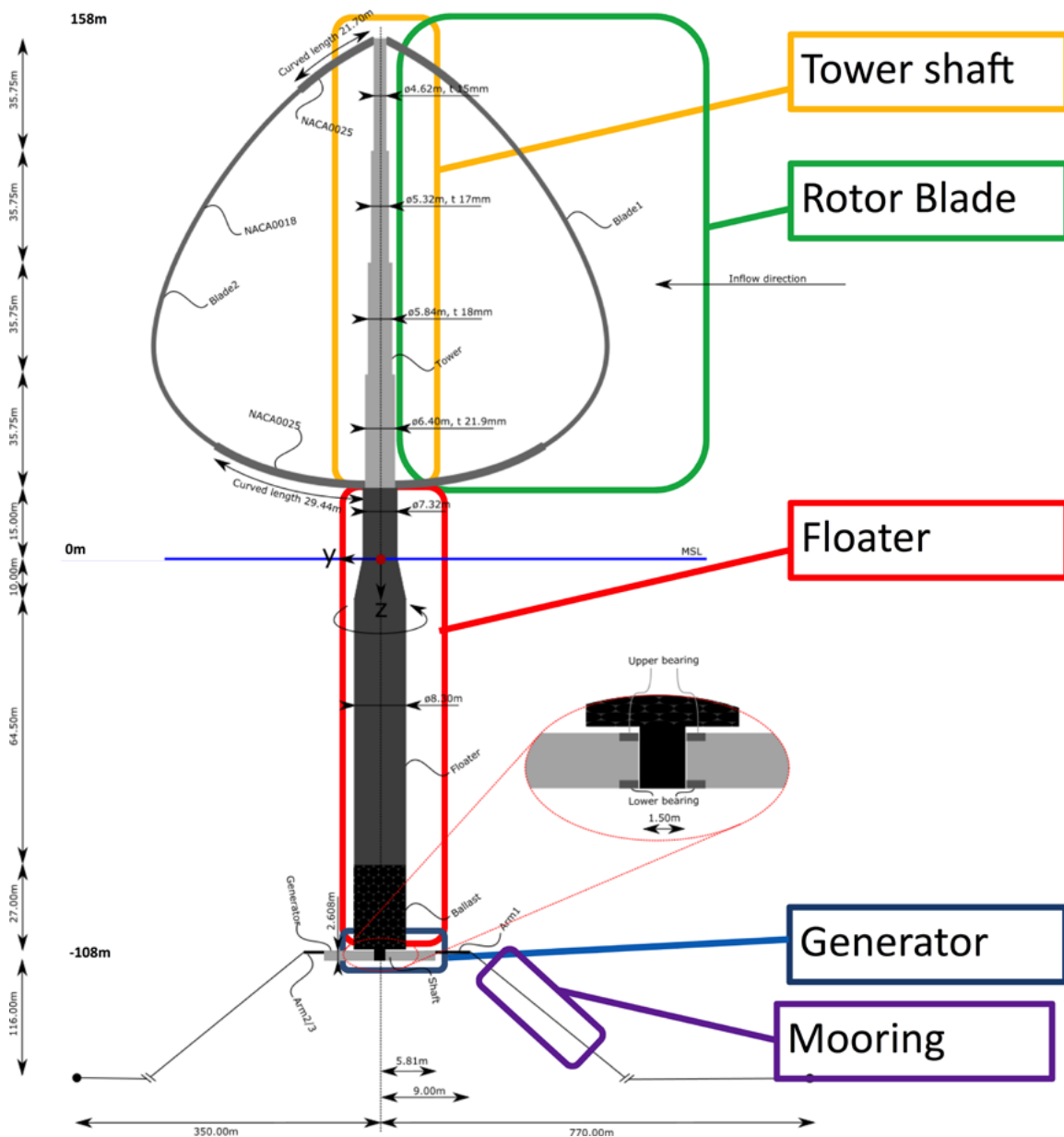
The main advantage of a floating VAWT is the lower position of the centre of gravity (estimated ~20% compared to a similar HAWT) which in the case of a floating system

may have implications on the design and cost of the support structure.

This 10 MW floating VAWT is an upscale of the DeepWind 5 MW and incorporates certain design modifications for improved structural strength. A schematic overview of the system is given in Figure 3.8. The rotor is a 2-bladed Darrieus type, while the floater is a typical spar buoy which houses the generator at its lower end and is equipped with catenary mooring lines.

FIGURE 3.8

Schematic overview of the 10 MW VAWT conceptual design



4.

INNOVATIONS NEEDED AT COMPONENT LEVEL

This section details the research performed at the main component level (rotor, drive train and offshore substructure). For each component, the state-of-the-art technology is presented first, followed by the innovative concepts researched in the project. Main scientific results and technological accomplishments are presented and discussed along with the lessons learnt.

4.1 BLADES

The research objectives concerning blades have been to define, assess and demonstrate innovative concepts for achieving lightweight and optimised rotor characteristics for very large offshore turbines. This has been done by using the new aerodynamic and structural design opportunities allowed by high rotational speeds and advanced load control obtained through a combination of adaptive characteristics from passive built-in geometrical and structural couplings between deformations and active control. This chapter describes some of the necessary initial modifications and validations of the design tools to cope with the extended operational regime and innovative concepts, a detailed evaluation and demonstration of the different aerodynamic, structural and smart control innovations and, finally, the main achievements from a more integrated blade design process applying these innovations.

4.1.1 STATE OF THE ART IN BLADE DESIGN FOR LARGE OFFSHORE TURBINES

Blade design has a long history, and has traditionally consisted of three more or less sequential processes: selecting an airfoil series, lay-out of the blade planform and design of the blade shell and internal structure to carry the loads. Design and optimization tools have been developed and applied for all three phases, and gradually with some interaction on a rather crude level, mainly with constraints concerning, for example, structural characteristics within the aerodynamic design.

A significant advancement beyond state-of-the-art during the INNWIND.EU project has been the full integration of the aerodynamic and structural design process under a common numerical optimization framework that handles all the describing parameters including some new properties such as material bend twist coupling, sweep and spar cap offset. This means that the number of parameters handled simultaneously in the design process (and thus the complexity) has much increased, along with the opportunities for designing aeroelastically tailored blades with advanced characteristics. This constitutes a major achievement of the project.

A further integration of the airfoil design process into the optimization framework offers additional opportunities which are a logical follow up on the INNWIND.EU project.

4.1.2 VALIDATION OF THE DESIGN TOOLS USED IN THE PROJECT AGAINST EXPERIMENTAL DATA / BENCHMARK

The design tools for application to the design of typical wind turbines had, to a large extent, already been validated at the time of initiation of the project. However, for very large and flexible turbines running at high tip speeds and for exploring innovative concepts, an extended validation was needed. The issues that were associated with major uncertainty are the focus of this section.

4.1.2.1 VALIDATION OF AEROELASTIC TOOLS

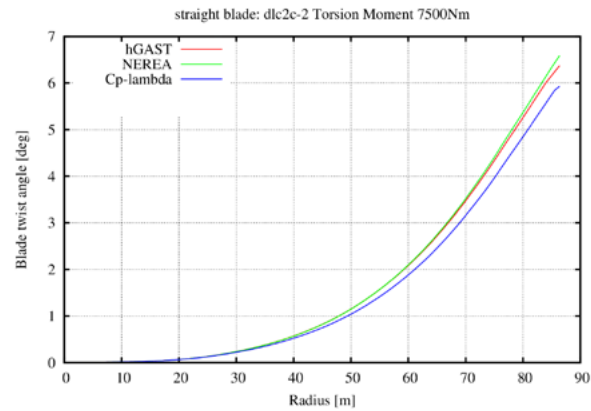
In the beginning of the INNWIND.EU project, a thorough validation of the applied aeroelastic design tools was performed with particular focus on the blade torsion. With the aim of being able to fully explore and use the potentials of the aeroelastic tailoring of blades, the torsional characteristics and coupling to deformations is of paramount importance. The numerical tools participating in the benchmark can be found in Table 4.1. With respect to mode results, all aeroelastic tools are found to compare well to 3D FEM (Finite Element Method) up to the seventh mode. The validation required a number of iterations; however, sufficient consistency between the tools was obtained to justify their application in a concerted search for innovative rotor and turbine solutions Figure 4.1.

TABLE 4.1
Different codes used by partners in benchmark comparison

CODE NAME	PARTNER	CODE TYPE
Cp-Lambda	PoliMi	Multibody
HAWC2	DTU	Multibody
hGAST	NTUA	Multibody
NEREA (GT)	GAMESA	Generalized Timoshenko
NEREA (modal)	GAMESA	Modal (Craig-Bampton)

FIGURE 4.1

Twist distribution along RWT blade length under torsion moment $M_y=7500\text{Nm/m}$ according to different codes.



4.1.2.2 VALIDATION OF REYNOLDS NUMBER EFFECTS

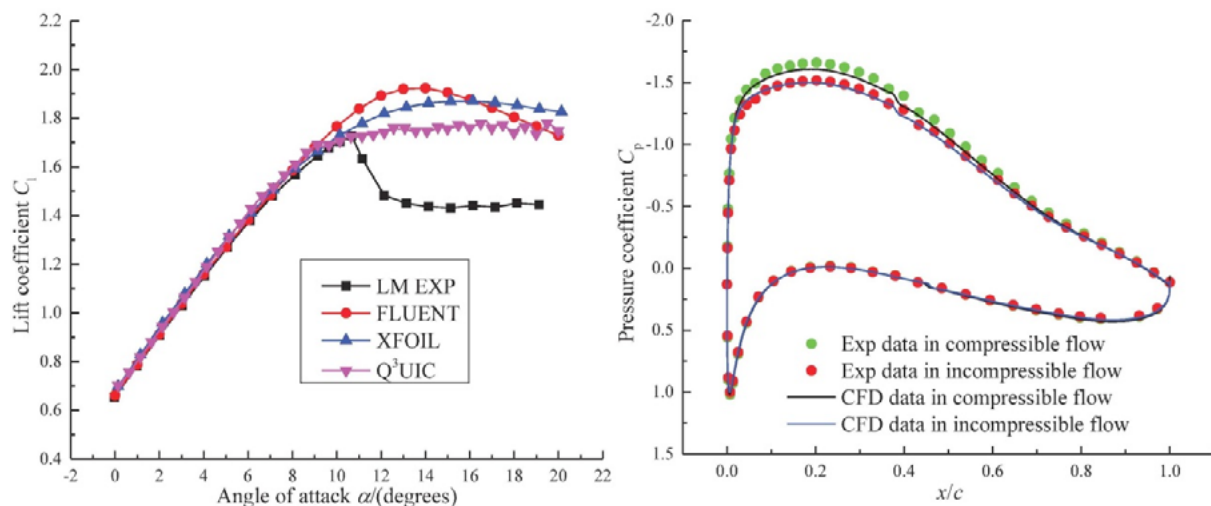
For the further upscaling of rotors, uncertainties at the beginning of the project were related to the airfoil and blade aerodynamic characteristics at large Reynolds Numbers. This challenge was solved in cooperation with the AVATAR project, concluding that while airfoil performance improves with increased size (Reynolds number) until a certain size, it levels out or even decreases between 10 and 20 MW, at least for the airfoil investigated. This effect can now be predicted with confidence and be taken into account in the design process.

4.1.2.3 VALIDATION OF COMPRESSIBILITY EFFECTS

To check the prediction capability on compressibility effects, tunnel tests for a low noise 18% thickness airfoil (DTU-LN218), performed at the LM wind tunnel, were used. In this experiment the highest Reynolds number appearing at an inflow speed of 105 m/s is about 6 million corresponding to a Mach number of 0.3. Due to the effect of wall interference and compressibility, the data obtained in wind tunnel flows was corrected into data in free-air with the consideration of compressibility. For the purpose of prediction on the aerodynamic characteristics of wind turbine airfoils including the influence of compressibility, the following were used: the commercial CFD software FLUENT, which solves both the incompressible and compressible Navier-Stokes equations; the viscous-in-

FIGURE 4.2

(a) Lift coefficients for compressible flows past a clean DTU-LN218 airfoil at a Mach number of 0.3 and a Reynolds number of 6×10^6 ; (b) Comparison between the compressible and incompressible surface pressure coefficient at a Mach number of 0.3 and a Reynolds number of 6×10^6 .



viscid interaction codes XFOIL and Q3UIC, which basically solve the incompressible equations and get compressible effects by correcting the incompressible data into compressible one by using the Karman-Tsien rule. Flows past a clean DTU-LN218 airfoil at Reynolds numbers of 4 and 6 million, which correspond to Mach numbers of 0.2 and 0.3, are considered. From Figure 4.2a it's found that FLUENT, XFOIL and Q3UIC codes can predict quite well the airfoil characteristics for compressible and incompressible flows. The compressibility effects are small at a Mach number of 0.2, while the effects become more important at a Mach number of 0.3. The compressible lift coefficient in the linear region is about 5% larger than the incompressible one at a Mach number of 0.3. Looking closer at the pressure distribution around the airfoil, the minimum pressure coefficient on the suction side is more negative than the incompressible one, in Figure 4.2b, which results in the increase of lift.

4.1.2.4 VALIDATION OF AERODYNAMIC MODEL FOR ACTIVE FLAPS

An investigation of the impact of trailing edge flaps on the flexible blade was performed by means of a CFD-based fluid structure coupling. The objective was to judge the impact of the change of the moment coefficient, which is connected to the flap deflection and causes additional

blade torsion. The resulting additional twist reduces the flap efficiency as it decreases the local AoA in comparison to stiff blade structure.

In order to investigate this objective, the CFD-code FLOWer is coupled to the commercial Multi-Body simulation tool SIMPACK. Initially, simulations of the rotor without flap were performed and compared to the BEM code HAWC2. Apart from the in-plane deflection a very good agreement was found. As the important parameters with respect to trailing edge flaps are the out-of-plane deflection and twist, an application of trailing edge flaps is, however, justified. Two extensions along the blade span (10 and 20%) and positive and negative deflection angles were investigated at a flap centered at 75% radius.

The impact of a flap deflection on the blade torsion is present in both sectional and integral loads. For the flexible blade, a flap deflection causes torsion of the blade, resulting in only 80% impact on turbine thrust and out-of-plane root bending moment, compared to a stiff blade. With regard to the sectional load distribution, a very good agreement to HAWC2 including the near wake model is observed, as with previous studies of the stiff rotor. Without near wake model, the effect of the flap is locally overestimated, as also illustrated in Figure 4.3.

FIGURE 4.3

Flapwise and edgewise load distribution and deflection for a positive trailing edge flap deflection.

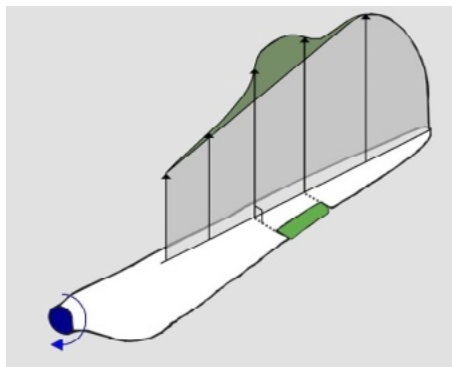
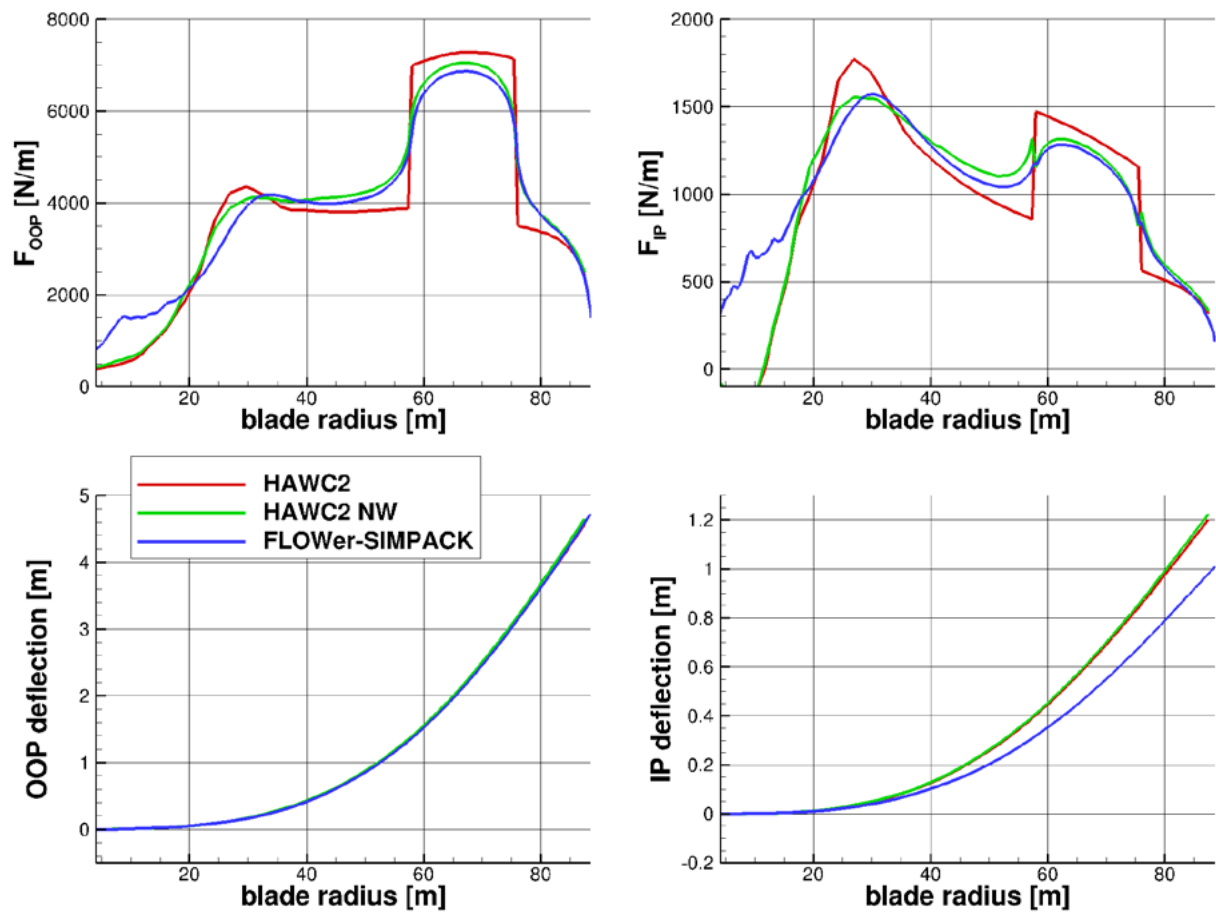


TABLE 4.2

Numerical tools used by partners for structural analysis

RESULTS FOR	CRES	CENER	DTU	POLIMI	UPAT	WMC
Global blade properties	3D FEM	2D FEM	4D FEM	3D FEM	3D FEM	FOCUS6
Natural frequencies	3D FEM	2D FEM	4D FEM	3D FEM	3D FEM	FOCUS6
Buckling analysis	3D FEM		4D FEM	3D FEM	3D FEM	3D FEM + FOCUS6
Section properties	THIN	BASSF		ANBA	PROBUST	FOCUS6
Displacements	3D FEM	2D FEM	4D FEM	3D FEM	3D FEM	FOCUS6
Strength analysis	3D FEM + THIN	BASSF	4D FEM	3D FEM	3D FEM + PROBUST	FOCUS6
Strains	3D FEM	BASSF	4D FEM	3D FEM	3D FEM	FOCUS6
Stresses	3D FEM + THIN	BASSF	4D FEM	3D FEM	3D FEM	FOCUS6

4.1.3 VALIDATION OF STRUCTURAL DESIGN TOOLS

During the INNWIND.EU project, a benchmark was conducted to account for the efficiency of structural modelling and analysis tools used by the participants. The benchmark was based on the reference wind turbine (DTU 10 MW) and its reference blade. Within this exercise, results on blade model data were provided, as well as results of modal, strength and elastic stability analyses under extreme loading. The results provided by each participant in the benchmark were estimated using different numerical tools, as shown in Table 4.2.

In general, the data provided by the partners are in good agreement. Especially regarding the global blade properties, i.e. mass, centre of gravity, natural frequencies and displacement results are quite close, irrespective of the differences in the modelling assumptions and the analysis methods used. Results regarding the strength of the blade, namely the strength against buckling and against extreme loading, are more dispersed. A close look at the stresses and strains estimated along the blade on specific lamination sequences on the sections also indicate differences.

4.1.4 INNOVATIVE CONCEPTS RESEARCHED REGARDING AERODYNAMIC DESIGN

4.1.4.1 LOW INDUCTION ROTORS

10 and 20 MW Low Induction Rotors have been designed and their performance and loading have been assessed against the reference wind turbines. Since the design procedures followed for the two turbine sizes are similar, we shall restrict this presentation to the 20 MW LIR.

Taking advantage of the higher Reynolds number at which a 20 MW turbine operates compared to a 10 MW one, new low lift 26% thick airfoils have been designed for the outer span of the 20 MW LIR blade with an aim toward increasing its structural performance without compromising power production. The assessment of the aerodynamic performance of the designed airfoils using high fidelity CFD-based tools demonstrated that such a 26% thick airfoil operating on a 20 MW rotor can indeed have similar performance with a 24% thick airfoil operating on a 10 MW rotor.

Using the CFD polars of the 26% airfoil the planform of a 20 MW LIR Rotor was redesigned. The LIR was optimized for increased annual energy capture constraining its blade root (mean) flap-bending loads. The optimization also resulted in a new rotational speed schedule, respecting the variable speed range of the 20 MW RWT.

The power performance of the 20 MW LIR versus the 20 MW RWT was then assessed using higher fidelity tools. Both CFD-RANS with free transition and a free-wake vortex method was used for this. Comparing LIR against the 20 MW RWT rotor we note that LIR blades are 13% longer and 7.6% heavier than the RWT. LIR increase the individual turbine capacity factor by 7.5% and the wind farm capacity factor by 9.8%. Overall, the anticipated reduction in LCoE in comparison to the 20 MW RWT is about 4%.

4.1.4.2 TWO-BLADED ROTORS

The two-bladed, downwind rotor concept has been explored from the beginning of the INNWIND.EU project because several studies in the past have shown that the concept might be competitive compared with the three-bladed rotor. Low frequency noise (LFN) from the downwind rotor due to the blade passage of the tower wake is known to be a major problem for such turbines. However for the off-shore application considered here it is not expected that LFN should cause problems.

A baseline 10 MW two-bladed RWT version derived by simple scaling rules from the three-bladed INNWIND.EU RWT was presented at an early stage in the project. The major influence on the cost is the saving of one blade and thus a decreased tower top mass. However, a major problem was considerably increased tower loading caused by the interaction of the 2p rotor frequency with the frequency of the 1st tower mode of vibration.

One innovative solution for offshore application is the use of the semi-floater supporting concept, as the 1st tower frequency for that design is much lower than a bottom-fixed structure with the tower on top of this.

In another design and optimization study of the two-bladed rotor, the inclusion of design parameters enabling passive load alleviation by a strong bend twist coupling (BTC) showed very promising results. The BTC is achieved by a

different chordwise position of the spar caps on the suction and pressure side of the blade and by a forward movement of the elastic axis. All these characteristics originate from the numerical optimization and were not pre-determined. The most promising design is a blade with an 8% increase in blade length, a more slender planform and a reduction of about 8% in blade weight from 37.8 to 33.7 tons when compared with the two-bladed RWT. The AEP increases with 8% and the loads are within the envelope of the baseline. The tower clearance is kept within the limit by 2.5 degrees pre-cone. In another design, the blade was stretched by 12% with an 11.9% increase in AEP. With a pre-cone of 4.5 degrees, the tower clearance was kept within the limit. In this case, some of the loads exceeded the envelope. However, it might be that advanced control with IPC or flaps could bring the loads back within the envelope.

As concluding findings for the 2B rotor investigations, it can be stated that such a rotor has to be mounted on a flexible tower like the semi-floater design mentioned above in order to avoid the 2p excitation problem.

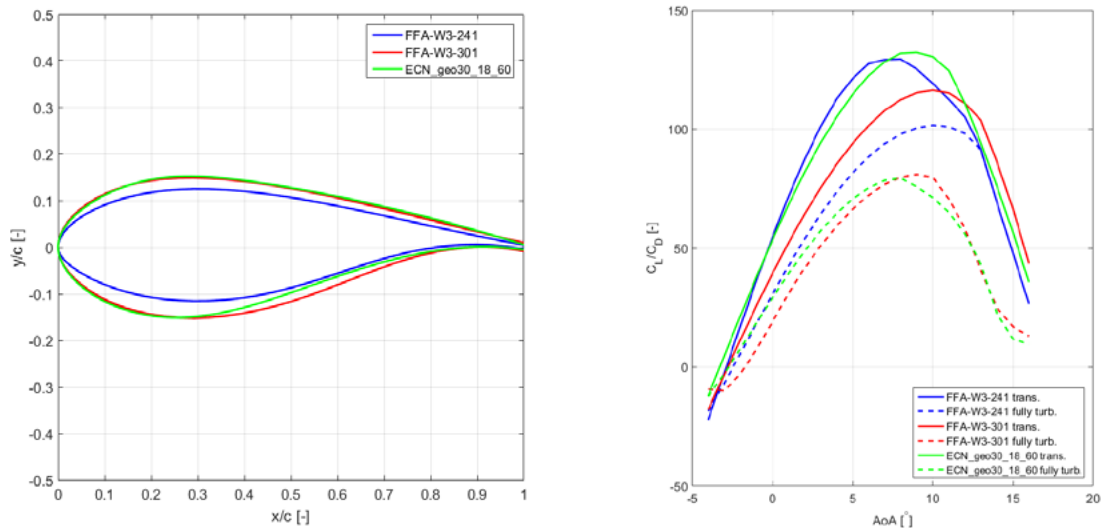
4.1.4.3 NEW AIRFOILS

The rotor concept studies of INNWIND.EU showed the need for dedicated airfoil designs to realize the full potential of the new rotor designs. One of the overall tendencies in the new rotor designs is the use of more slender and longer blades. Slender blades can be achieved by using thicker airfoils which means that the chord can be decreased for the same load on the blade.

One study has focused on the design of a 30% thick airfoil for outboard application on a blade where a 24% airfoil is used on the 10 MW RWT. The new airfoil contour is shown to the left in Figure 4.4 together with the two FFA airfoils that it will replace. To the right in the same figure it can be seen that the new 30% airfoil has a lift-to-drag ratio that is almost the same as for the 24% airfoil it will replace. However, the detailed analysis of the airfoil characteristics has shown that the large roughness sensitivity of the new airfoil results in a larger penalty in terms of power coefficient decrease than with the FFA 24% airfoil.

FIGURE 4.4

The new 30% airfoil design in comparison with the two FFA airfoils (Left) and the lift-to-drag ratio for turbulent and transitional flow (Right)

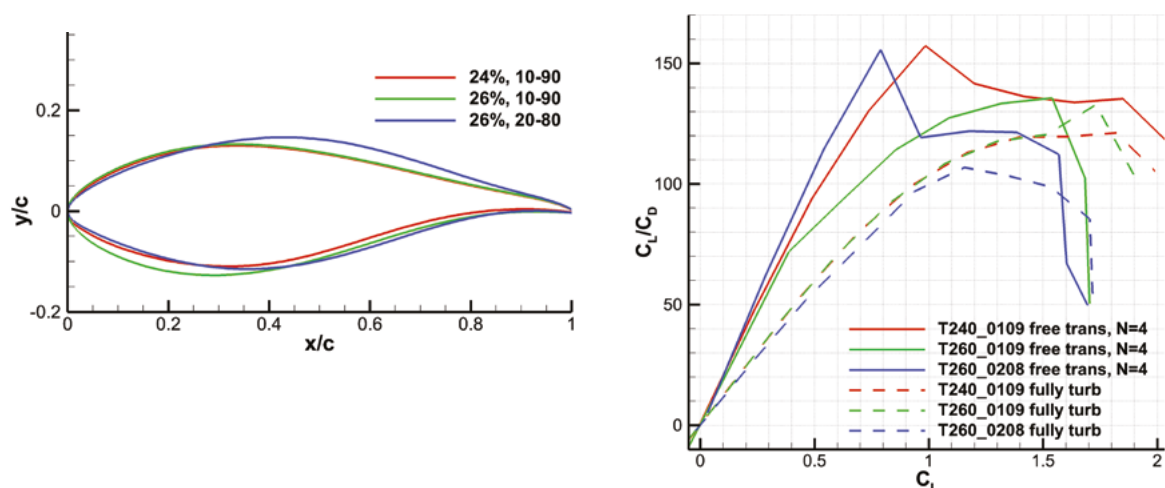


LIR rotor designs, in particular, require dedicated airfoil designs as the low loading giving the low induction is achieved by operation at a low design lift, typically around 0.8. A complete airfoil family with a low lift 24% airfoil for the outboard part of the blade was designed for the 10 MW LIR. For the 20 MW LIR, the increase in Reynolds

number made it possible to increase the thickness to 26% for a new low lift airfoil to be used outboard on the blade, Figure 4.5 left. The improved operational conditions at the higher Reynolds number made it possible to design the 26% airfoil so it has almost the same lift-to-drag ratio as the 24% airfoil used on the 10 MW rotor, Figure 4.5 right.

FIGURE 4.5

To the left, the new 26% (10-90) low lift airfoil for use on the outboard part of the 20 MW LIR rotor. To the right, the lift-to-drag characteristics.



4.1.5 INNOVATIVE CONCEPTS RESEARCHED IN STRUCTURAL DESIGN

4.1.5.1 PASSIVE CONTROL THROUGH BEND-TWIST-COUPLING (BTC). ALTERNATIVE WAYS OF BTC.

Ten different structural solutions were presented with the aim to achieve passive load alleviation while maintaining the power output, reduce the cost of the wind turbine components, and thereupon reduce the cost of wind energy generation. In one design the structure of the blade was optimised, running the complete design circle to achieve a solution complying with all design requirements, including fatigue, while introducing passive load reduction through the incorporation of bend-twisting coupling. The optimal solutions when changing the angle in the spar cap (SC) of 3, 4, 5, 6 and 7deg and in the skin (SK) of 5, 10 and 15deg, are presented in Figure 4.6. The same figure shows the reduction of the LCOE with respect to the RWT. A 3% mass reduction was achieved with about 1% increase in annual energy production, leading to an approximate 1% reduction of the levelised cost of energy. Nevertheless, the effect of the load reduction achieved on other wind turbine components was not taken into account, leading to conservative results regarding the gain on LCOE.

In another part of the work seven different solutions were investigated, combining the concept of bend-twist coupling, swept blade, and single shear web (reduced torsional stiffness). The combination of all three passive control strategies in the same reference blade was found effective mainly with respect to the blade root flap-wise extreme and fatigue moments. The concept of bend-twist coupled blade was investigated from different perspectives. One solution studied is based on the same concept of introducing bend-twist couplings, yet in this case, the angle of the fibre orientation for the drive of the coupling is not constant along the blade length, but rather varies with the radial position, see Figure 4.7. Optimized coupling behaviour is achieved in this way, yet at a higher manufacturing cost. By combining tow-steered fibres and a variation of the spar geometry and orientation, the new blade design produced an induced elastic twist which better approximates the optimum twist of the blade across its entire operating range. At the rated wind speed, the concept adaptive design reduced the amplitude in flapwise bending oscillations by 16% compared to the reference blade.

Finally, focus was on the development of a tool that enables accurate prediction of the blade response in the presence of bend-twist coupling terms. The incorporation of the bend-twist coupling is performed by suitably adjusting the fibre orientation of the composite material at the spar cap. Using this tool the blade is then designed to achieve load alleviation in comparison to the reference blade design.

FIGURE 4.6

LCOE reduction compared to RWT for optimal solutions (Skin Angle (SK) 5, 10 and 15deg, Spar Cap Angle (SC) 3, 4, 5, 6 and 7deg).

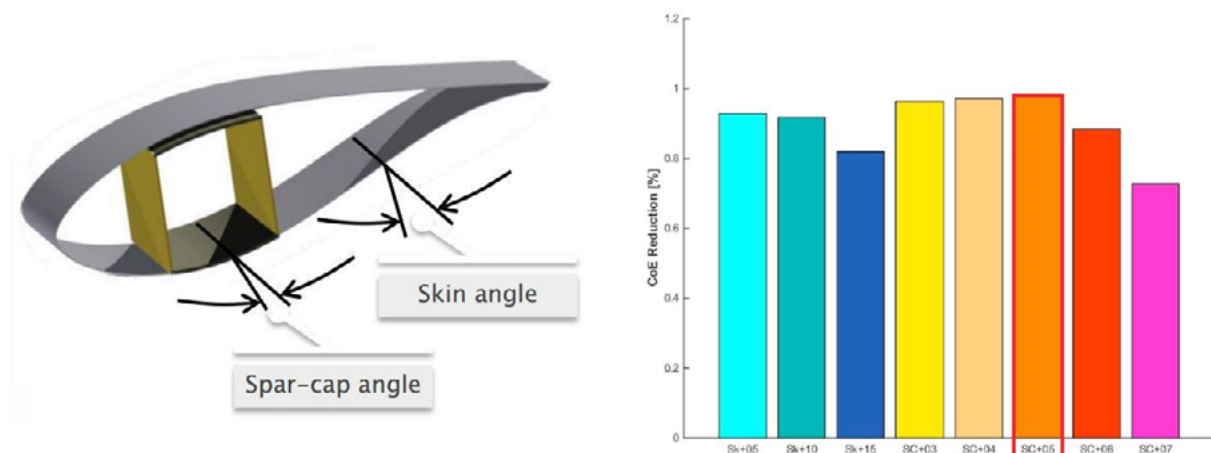
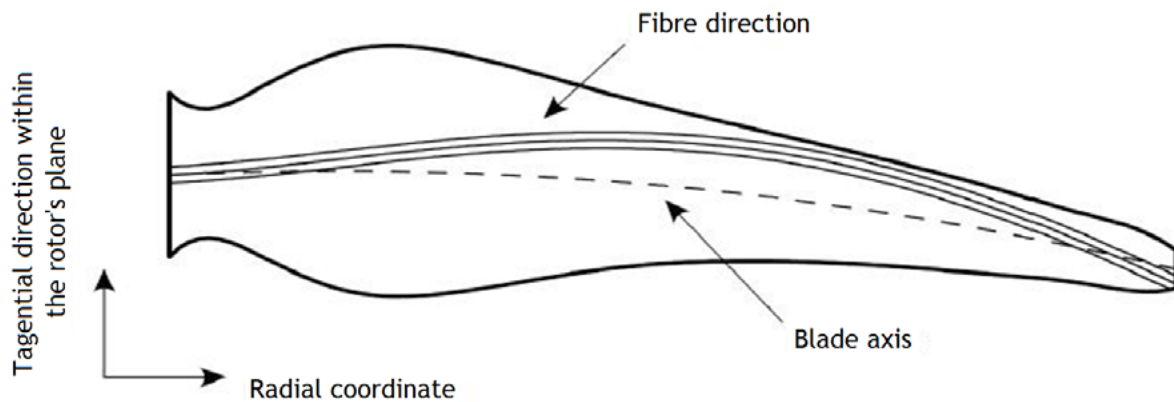


FIGURE 4.7

A schematic design of the fibre path along the curved blade planform representative of the concept used to investigate bend twist coupling.



4.1.5.2 NEW INNER STRUCTURE

In the framework of the INNWIND.EU project, a variation of innovative proposed solutions for the internal structure of the blade was examined. The objective was to assess the feasibility of the concept and validate the mass savings introduced by replacing structural parts of the blade with other manufacturing technologies. The examined solutions were:

- Internal truss structure; whereby the spar box and 3rd web of the original configuration is replaced by a truss structure made of composite materials, and reducing the mass of the blade skin, see Figure 4.8 (a);
- Grid reinforced skin; whereby the sandwich panels of the trailing edge are replaced by grid-stiffened panels, keeping the rest of the blade structure as

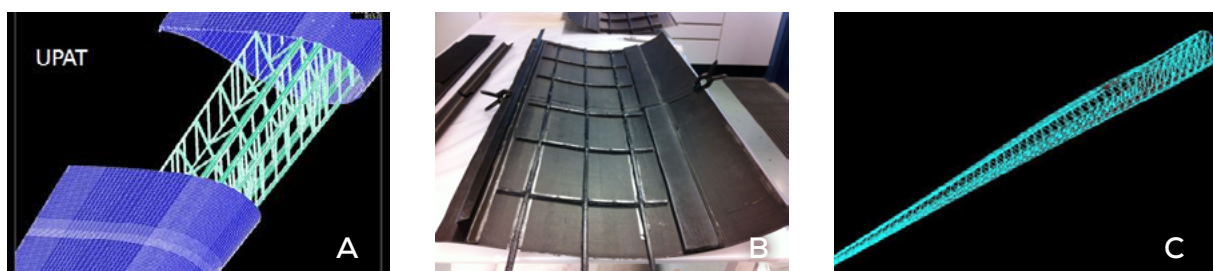
per traditional designs. A scaled prototype was manufactured and can be seen in Figure 4.8 (b);

- Rib reinforced skin; whereby the load-carrying structure of the blade is completely replaced by a truss structure having composite material members. The outer surface of the blade is no longer designed to carry the loads, but rather only to form the aerodynamic shape needed for the operation of the blade, see Figure 4.8 (c).

Results showed that a reduction to the blade mass is possible when implementing each of those innovative solutions. However not all aspects of the introduced concepts have been covered; for example, structural details such as the joints between truss members have not been considered in the design process. Further research is needed to ensure the feasibility of the proposed concepts.

FIGURE 4.8

Innovative concepts for the inner structure.



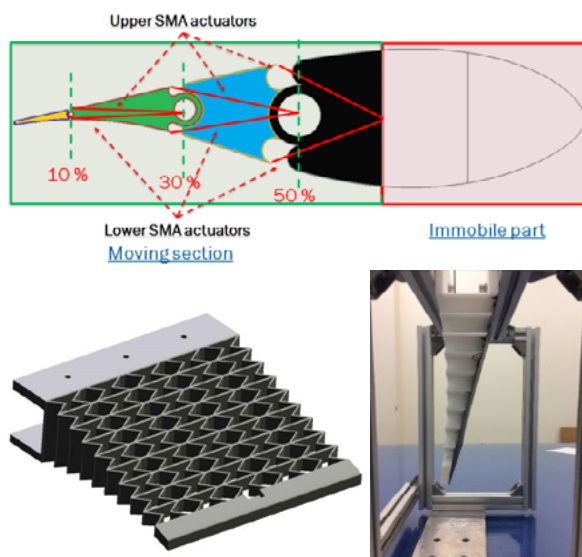
4.1.6 ACTIVE CONTROL USING FLAPS

4.1.6.1 ALTERNATIVE TECHNIQUES FOR ACTUATING FLAPS

Different rotor (re)design concepts for blade load reduction were explored in terms of advantages and limitations. Within the project there was a strong focus on the technical feasibility and readiness level of various technologies for their implementation in the field. It was concluded that active trailing edge flaps, which can modify airfoil camber in response to varying wind loads, show the highest technology-readiness level. Other concepts, namely passive trailing-edge flaps and material/geometric coupling, need further validation in the simulation and experimental environment.

FIGURE 4.9

Left, shape memory alloy actuator; right, morphing flap inner structure and flap mounted in test rig.



The advantages and limitations of shape memory actuators (see Figure 4.9, left) for the application of wind turbine blade trailing edge flaps were investigated in the project, and significant potential for blade load reduction was identified. Technical limitations include a moderately low fatigue lifetime of the material, and low bandwidth without active cooling. Trailing edge flaps, using other smart materials, have already been demonstrated in wind

tunnels on wind turbine-scaled prototypes and, in one instance, on a small-scale field turbine using large conventional actuators.

A novel morphing flap has been proposed which features structural multi-stability with scope for minimizing actuation force requirements (see Figure 4.9 right). The flap provides spanwise continuous deformed shapes and a constant morphing angle variation. Wind tunnel testing indicates that controlling geometry over the deformed shapes can enhance blade performance. Due to promising lab test results it was decided in the last part of the project to test this flap concept on a rotating test rig under operating conditions close to those on a full scale turbine. In particular, the important influence of the centrifugal loading is almost equal to full scale conditions. What is more, the Reynolds number and the turbulent inflow conditions are quite realistic. The experiment is further described below.

It is necessary to understand the fundamental behavior of trailing edge flaps and the uncertainties associated in order to be able to integrate these smart actuators with conventional aeroelastic rotor design. As a result, the current numerical tools for wind turbine analysis have been extended such that they are able to incorporate the new actuators, and furthermore are validated for prediction of turbine lifetime load cases. These engineering tools are able to model the influence of the actuators to an acceptable degree of fidelity, specifically capturing the effect of actuator variations on the load profile of the wind turbines. Furthermore, they are able to run within a reasonable amount of time such that design iterations can be carried out efficiently.

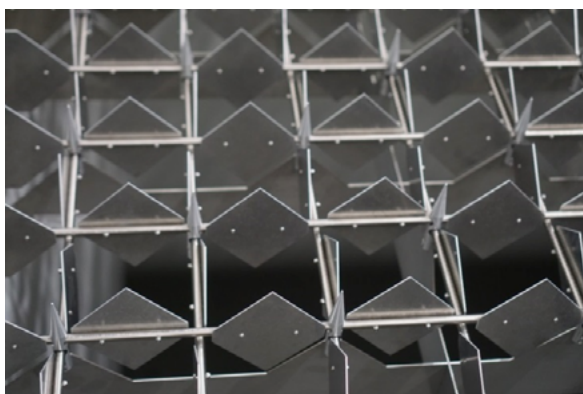
4.1.7 DEMONSTRATION IN THE WIND TUNNEL AND ON A ROTATING TEST RIG IN THE PRESENCE OF WIND TURBULENCE

A successful experimental proof of concept has been achieved for the first time of free-floating flaps for wind turbines and of combined pitch and flap control for blade load mitigation. Free-floating flaps were designed for the first time for the application of wind turbine load control. Numerical aeroelastic analysis concluded that such flaps

show significant control authority in the desired frequency band (2P and beyond). However, the additional degree of freedom couples aerodynamically with the flapwise flexible mode of the blade and causes flutter at low wind speeds, just outside the design envelope. Using a data-driven feedback controller, the blade can be stabilized in the post-flutter region. Both of these results were validated experimentally in the wind tunnel.

The experiment was conducted in the wind tunnel of the University of Oldenburg. The wind tunnel had a cross section of $3 \times 3 \text{ m}^2$ and a test section of 30 m. Wind speeds up to 30 m/s could be achieved. The inflow of the wind tunnel was modulated by an active grid which was mounted to the wind tunnel inlet. The active grid was used to generate customized turbulence for wind tunnel applications. The used active grid divided the cross section by 80 horizontal and vertical rods, resulting in a mesh width of about 0.14m. A photograph of the active grid is given in Figure 4.10 and Figure 4.11. Each of its axes was connected to a servo motor in a manner that each could be controlled individually by a real time system. Mounted on the rods are square flaps which depend on the orientation to the inflow blocking and deflecting the wind. Dynamic changes of the angle of attack of the flaps to the flow are in the following described as excitation protocol. The excitation protocol defines the dynamics of the generated turbulence.

FIGURE 4.10
Photo of the active grid with the square rods.



During the wind tunnel tests, the concept of Subspace Predictive Repetitive Control (SPRC), a dedicated data-driven control technique, was used to achieve blade load reduc-

tions. The pitch control action was composed of a superposition of 1P and 2P sinusoidal basis functions where the gains are automatically adapted to the time-varying wind conditions. It was shown that significant rejection of 1P and 2P loads in the blade load spectrum could be achieved with combined pitch and flap control. A typical result can be found in Figure 4.12.

FIGURE 4.11
Wind tunnel experiments in Oldenburg with the active grid and an scaled innovative two-bladed wind turbine

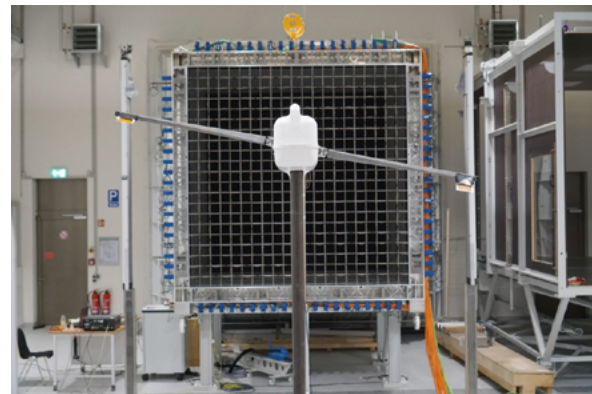
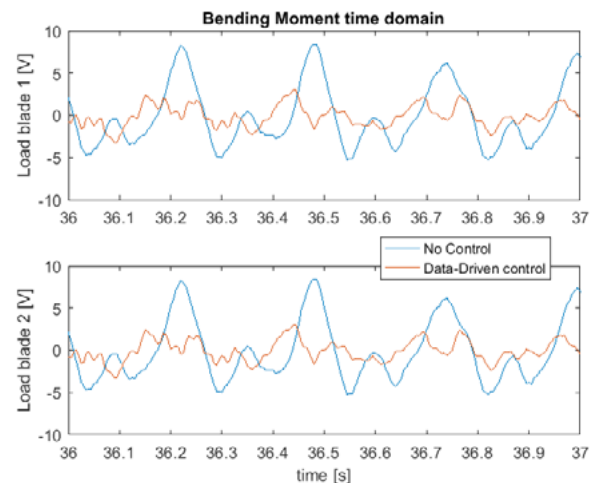


FIGURE 4.12
A typical result of the wind tunnel experiments using an advanced data-driven feedback controller that mitigates the loads. Turbulence intensity 3%



4.1.8 MANUFACTURING AND TESTING OF A MORPHING TRAILING EDGE FLAP

A morphing trailing edge (MTE) flap has been developed for the alleviation of unsteady loads within Task 2.3. It

consists of an inner, printed cell structure which allows a deflection of the flap. On the suction side, the flap is covered with a Carbon Fiber Reinforced Polyester (CFRP) skin and a pre-stressed silicone skin on the pressure side, Figure 4.13. The flap is actuated with a carbon rod attached to the trailing edge of the flap, Figure 4.14.

FIGURE 4.13

The inner structure in the morphing flap is printed. Then a Carbon Fiber Reinforced Polyester (CFRP) skin is glued onto the suction side and a pre-stressed silicone skin on the pressure side.

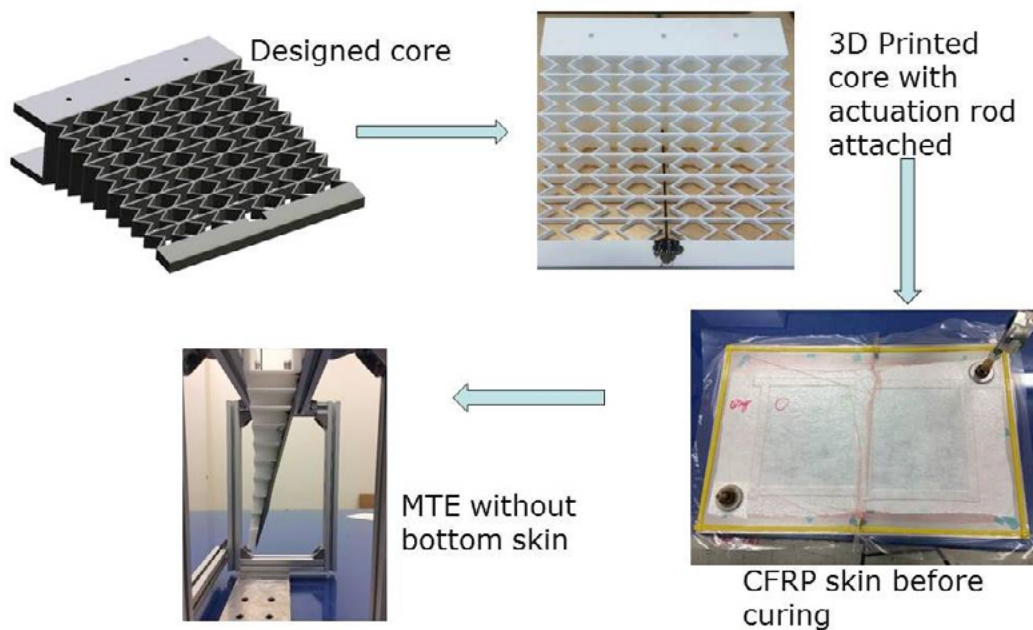
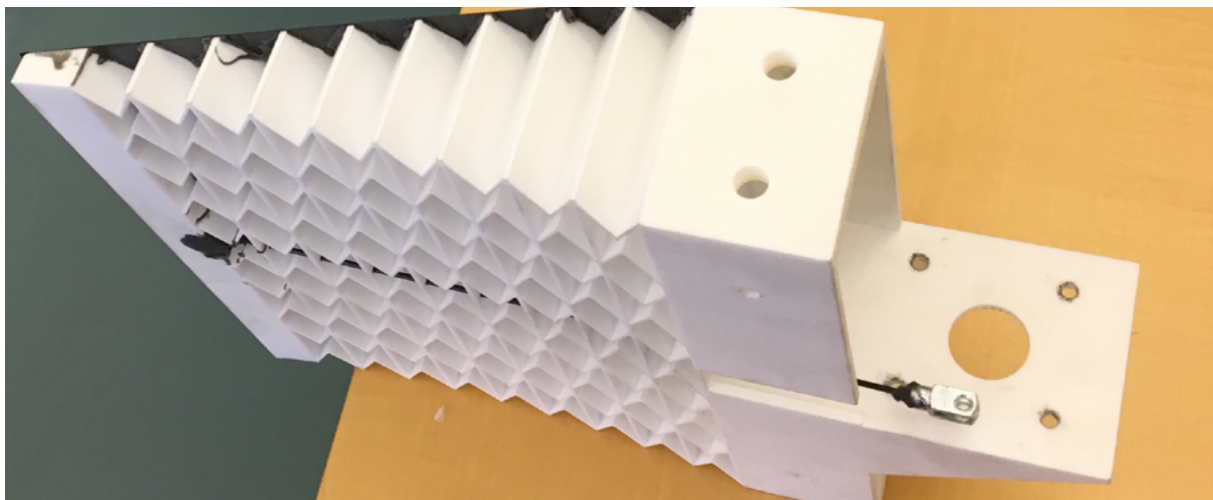


FIGURE 4.14

A flap prototype. The silicone skin on the pressure side is not glued on at this stage. The actuation rod is visible at the lower part of the flap.



The flap is tested under realistic conditions on a rotating test rig, developed previously in a National Danish project INDUFLAP in the period from 2011-2014. It is a test facility based on a 100 kW turbine platform where the rotor has been taken down and instead a 10m long boom with a 2m blade section at the end is mounted, Figure 4.15.

FIGURE 4.15
Rotating test-rig at DTU, Campus Risoe.



The flap system is integrated on a 2m blade section and then tests can be run with the boom rotating, simulating conditions close to the ones on a full scale turbine. The boom can be pitched, which means that a combined pitch and flap actuation can be performed.

A new blade section for testing the flap system on the rotating test rig has been manufactured using the 30% airfoil, developed within the INNWIND.EU project, Figure 4.16. A comprehensive instrumentation comprising about 120 pressure tabs is conducted so that the flap influence on the loading can be monitored in details. The flaps are manufactured in sections and therefore eight flaps are assembled to constitute a complete flap section for the 2m blade section, Figure 4.17.

FIGURE 4.16
A new 2m blade section has been manufactured for the INNWIND.EU flap testing on the rotating test rig.



FIGURE 4.17
The flaps are manufactured in sections of 25cm. Therefore 8 flaps are mounted side by side to constitute a complete 2m long flap section.



4.1.9 INTEGRATED BLADE DESIGN

4.1.9.1 METHODS USED

A combination of load alleviation techniques and automatic design procedures has been employed to design a new rotor for the INNWIND.EU 10 MW wind turbine. Redesign-

ing the 10 MW RWT rotor it has been shown that a combination of geometric spar offset (O-BTC), a classic fiber rotation coupling (F-BTC) and an IPC supervisor can dramatically reduce ultimate and fatigue loads in all the main components of the wind turbine. The study exploited the benefit of designing for an elongated blade, which gives 4.5% more AEP when compared against the baseline. The new rotor has been obtained after an aero-structural optimization which was used to redesign the chord and twist in order to maximize performance and reduce loads. The resulting configuration produces ultimate loads which do not exceed a range of 10% from the baseline, while some key fatigue loads (DEL) like blade flap and tower base fore-aft are even reduced. Some DEL, especially in the hub, are higher than the original, which may require a careful re-evaluation of the hub and tower components but, in our view, the advantages in terms of AEP and LCOE reduc-

tions broadly justify the findings of this study. Finally the load reduction on critical wind turbine components was validated by testing a scaled wind turbine employed with BTC blades and IPC in Polimi's wind tunnel, see Figure 4.18.

Possible continuations of this work may imply a complete redesign of the wind turbine, including rotor solidity, cone, tilt and control laws. Thorough assessment of the tower and hub loads for the new system is highly recommended.

Multidisciplinary design optimization has also been performed with the three passive control concepts – spar cap placement, material bent twist coupling and sweep in combination – resulting in designs illustrated in Figure 4.19 that has an increased AEP in the order of 4-8%. The combination with active blade control has also been investigated, and this gives further potentials.

FIGURE 4.18

(a) Partial wake tests configuration: Rigid blades wake generator in front, BTC model in downwind position, **(b) results of load reduction on critical components for various wake cases for the scaled wind turbine.**

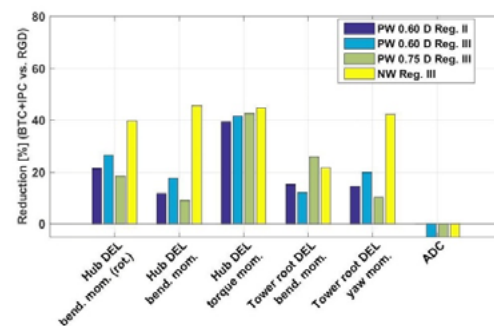
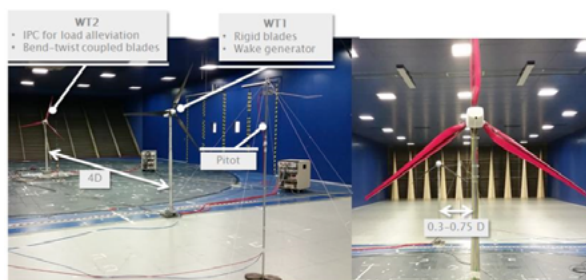
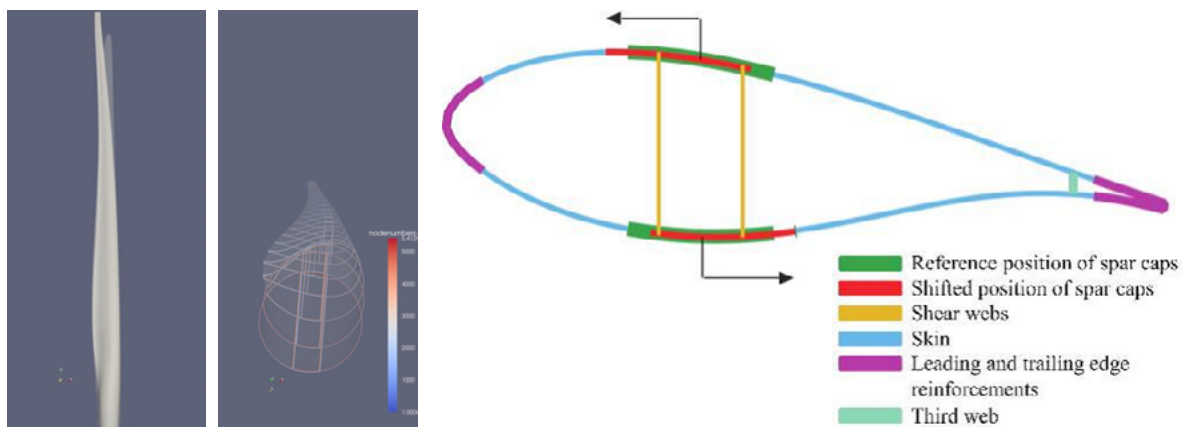


FIGURE 4.19

Optimised blade with combined passive control concepts (left), and illustration of spar cap movement to facilitate bend twist coupling (right).



4.1.10 MAIN SCIENTIFIC AND TECHNOLOGICAL ACCOMPLISHMENTS

4.1.10.1 GENERAL

An overall main accomplishment regarding rotor design is the general recognition that lightweight is not necessarily equal to optimal from a cost perspective. However, energy production is a more universal parameter in this process. This has led to the concept of low induction rotors, what are not necessarily designed for maximum efficiency, but maximum energy production with constrained loads. This again has led to the effective development concept of stretching the blades, and at the same time limiting the loads via the introduction and application of new and innovative technology. The number of parameters in the design process has thus increased considerably, and a main accomplishment here is the development and application of multidisciplinary design optimization tools to handle the combined aero-structure-control parameters simultaneously. This has led to the identification of a number of favourable innovations in new blade designs.

4.1.10.2 SCIENTIFIC ACCOMPLISHMENTS

At the beginning of the INNWIND.EU project, there were a number of scientific challenges associated with the further upscaling of rotors and the application of innovative technologies. The main challenges and uncertainties here were related to the following factors: the airfoil and blade aerodynamic characteristics at large Reynolds Numbers; the importance of the compressibility effect for increased tip speeds; the prediction of the torsional deflection of blades in aeroelastic simulations; and the unsteady aerodynamic effects of active trailing edge flaps. These challenges have been tackled in a concerted action with the AVATAR project, and represent significant scientific accomplishments within the projects.

The airfoil aerodynamic characteristics improve with increased size (Reynolds number) until a certain size, however, levels out or even decreases between 10 and 20 MW. The compressibility effect increases airfoil lift curve slope and drag at tip-speeds beyond about 100m/s. However, both effects can now be predicted with confidence

and taken into account in the design process. The same accounts for the aeroelastic prediction of blade torsional response and the effect of trailing edge flaps, to the degree that it is necessary for the investigations performed within the project to be representative for innovative large wind turbine design.

4.1.10.3 TECHNOLOGICAL ACCOMPLISHMENTS

The discovery of the concept of obtaining flap-torsion deflection coupling by proper placement of the spar-caps and shear-webs in a blade is a major accomplishment which, already during the timespan of the project, has been adopted by the industry.

The handling of the different passive control concepts (spar cap placement, material bend twist coupling and sweep) in the combined aero-structure optimization tools (leading to optimized stretched rotors with an increased AEP in the order of 4-8 % in comparison to the RWT), is a main accomplishment, one which is further supporting the trend in the industry. The combination of the passive control concepts with active trailing edge control has also been demonstrated in the project, and this revealed a further potential for AEP increase.

A 30% thick airfoil series was developed to substitute a 24% series for the outer part of the blade, which corresponds to a 56% increase in the bending moment resistance. The airfoil performance could match that of the 24% airfoil for clean conditions; however, for rough conditions the performance would be much lower. There might be a good potential for thicker airfoils for stretched rotors. However, the means to overcome sensitivity to roughness must be developed.

Innovative inner structures, such as truss structures that are more or less integrated into the skin, and grid reinforced skin, a substitute to traditional spar caps, shear webs and sandwich panels, have shown perspectives for weight reduction. In particular, they offer possibilities for advanced tailoring of deformation coupling. However, these solutions are still at a low TRL level, and have only to some extent been demonstrated in the laboratory.

The concept of active airfoil (camber line) trailing edge control has been developed and demonstrated in both

the laboratory, the controlled wind tunnel environment and in an open-air scaled experiment. The demonstrations are validated with aeroelastic simulations on MW turbines to an extent that justifies its readiness for full scale demonstration.

The change of concept to a two-bladed rotor offers further options for stretching of blades or weight reductions due to the different ratio between blade chord and radius. By further application of a teeter hinge (or individual pitch control) the rotor weight for the same radius can be reduced to nearly 50%, corresponding to a large potential for stretching of the blades within the load envelope of the three-bladed RWT. The main challenge is the turbulence excitation of the tower due to the proximity to 2P. This challenge has been solved by application of the semi-floating tower developed within WP1, which has a very low natural frequency.

4.2 ELECTROMECHANICAL CONVERSION

4.2.1 STATE OF THE ART IN DRIVE TRAIN DESIGN FOR LARGE OFFSHORE TURBINES

The goal of the INNWIND.EU drive train demonstrations was to evolve non-contact drive train technologies with as few moving parts as possible, but at the same time holding a potential to be more compact and lightweight than the permanent magnet direct drive generators used by the industry. The focus was therefore on:

- Superconducting direct drive generators, where the magnetic field is created by superconducting field coils, and
- Magnetic Pseudo-direct drive generators, where a magnetic gearbox is integrated into a ring generator.

Suitable power electronic converters to connect these generators to the grid were investigated, as well as the challenge of constructing a nacelle structure which will be able to support these drive trains at power ratings between $P = 10\text{--}20$ MW.

4.2.2 SUPERCONDUCTING GENERATORS (SC)

4.2.2.1 CONCEPT AND ALTERNATIVE SC TECHNOLOGIES

Superconductors are materials with no electrical resistance ($R = 0 \Omega$) when cooled below their critical temperature. Superconducting wires can be used to produce magnetic fields in coils without any Joule heating $P = RI^2$, where I is the current in the wire. Such coils can provide the magnetic field in a generator. The main advantage of the superconducting coils in a generator is the possibility to provide airgap magnetic flux densities considerably higher than what is possible in conventional machines. The challenge, however, is that the coils must be cooled down to temperatures in the range of -263°C to -180°C using advanced cooling machines. By mounting many superconducting coils on a large tube, one can construct a superconducting direct drive generator, which has the potential to be smaller and more lightweight than the permanent magnet direct drive technology.

Superconducting materials have been known for more than 100 years and the most mature superconducting wires, made of the niobium and titanium alloy NbTi, are used for building the main magnet coil of Magneto Resonant Imaging (MRI) scanners used at hospitals around the world. These superconductors are cheap and cost in the order of 0.5 €/m, but they have to be cooled to -269°C in order to work. This will be difficult in a wind turbine. Several other superconducting wires with higher operation temperature have been developed: the two main candidates for a superconducting wind turbine generator are the magnesium-di-boride MgB_2 and the high temperature superconductor $\text{RBa}_2\text{Cu}_3\text{O}_{6+x}$, where R can be most of the Rare Earth Element of the periodic table as well as Yttrium. They have a critical temperature T_c of -234°C and -180°C , which can simplify the cooling equipment considerably, but they are also more expensive than NbTi with unit costs in the order of 4 €/m and 20-100 €/m.

The goal of the work on superconducting generators was to determine which combination of superconductors and machine topologies would provide the lowest Levelized Cost of Energy (LCoE) for the INNWIND.EU turbines with a power rating $P = 10\text{--}20$ MW.

4.2.2.2 DESIGNS AND DEMONSTRATORS

Two independent generator designs and demonstration tracks have been carried out based on the MgB_2 superconductor and the high temperature superconductor $\text{Rb-a}_2\text{Cu}_3\text{O}_{6+x}$ (RBCO). Since the Technology Readiness Level (TRL) of superconducting direct drive wind turbine generators is still 2-3 these demonstrations are focused on constructing only a pole pair segment of a full scale direct drive generator. The first logical step is to show the superconducting field coils can be made.

The MgB_2 track was performed by Delft University of Technology (TUD) and the Technical University of Denmark (DTU) in collaboration with SINTEF energy, who constructed and tested a 0.8 m long and 0.5 m wide race track coil constituting a shorter version of a 10 MW generator pole with a length of 2 metres. Figure 4.20 shows the design

of the demonstration coil connected to a cryocooler cold-head inside a cryostat at SINTEF and the coil during the assembly. The race track coil consists of 10 double pancake coils wound from 4.5 km of wire. The race track was cooled to -253°C and the current in the coil was ramped to $I = 145$ Ampere. It was observed that 7 out of the 10 double pancake coils showed full superconductivity, whereas signs of non-superconducting sections were observed in 3 of the coils as shown in Figure 4.21.

In conclusion, it has been shown that long superconducting wires can be provided by the European wire manufactory Columbus Superconductor and that it can be wound into a race track pole coil. It is clear, however, that more work is needed to industrialize the coil manufacturing in order to increase the number of successful coils, but it is believed that the TRL has been lifted from 2-3 into 4, i.e. validated in the laboratory.

FIGURE 4.20

Left) Design of MgB_2 race track coil with Cu thermal support (red), mechanical steel support (grey) and glass fibre support (yellow). **Right)** Stacking of 10 pancake coils into the final MgB_2 race track coil being glued together using Stycast epoxy (black).

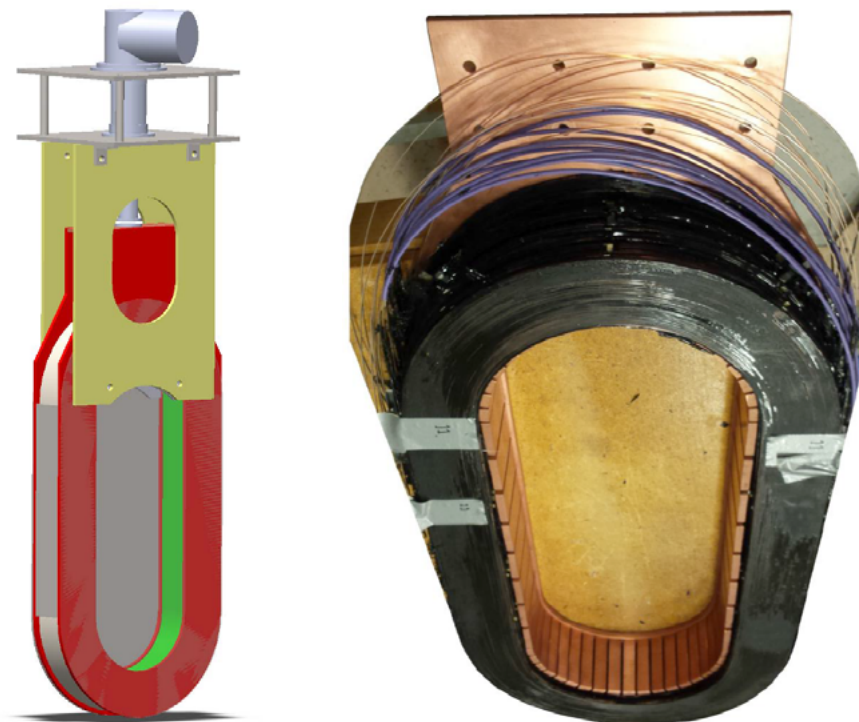
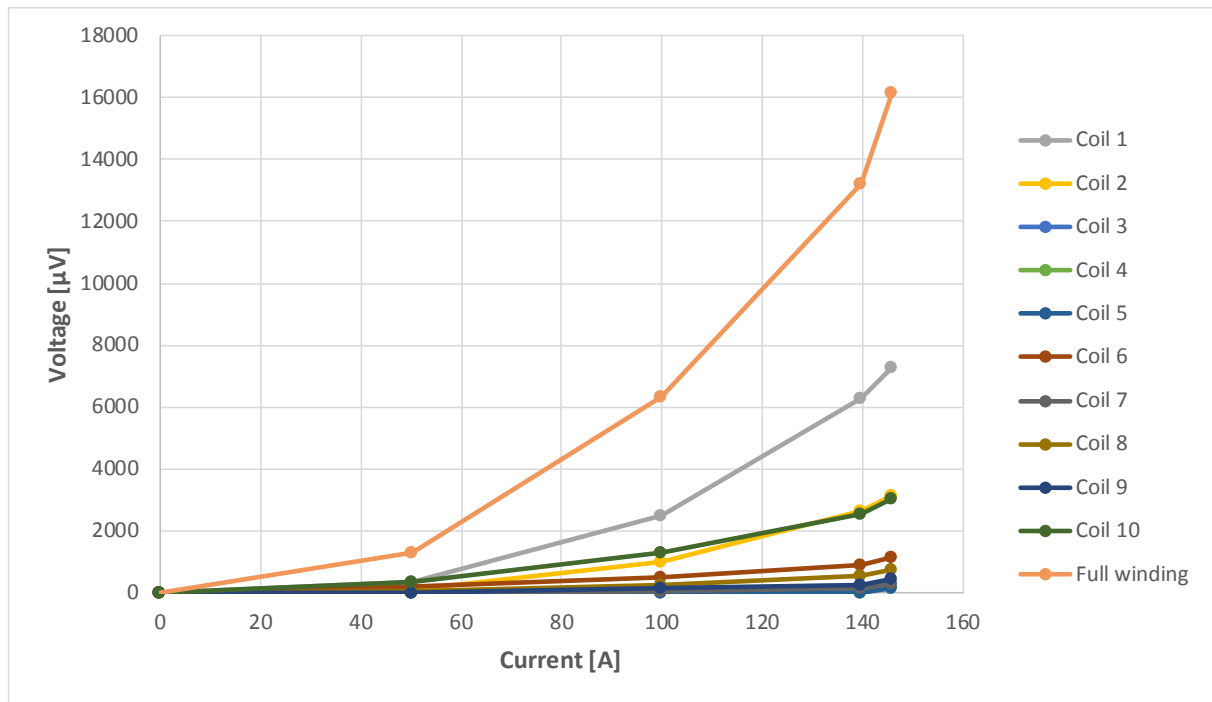


FIGURE 4.21

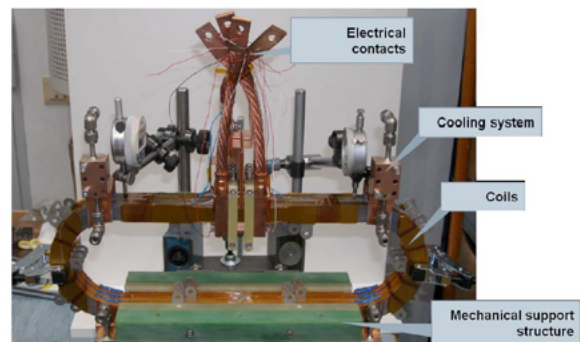
Voltage drop across the 10 pancake coils of the MgB_2 race track demonstration coil.



The RBCO generator demonstration was performed by Siemens Wind Power with the design, construction and test of a race track coil based on RBCO high temperature superconducting tape, as shown in Figure 4.22. The coil consisted of 3 single race track coils stacked on top of each other. The coil test provided the properties of the superconducting tape, which were used for the design of a direct drive high temperature superconducting wind turbine generator. It was concluded that several single race-track coils were damaged during construction or testing, with the result that the TRL level of the coil technology was only lifted from 2-3 to 4 (validation in the laboratory).

FIGURE 4.22

Race track coil based on second generation high temperature superconducting $\text{RBa}_2\text{Cu}_3\text{O}_{6+x}$ coated conductor tape, as tested by Siemens Wind Power. The straight section of the coil is 300 mm and the opening is 120 mm with a winding width of 22 mm.



4.2.2.3 GENERATOR DESIGNS

Figure 4.23 and Figure 4.24 show the magnetic flux density distribution of the 10 MW superconducting direct drive generators based on MgB_2 and RBCO tape developed during the INNWIND.EU project. The main characteristics of the two generators are listed in Table 4.3 and Table 4.4 after

optimization for lowest Levelized Cost of Energy has been performed. It is seen that both development tracks find that one must include more iron in the machines in order to reduce the usage of superconducting wire, thereby driving the cost down. This, however, leads to an increased mass, which will not become lower than what is expected for the currently-used permanent magnet direct drive generator.

FIGURE 4.23

(left): Magnetic flux density of MgB_2 pole in a 10 MW direct drive generator with a diameter of 6.0 m and a length of 2.6 m

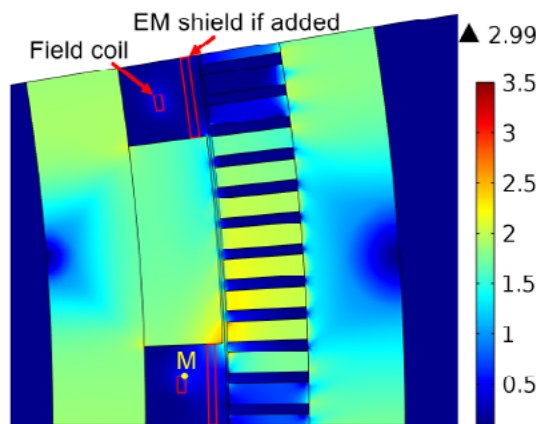


FIGURE 4.24

(right) Magnetic flux density of high temperature superconducting pole in a 10 MW generator with a diameter of 7 m and a stack length of 1.2 m

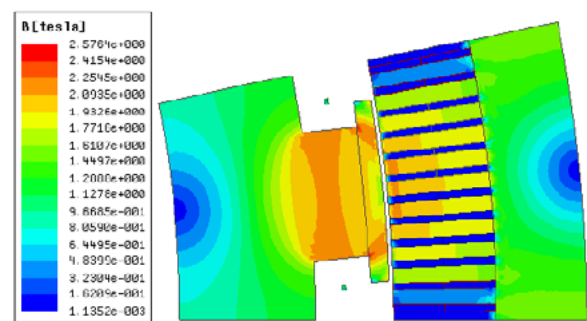


FIGURE 4.25

Dimension of active materials of MgB_2 10 MW direct drive generators found by optimizing the generator topology at a diameter of $D = 6.0$ m, 8.4 m and 10.8 m.

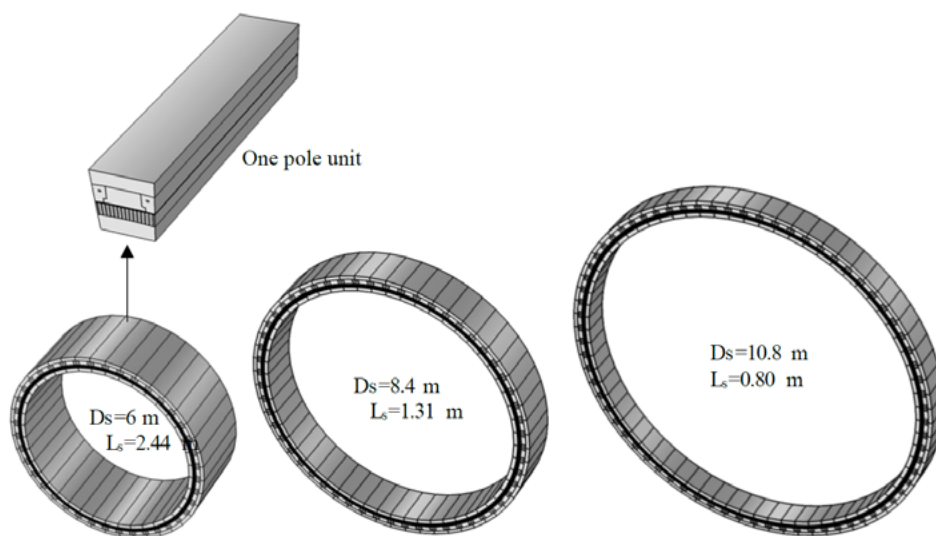


TABLE 4.3

The size of the MgB_2 generators as function of the generator power as well as the active masses and cost of active materials

SIZE AND WEIGHT OF MGB2 SUPERCONDUCTING GENERATORS		10 MW			20 MW
	Stator outer diameter D_s (m)	6.0	8.4	10.8	10.8
	Stack length (m)	2.44	1.31	0.80	2.25
Rotor	Field winding mass, including end winding (ton)	0.36	0.32	0.30	0.52
	Rotor iron mass (ton)	70.78	51.77	40.59	111.5
	Cryostat mass (ton)	3.87	3.38	3.16	8.89
Stator	Stator iron mass (ton)	63.99	49.37	38.86	106.7
	Copper mass, including end winding (ton)	13.93	13.06	13.02	24.27
Total rotor mass (ton)		75.00	55.46	44.04	120.39
Total stator mass (ton)		77.92	62.43	51.88	130.97
Total mass (ton)		153	118	96	251
Superconducting wires (k€)		93	80	75	140
Copper conductors (k€)		209	196	195	364
Rotor iron (k€)		212	155	122	334
Stator iron (k€)		192	148	117	321
Total cost (k€)		706	579	509	1159

TABLE 4.4

Properties of high temperature superconducting generators

	10MW	20MW-I	20MW-II
Stator outer diameter D (m)	7	7	11
Stack length L (m)	1.2	1.95	1.16
Speed n (rpm)	9.6	6.8	6.8
Torque T_{em} (MNm)	10.5	30	30
Stator current density J_s (A/mm ²)	3.5	3.5	3.5
Stator slot packing factor	0.6	0.6	0.6
Number of poles $2p$	32	32	64
Number of stator slots Q	384	384	768
Air gap length g (mm)	9	9	13
SC current density J_{sc} (A/mm ²)	340	273	340
SC area per pole (mm ²)	200	1000	200
Length of SC wire (km)	5.35	39.2	10.54
Ampere turns of SC per pole (AT)	34,000	136,500	34,000
Type of stator core	Iron-core	Iron-core	Iron-core
Type of rotor core	Iron-core	Iron-core	Iron-core
Volume of generator (m ³)	42.3	68.7	100.5
Mass of Iron (t)	141	271.9	208
Cost of SC (million €)	0.543	3.92	1.054
Cost of Cu (million €)	0.117	0.215	0.192
Cost of iron (million €)	0.112	0.217	0.166
Cost of total (million €)	0.764	4.35	1.412

4.2.2.4 LESSONS LEARNT

- Rotor coils of MgB_2 wire and RBCO high temperature superconducting tape can be wound and the TRL has been lifted from 2-3 to 4.
- Further work is needed to increase the success rate of winding superconducting coils from the observed rate of 60-70% towards 99.9%.
- The cost of superconducting generators can be lowered by increasing the amount of magnetic steel in the topology, but this will cause a weight increase making the superconducting generator heavier than the permanent magnet direct drive generator with the current properties of MgB_2 and RCBO superconductor wires and tapes.
- Superconducting generators are not rewarded for being “lightweight” and thereby cause savings in the tower and foundation for bottom-mounted offshore wind turbine due to resonance of the turbine and foundation’s first global frequency during variable speed operation. This calls for a design strategy of “cheap and not too heavy”.
- More lightweight superconducting wind turbine generator topologies will be possible if either the cost of the superconducting wires is reduced or if the critical current density of the wires is improved.

4.2.3 MAGNETIC PSEUDO-DIRECT DRIVES (PDD)

4.2.3.1 CONCEPT

The PDD is a mechanical and magnetic integration of a non-contacting magnetic gear and a Permanent Magnet Generator (PMG). The high torque rotor blade loads are handled by the magnet-magnet coupling of the gear, which reduces the generator torque requirement, and increases the rotational speed of the excitation rotor. It is therefore analogous to a single stage PMG hybrid WT architecture, but with the benefits of eliminating a mechanical transmission. The PDD achieves a very high airgap shear stress, allowing for a more compact machine and

reduced Rotor Nacelle Assembly mass, and the reduction in stator electrical loading leads to high efficiency, even at part load.

The INNWIND.EU project has advanced the development of the PDD technology significantly by addressing a number of challenges to the adoption of this promising technology at larger scales. These challenges included the following:

1. Due to its infancy, there were no established design rules and no analytical models to efficiently establish performance parameters and facilitate rapid optimization;
2. The size of the available laboratory demonstrators meant it was difficult to assess scaling effects;
3. Whilst most of the PDD components are similar to those used in a conventional PMG, the modulating rotor or pole-piece rotor is unique and represents new challenges in terms of its construction.

Analytical models of the PDD (Figure 4.26: Analytical model of PDD for predicting field quantities and performance parameters) have been developed and benchmarked against FEA and measurements on a 5 kNm demonstrator model. These models were employed to optimize 10 and 20 MW designs in terms of minimizing magnet material, overall mass and cost while maximizing efficiency considering both copper loss and iron losses. The predicted size and mass of the PDD (Table 4.5) is a significant improvement on direct drive PMG and is favourable compared to the Superconducting Direct Drive (SCDD) generators. The predicted efficiency curve will also have a beneficial impact on the LCOE.

FIGURE 4.26

Analytical model of PDD for predicting field quantities and performance parameters

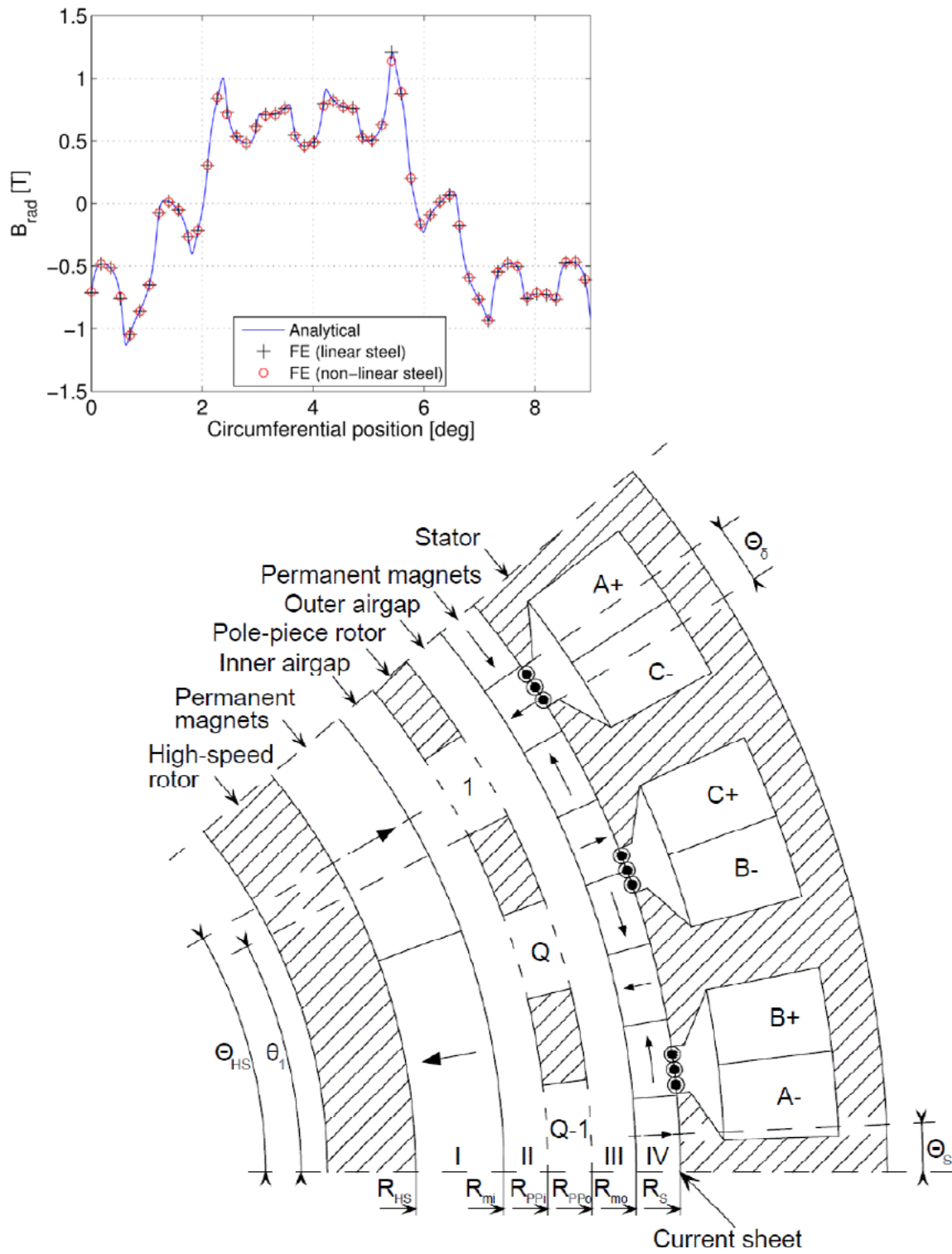


TABLE 4.5

10 MW and 20 MW design established using analytical model. ** Updated after deliverable D3.21. *** Revised efficiency after including scaled magnet eddy current loss to the original analysis.

SYMBOL	QUANTITY	VALUE FOR 10MW	VALUE FOR 20MW
	Rated power	10 MW	20MW
$\Omega_{PP,R}$	Rated speed of PP rotor	9.65 rpm	6.82 rpm
	Rated torque on the PP rotor	9.9 MNm	28.0 MNm
	Analytical pullout torque of the MG	11.9 MNm	33.7 MNm
$f_{out,R}$	Rated electrical output frequency	48.25 Hz	34.1 Hz
G	Gear ratio	7.5	7.5
P_{HS}^i	Pole-pairs on HS rotor per section	2	2
P_S^i	Pole-pairs on stator per section	13	13
M_S	Halbach segments per pole-pair on the stator	4	4
Q^i	Pole-pieces per section	15	15
S	Number of identical sections	20	20
	PP slot opening angle	$\pi/300$ rad	$\pi/300$ rad
D	Airgap diameter	6.0 m	8.5 m
W_{PP}	Radial thickness of PPs	31.4 mm	44.4 mm
	Radial thickness of HS rotor PMs	39.8 mm	56.3 mm
	Radial thickness of stator PMs	25.2 mm	35.6 mm
	Length of inner airgap	6.0 mm	8.5 mm
	Length of outer airgap	6.0 mm	8.5 mm
l_a	Active axial length	1.66 m	2.35 m
	HS rotor pole arc to pole pitch ratio	0.8	0.8
B_r	Remanence of N48SH PMs at 100°C	1.25 T	1.25 T
μ_r	Relative recoil permeability of PMs	1.05	1.05
	Copper packing factor	0.5	0.5
	Current density at rated power	$2.0 A_{rms}/mm^2$	$2.0 A_{rms}/mm^2$
	Annual energy efficiency	98.4%***	98.4%***
	PM mass	13.5 tons	38.2 tons
	HS rotor and PP rotor laminated steel mass	14 tons	39.6 tons
	Stator laminated steel mass	15.5 tons	74 tons
	Copper mass	7 tons	14 tons
	Estimated structural mass **	100 tons	254 tons
	Estimated total mass	150 tons	420 tons

FIGURE 4.27
5 kNm demonstrator during dynamometer testing

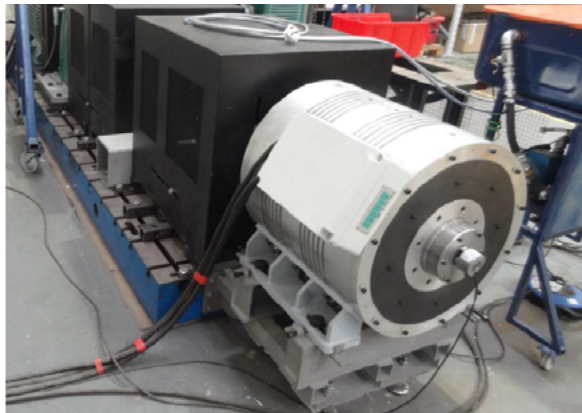


FIGURE 4.29
Insertion of search coils on pole-piece rotor



4.2.3.2 DESIGNS AND DEMONSTRATORS

An initial 5 kNm Industrial demonstrator was designed and built during Years 2-3 of the project (Figure 4.27). This was used to validate the analytical models from the University of Sheffield. As well as bulk properties such as emf, torque and efficiency (Figure 4.28), a bespoke telemetry system was developed to measure the complex flux waveforms using search coils embedded in the magnetic gear rotor (Figure 4.29) in order to also validate the models at the local spatial level (Figure 4.30).

The initial 5 kNm demonstrator was manufactured using Magnomatics existing approach with glass-fibre rods

FIGURE 4.28
Measured and predicted efficiency of 5 kNm demonstrator

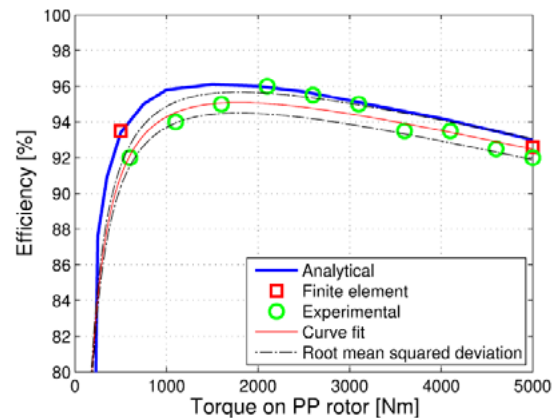
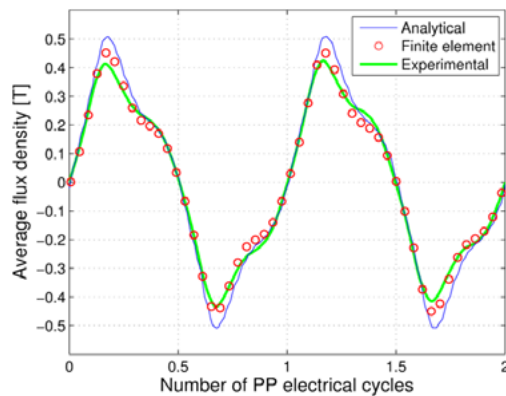


FIGURE 4.30
Measured and predicted (thru analytical model & FEA) complex flux waveforms in PPR



holding hourglass shaped pole-pieces, reliant on stiff bond-lines. The pole-piece rotor is subject to complex loads from the torsional loads and radial pull of the magnets. There is potential for modes to be excited in this structure which can lead to undesirable noise and vibration and potential issues of fatigue. Novel pole-piece rotor structures to overcome these issues were demonstrated under INNWIND.EU, consisting of a monocoque structure with additional layers of damping materials. Initially, these were de-risked on the 5 kNm demonstrator (Figure 4.31) showing a significant improvement in the resonant response measured using laser vibrometer (Figure 4.32),

FIGURE 4.31

Monocoque pole-piece rotor structure for 5 kNm prior to insertion of pole-pieces



FIGURE 4.32

Comparison of vibration response of original and modified pole-piece rotors

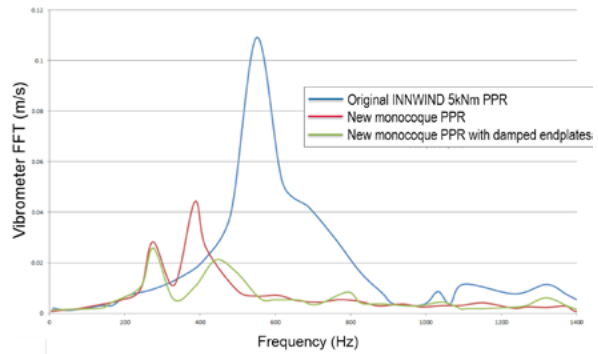


FIGURE 4.33

16 kNm PDD demonstrator

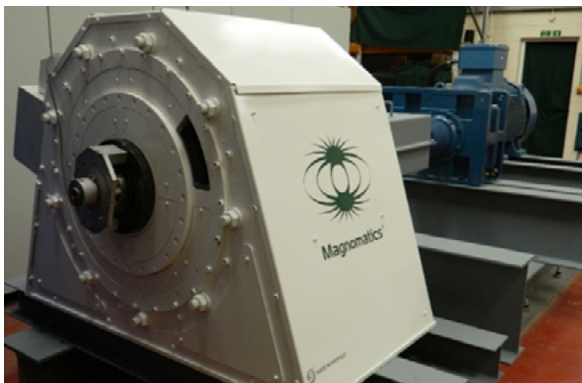


FIGURE 4.34

Rewound stator of the 16 kNm demonstrator

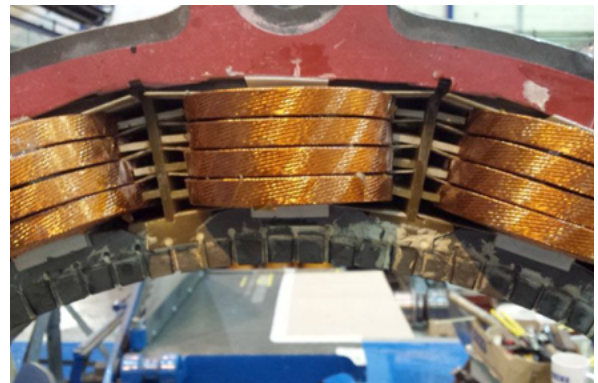


FIGURE 4.35

Revised pole-piece rotor structure for 16 kNm demonstrator

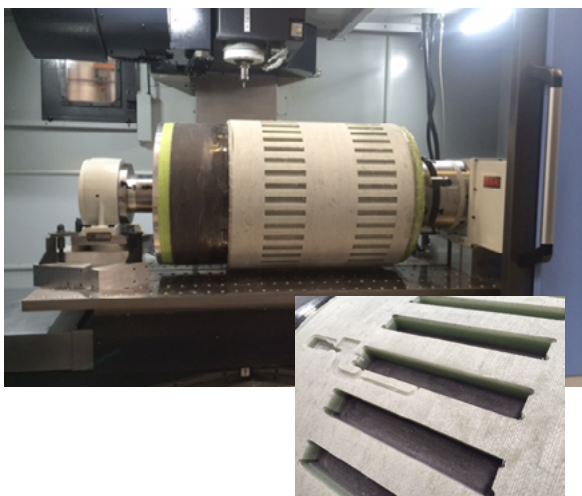
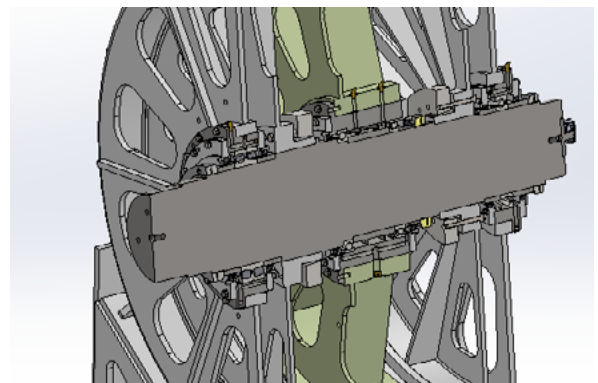


FIGURE 4.36

Model of 200 kNm, 500 kW demonstrator

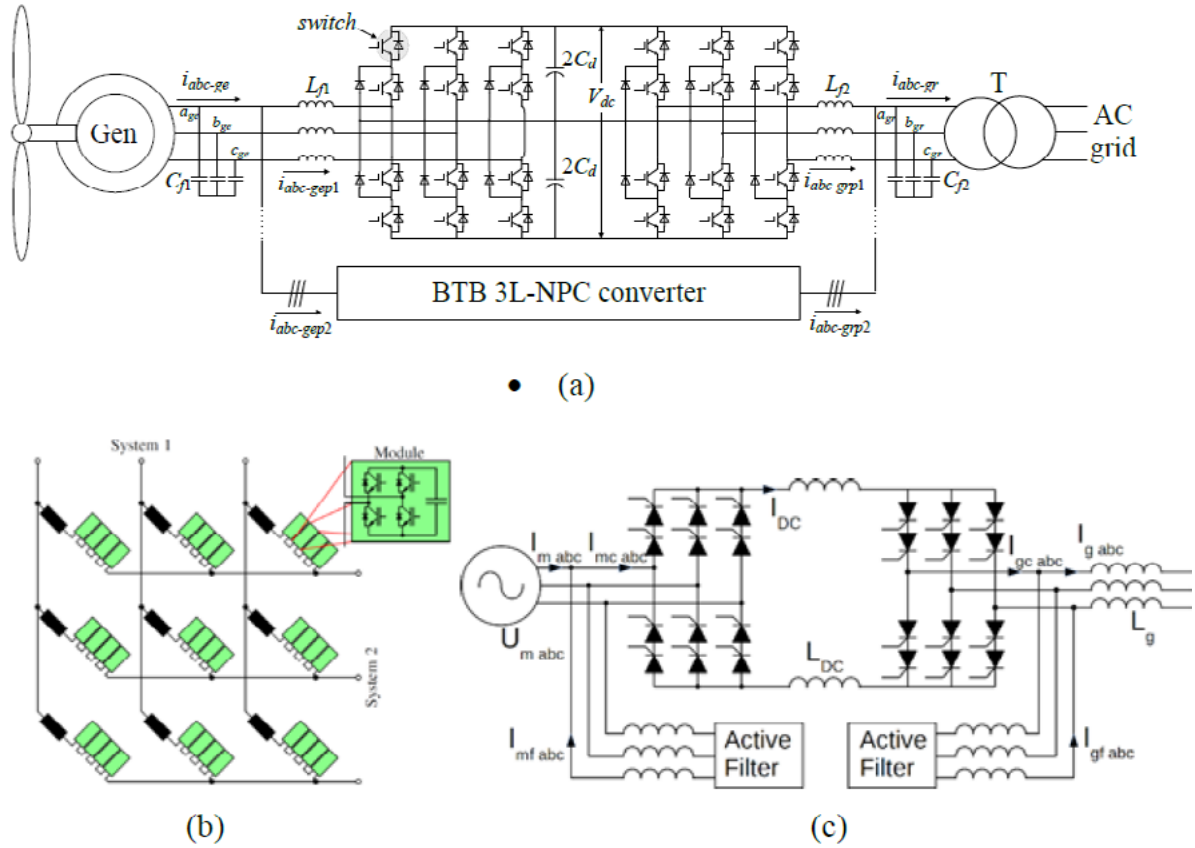


At a later stage (Y4), a 16 kNm PDD (Figure 4.33) built under an industrially-funded project was made available to the INNWIND.EU project. This machine was then further developed to address issues associated with the manufacture and potential noise and vibrations of the pole piece rotor (as identified on the 5 kNm unit) and additional parasitic AC copper losses in the strip wound conductors. The machine has been rewound with a revised winding layout (Figure 4.34) and a novel composite structure of pole-piece manufactured with integral damping layers (Figure 4.35). The efficiency of this machine has been improved from 94% at the start of INNWIND.EU to 95.5% following the rework.

The lessons learned and validated models from the 5 kNm and 16 kNm industrial demonstrators are now being applied to the development of a 200 kNm (500 kW) WT generator, funded under the Demowind CHEG (Compact High Efficiency Generator project). The generator (Figure 4.36), with a 2.4m outer diameter, will be built in Q1 2018 and test results made available Q2 – 2018.

FIGURE 4.37

(a) Converter configuration of BTB 3L based VSC. (b) Converter configuration of MMC based VSC. (c) Converter configuration of CSI-Actfilt



4.2.4 POWER ELECTRONICS FOR SUPERCONDUCTOR DIRECT DRIVE (SCDD) AND PSEUDO DIRECT DRIVE (PDD) GENERATORS

The power electronic converters are investigated for the 10 & 20 MW wind turbine with superconducting generator (SCG) and magnetic pseudo direct drive generator (MPDDG) concepts, where the unsegmented and the segmented SC and PDD generators are both considered.

4.2.4.1 CONCEPTS

Three types of power electronic converters for the 10 & 20 MW wind turbines based on SCG and MPDDG have been selected for detailed investigations, including

(1) the back-to-back (BTB) 3-level (3L) neutral-point clamped (NPC) voltage source converter (VSC) shown in Figure 4.37(a), where several BTB 3L-NPC converters are connected in parallel for the high power with good reliability.

(2) The modular multilevel matrix converter (MMMC) based VSC, as shown in Figure 4.37(b), which is a direct AC/AC converter.

(3) The configuration of combining a current source converter with active filters (CSI-Actfilt), as shown in Figure 4.37(c).

4.2.4.2 DESIGNS

For each of the above power electronic systems, the passive components and the active components are designed and the total cost for the power converters is evaluated. In addition, the size and the weight of the power converters are assessed. The efficiency, energy production and wind energy cost contributed by the power electronic system are also investigated. Finally, the control systems for the power converters are designed and simulations are performed for both normal operation and grid faults.

4.2.4.3 LESSONS LEARNT

The MMC-based converter requires a large number of components and would be rather expensive. The cost of CSI option may be significantly influenced by the rating of active filters which are voltage source converters. If the active filters are required to support the operation of thyristor converters during a grid fault, such as fault ride through, larger current ratings would be necessary than those required for only harmonic compensation. Further investigations are needed to determine the required rating of the active filters and the cost, as well as the operation and control strategies under both normal situation and disturbance conditions. Consequently, the 3-level NPC converter-based VSC can meet the technical requirements of interfacing the discussed generators, and may be cheaper overall, with the increased uses in multi-MW

industrial applications and increased production volumes on the market. The cost level of the power converters are found to be ~ 80 K€/MW for the INNWIND.EU drive trains.

4.2.5 INTEGRATING SC AND PDD GENERATORS IN 10-20 MW TURBINES NACELLE DESIGNS

4.2.5.1 NACELLE CONCEPTS

Direct drive wind turbines and wind turbines with gear-boxes often have very different nacelles because direct drive generators are so large that they determine the nacelle layout. This project focused on SCDD and PDD generators for 10-20 MW wind turbines and therefore on nacelle layouts that make these generator systems possible.

After considering different nacelle concepts, it was concluded that nacelle concepts based on a king-pin design were more realistic than other concepts based on availability and feasibility of nacelle components such as bearings.

In most direct drive wind turbines, the generator is located between the rotor and the tower to place the heavy weight of the generator close to the tower and to increase the tower-blade tip clearance. However, for the PDD it is not possible to do that, because the shaft or kingpin diameter is too large for mounting a PDD. Therefore, we investigated if the generator could be mounted upwind of the aerodynamic rotor. That appeared to work out very well, because in this construction, the main loads coming from the aerodynamic rotor are transferred to the tower in an optimal way. Therefore, a PDD is preferably mounted upwind from the rotor. For an SCDD generator, the generator can also be mounted upwind from the rotor or between the rotor and the tower.

FIGURE 4.38

Illustration of the 10 MW MgB_2 superconducting direct drive generator with a diameter of $D_{\text{gen}} = 8.4$ m, a length of $L_{\text{gen}} = 1.3$ m and a weight of $m_{\text{gen}} = 286$ ton mounted in front of turbine blades of the King-Pin nacelle (top) and behind the turbine blades (bottom). Both configurations seems possible to be scaled to power ratings up to 20 MW.

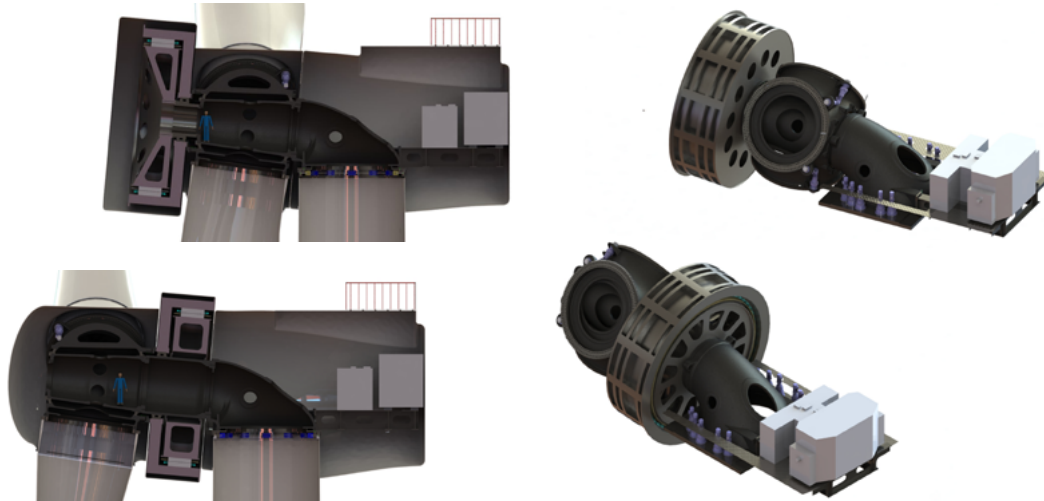
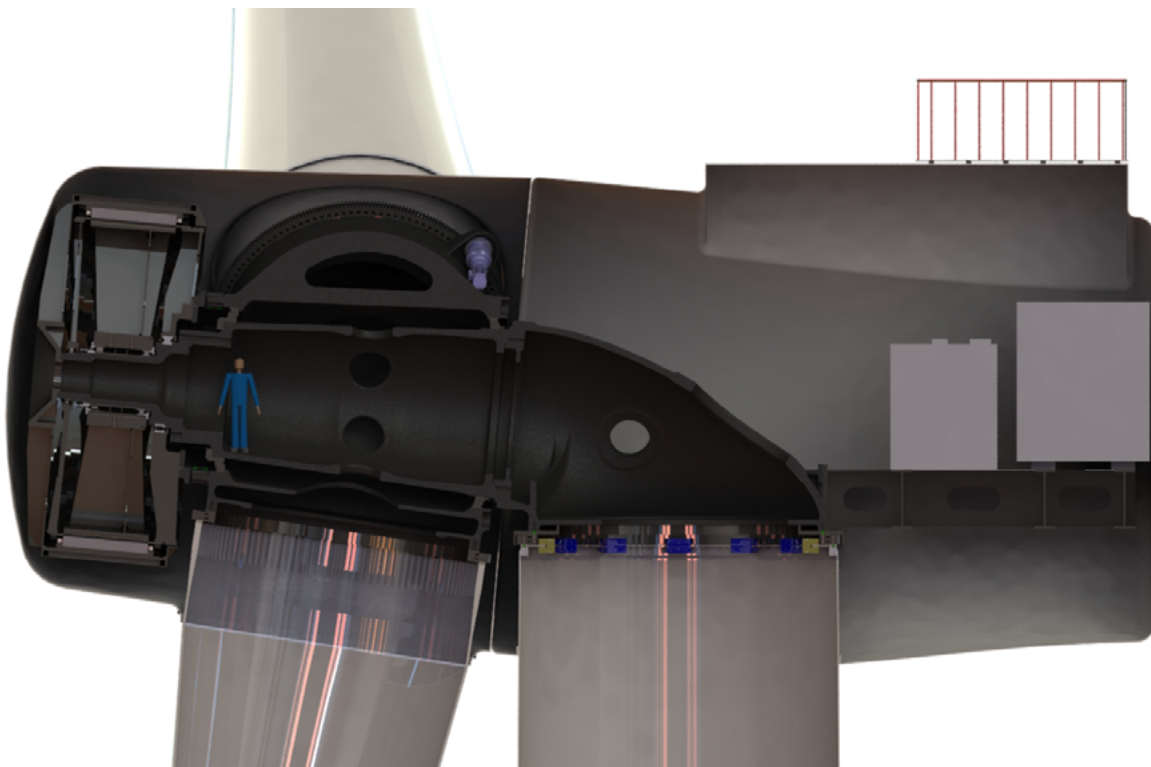


FIGURE 4.39

Illustration of 10 MW Pseudo Direct Drive generator with a diameter $D_{\text{gen}} = 6.0$ m, $L_{\text{gen}} = 1.7$ m and a weight of $m_{\text{gen}} \sim 150$ ton mounted in front of the turbine blades of the king-pin nacelle.



4.2.5.2 DESIGN OF KING-PIN FORWARD-MOUNTED GENERATOR

The resulting designs for 10 MW superconducting direct drive and Pseudo Direct Drive are shown in Figure 4.38 and Figure 4.39 respectively.

To reduce the risk of large generator air gap deviations introduced by deflections of the main load carrying components, a separate generator bearing was introduced with the purpose to isolate the generator from these deflections. The rotor of the generator is connected to the hub via a torque-only connection.

4.2.5.3 LESSONS LEARNT

- King-pin based nacelle layouts seem to be most suitable for large direct drive generators.
- 10 MW king-pin based nacelles can be manufactured now using available components and manufacturing technologies. In order to develop 20 MW wind turbines, new components (bearings) and manufacturing technologies have to be developed.
- For large direct drive wind turbines, forward-mounted generators are a good solution.
- The high short circuit torque of superconducting direct drive generators can be mitigated by segmentation of the machine.
- The low frequency of superconducting wind turbine generators can be handled by conventional power, electronic and added cost can be neglected.
- Providing light weight superconducting machines does not cause weight reductions of either the tower nor the foundation for the bottom-mounted INNWIND.EU turbine, since the generator weight is not the main design driver of the tower and foundation.
- A nacelle layout based on the king-pin concept has been established up to 20 MW and the limitations and issues related to the manufacturing has been identified.

4.2.6 MAIN SCIENTIFIC AND TECHNOLOGICAL ACCOMPLISHMENTS

The Pseudo magnetic direct drive technology has been demonstrated and the Technology Readiness Level has been lifted considerably to a stage where a 0.5 MW wind turbine generator is being designed as a commercial product.

The superconducting direct drive technology based on MgB_2 and RBCO has been investigated and the impact on the Levelized Cost of Energy has been obtained. It has been found that the current properties and cost of the superconducting wires is still too high to make the technology competitive, because iron steel must be introduced to reduce the usage of the superconductor and this results in overly heavy machines. The following issues of the superconducting generators have been solved during the project:

4.2.6.1 CONCLUSION

The partial load efficiencies of the PDD and the two superconducting direct drive generator at 10 MW are shown in the Figure 4.40 as function of the wind speed. The partial load efficiency includes the efficiency of the power electronics, but the cryogenic cooling losses of the superconducting generator have to be subtracted. In case of the 10 MW MgB_2 generator this is about 1%. It is clearly seen that the PDD has a superior efficiency resulting in a decrease of the LCoE of the 10 MW INNWIND.EU offshore turbine in the order of 4% compared to the reference drive train. The weight scaling of the PDD and the MgB_2 superconducting generators is shown in Figure 4.41 as function of the turbine rotor diameter, which is the main design driver for the mass upscaling. It is seen that the MgB_2 superconducting direct drive generator is scaling similar to the reference drive train, since iron has been introduced in the SCDD in order to reduce the cost of the generator. The PDD is showing a better mass scaling than the reference drive train and has therefore been selected as the INNWIND.EU candidate for an innovative non-contact drive train.

FIGURE 4.40

Efficiency of 10 MW drive trains as function of the wind speed and design Weibull wind speed distribution. MgB_2 : 10 MW superconducting direct drive generator based on an iron cored generator topology with 0 kW, 50 kW and 100 kW power consumption of the cooling system. RBCO: High temperature superconducting RBCO coated conductor based direct drive generator based on an iron-cored topology without the cooling system. PDD: Magnetic Pseudo Magnetic Direct Drive generator being a combination of a magnetic gearbox and a ring generator.

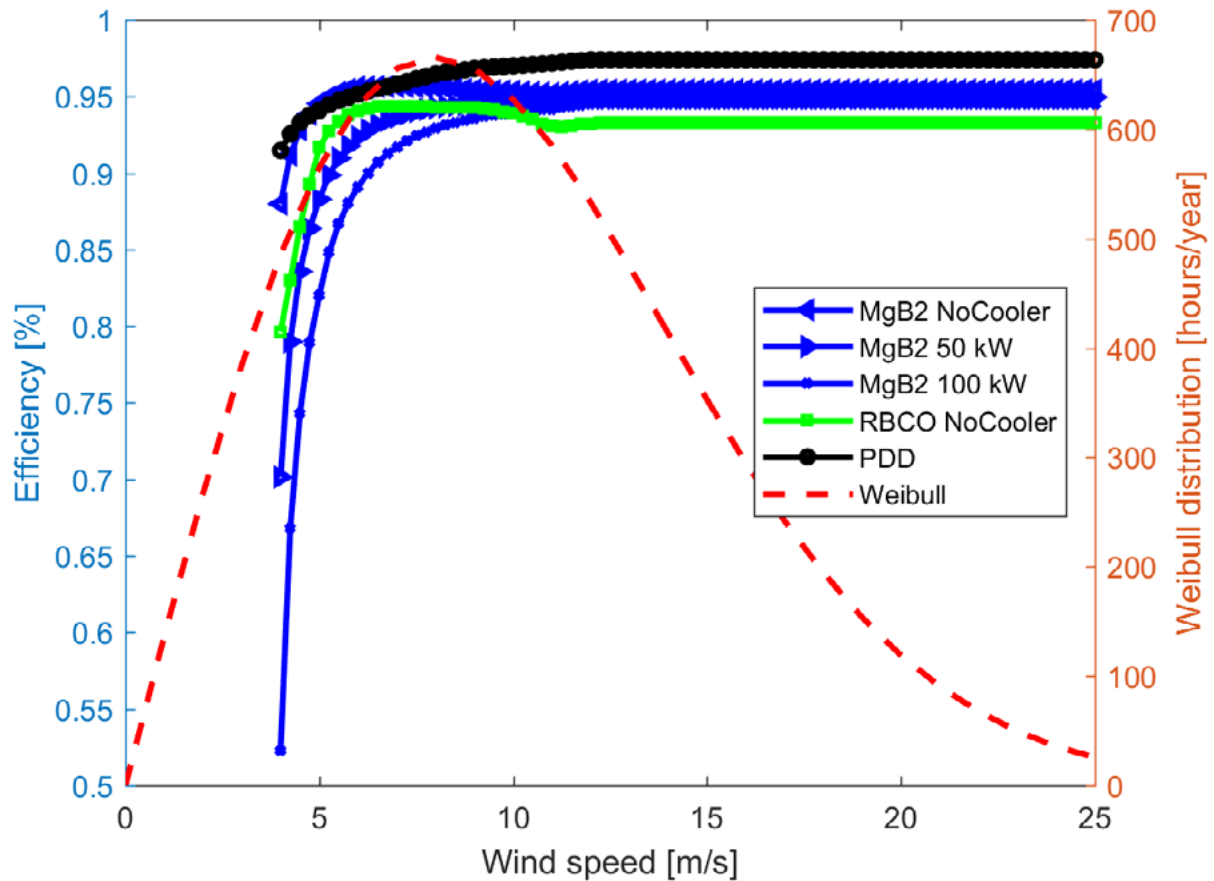
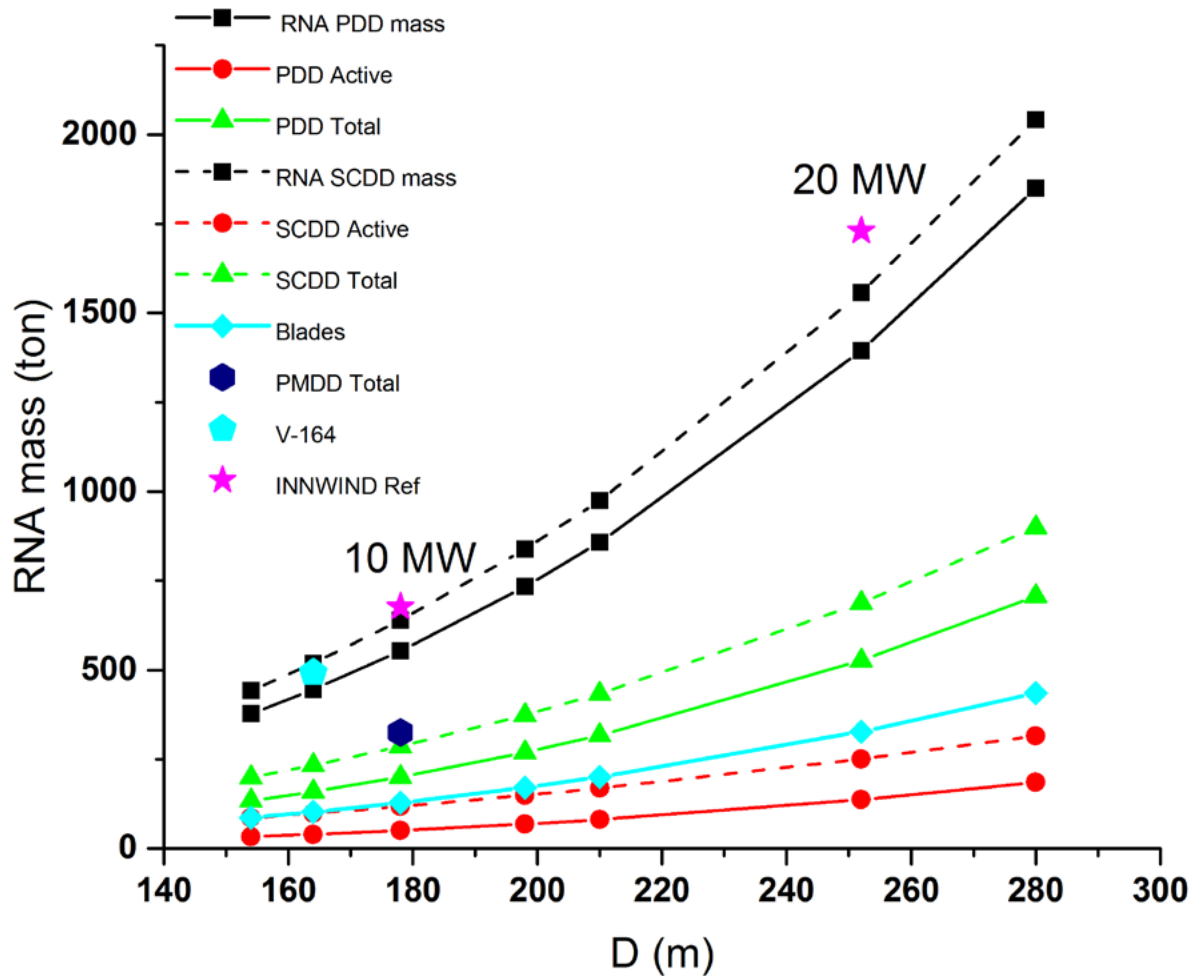


FIGURE 4.41

Scaling of the active material of the MgB_2 Superconducting Direct Drive (SCDD) and the Magnetic Pseudo Direct Drive (PDD) as well as the total generator mass. The generator mass is combined with the blade mass (Blades) and the king-pin nacelle mass in order to obtain the Rotor Nacelle Assembly (RNA) mass. The RNA mass of the INNWIND.EU reference drive trains are plotted for comparison as well as the RNA mass of the Vestas V-164²⁰. The total generator mass of a 10 MW Permanent Magnet Direct Drive (PMDD) generator²¹ is shown for comparison.

Rotor Nacelle Assembly mass scaling of INNWIND.EU generator



20 E. de Vries, "Close up - Vestas V164-8.0 nacelle and hub", Wind Power Monthly, September 9 (2013), www.windpowermonthly.com.

21 Polinder, H., Bang, D., van Rooij, R., McDonald, A., & Mueller, M., "10 MW Wind Turbine Direct-Drive Generator Design with Pitch or Active Speed Stall Control", Proceedings of the International Electric Machines and Drives Conference, 2, p. 1390 (2007).

4.3 SUPPORT STRUCTURES

4.3.1 STATE OF THE ART IN SUPPORT STRUCTURES DESIGN FOR LARGE OFFSHORE TURBINES

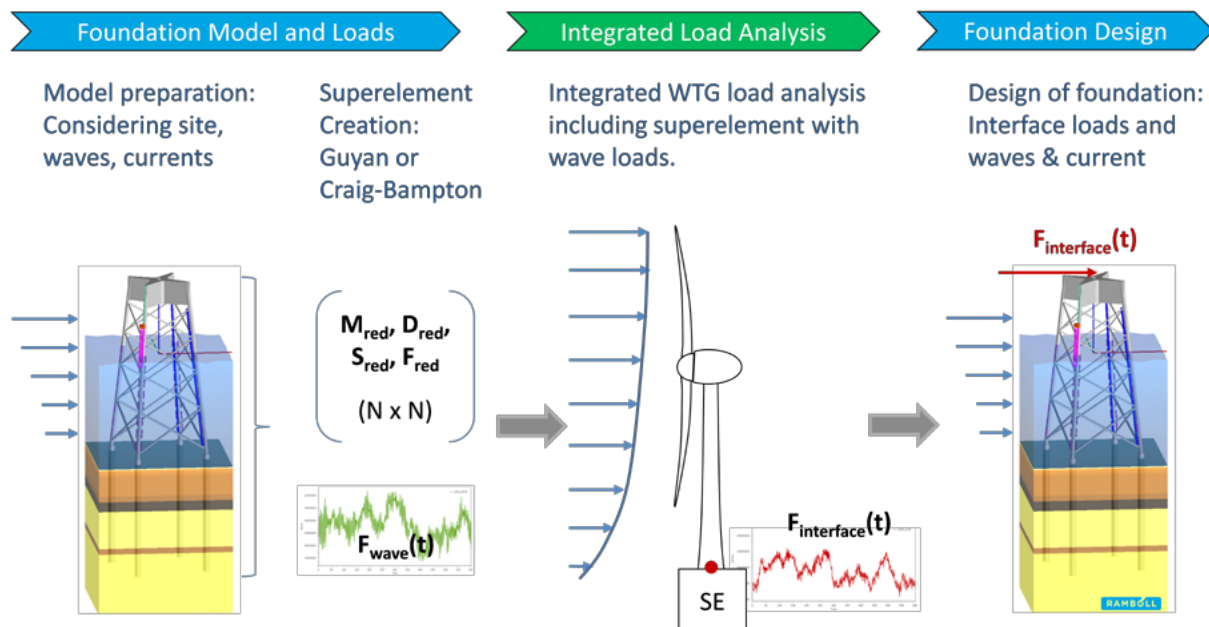
The design of support structures requires a common approach from different involved parties to ensure a cost-efficient design. Wind turbine manufacturers and foundation designers need to apply integrated models to accurately consider all relevant dynamic effects from wind and wave loading and structural response. It should be noted that the foundation design is always a site-specific design and often differs between positions of a windfarm due to water depth variations and variances of soil layers. In contrast, the wind turbine is designed for a particular IEC wind turbine class²², which considers a maximum allowed reference wind speed and turbulence intensity for the classification. This means that the wind turbine loads from simulations based on IEC class conditions are usually conservative for a site (which shall not exceed the wind turbine class definition) and in conceptual design the wind turbine loads do not consider the influence from the support structure accurately. Therefore it is recommend-

ed to apply site-specific met-ocean data (for wind and waves) and soil conditions for the integrated load analysis and the support structure design.

It is mandatory to define a common design basis, which accurately describes the met-ocean conditions of the site. Often a superelement approach and exchange of interface load time series between the wind turbine and the foundation model are applied, as illustrated in Figure 4.42. It is of crucial importance to perform multiple load iterations, especially if geometrical changes are implemented and if other boundary conditions at the site change, e.g. soil parameters. Although it seems negligible, even very small changes in local details of wall thickness or thickness transitions can significantly change the calculated loads and thus fatigue life of a hot spot. The results of the load simulations are the nominal sectional forces of each structural component and structural stresses in the hotspots. The design assessment – with respect to natural frequencies, ultimate limit state, fatigue limit state, serviceability limit state and accidental limit state – is required according to guidelines and standards, e.g. DNVGL-ST-0126²³ or NORSOK N-004²⁴

FIGURE 4.42

State of the art design load iteration between foundation and wind turbine



²² International Electrotechnical Commission (2009). IEC 61400-3. Wind turbines – Part 3: Design requirements of offshore wind turbines.

²³ DNVGL (2016). Support structure for wind turbines. Available at <http://rules.dnvgl.com/docs/pdf/dnvgl/ST/2016-04/DNVGL-ST-0126.pdf>

²⁴ Norsok Standard (2004). Design of steel structures. Available at <http://www.standard.no/pagefiles/1145/n-004.pdf>

Floating wind turbines are typically classified into three main typologies: spar, semisubmersible and TLP. Categorisation depends on the main physical mechanism used by these turbines to stabilize the system: gravity forces, buoyancy forces or tension of the mooring lines. Nevertheless, there are a great number of proposed designs that combine or modify these basic concepts. Such a variety of typologies makes it difficult to converge on an optimized cost-effective design. The first design challenge to face, then, is the correct selection of the appropriate concept for specific location of the floater.

The simulation of floating wind turbines requires integrated tools because physical effects like rotor aerodynamics and platform hydrodynamics present a strong coupling. An effect of particular importance for floating wind turbines is non-linear hydrodynamics, which can excite low and high frequencies of the system, not present in the wave spectrum. Non-linearities are important in the design of mooring lines and influence the lateral drift of the structure. The inclusion of these non-linearities can imply a high computational cost. Mooring lines dynamics can also have an important impact on the system design. Although dynamic mooring models imply higher computational cost, they should be included in the integrated simulation approach.

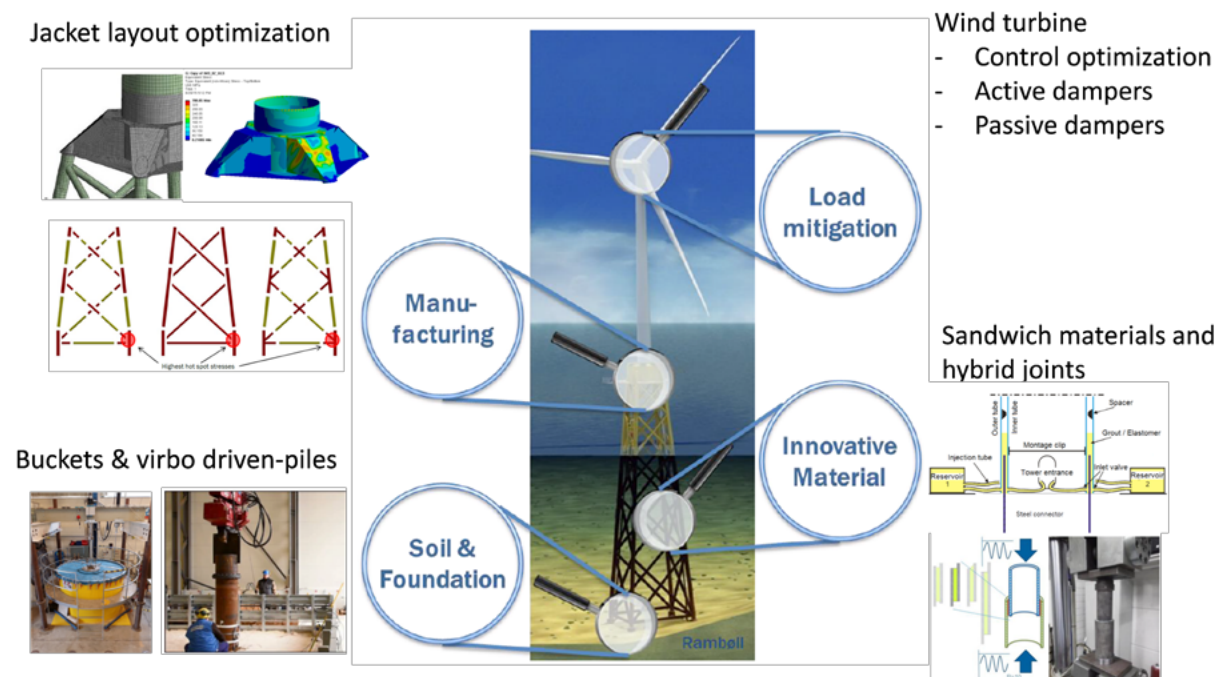
The wind turbine control strategies can have a great impact on the floating system dynamics, the loads and the production. The control has the objective of maximizing the power production, reducing the loads of the different components and ensuring stability for the whole system. Floating wind turbines have very different dynamics from onshore turbines or offshore bottom-fixed turbines. The lowest natural periods of the platforms are significantly different and require other control strategies.

4.3.2 INNOVATIONS FOR SUPPORT STRUCTURES

New innovations for future cost-effective, mass-producible designs are investigated, such as new foundation types, soil-structure-interaction of large piles or suction buckets, innovative transition piece designs or designs using hybrid materials which have never been employed before in wind energy. In addition, design integration using jacket-specific controls and innovative fabrication and installation processes shall complete the overall cost saving potentials. Figure 4.43 illustrates the considered innovations for the support structure which are summarised as follows.

FIGURE 4.43

Considered innovations for the support structures of large offshore wind turbines



Innovations of load mitigation

Novel 10-20 MW Offshore wind turbines need to have a lightweight design to reduce the material cost. The increased size of the rotor and tower height results in magnified vibration amplitudes which need to be reduced. In addition, the offshore wind turbine dynamics need to be reconsidered when upscaling the substructure design.

In principle, load mitigation strategies are classified under two main categories: control concepts and damping devices. Three dedicated load mitigation concepts are studied on the operational control level: speed exclusion zones, soft-cut out, and peak shaving.

Firstly, active load reduction technology has been implemented for the reduction of the thrust around rated wind speed by the so-called Peak Shaver. Also, a speed exclusion window to avoid resonances during operation is considered for the 10 MW design. Secondly, passive damping systems have been analysed for the support structure. The considered damping systems include the passive Tuned Vibration Absorbers (TVA), Tunde Mass Dampers (TMD) and Viscous Fluid Dampers (VFD) for the 10 MW wind turbine class. It has been shown that the passive dampers are more effective in a sideways direction while the effectiveness of these devices is marginal in fore-aft direction.

For the 20 MW wind turbine class, the application of passive TMD will become less effective and the integration into the available space in the tower top will become more difficult. Therefore, the employment of semi-active or active damping systems is becoming more attractive. Semi-active dampers operate in a broad frequency bandwidth and are more effective in both directions. The numerical modelling of a semi-active magnetorheological (MR) damper is implemented and integrated in both the jacket and the tower structure to mitigate loads. The study reveals the potential of MR dampers to alleviate fatigue damage in all conditions. Further investigations are required to propose an optimal configuration for reliable full-scale implementation in the field.

Innovation of hybrid materials

The sandwich material for a monopile, as well as the chords and braces of a jacket sub-structure, have never been used in the offshore wind industry. Sandwich

tubes are rod-like structural components consisting of three components: two relatively thin steel tubes and a core made of ultra-high performance concrete (UHPC). Due to its high strength, UHPC is an appropriate solution to save material and weight. The project studied the numerical and experimental investigation of sandwich tubes, as well as the development of the pre-design methods for sandwich tubes and their application on the chords and braces of the jacket structure. The bearing capacity of sandwich tubes under combined axial loading and bending moments was also investigated.

Taking the basic geometric parameters into account, variations of the member parameters, such as the ratio of steel to sandwich material, were investigated and the effect on natural frequencies compared to the reference structure was evaluated. It should be noted that the current TRL of sandwich tubes for jacket sub-structures is 3. The estimations show that if the necessary manufacturing time is summed up, the steel tubes for hybrid jackets allow a saving of up to 50% in time in relation to the thicker common steel tubes.

The second innovation considered is the potential of adhesively bonding instead of welding. In this regard, the considered innovation is to adhesively bond the trusses connected to the main pillars in the jacket substructure connections. The main potential benefit is that an adhesively bonded connection can be less fatigue-sensitive than a welded connection. On the other hand, potential disadvantages are issues during installation (can the adhesive be applied in a controlled manner?), sensitivity to temperature and humidity influences during operation, as well as sensitivity to multi-axial strains during operation.

Innovation of vibro-driven piles

Vibratory-driven (VD) technology, as an alternative to impact-driven (ID) technology, has the potential to significantly reduce the costs associated with installing piled foundation for offshore wind turbines. The economic advantages of this technology include: the absence of noise mitigation systems, the reduction of the installation time and the reduction of the fatigue load in the pile steel otherwise induced by impact hammers.

The results of an experimental campaign including two large-scale impact-driven piles have been presented and

interpreted by using CPT methods. Soil profile and steel price were assumed and are regarded to be rather realistic values. The analysis carried out with loads referring to a 10 MW wind turbine reveals that, on the basis of the tests carried out, the price difference between impact-driven and vibro-drive piles is around €38k when adopting UWA-05, and around €47k when adopting ICP-05.

Innovations of suction buckets

Jacket structures are usually founded on pre-installed piles. However, bucket foundations are an option that can decrease the overall cost and allow alternative installation strategies. Since wind turbines are dynamically sensitive structures, where stiffness requirements must be satisfied, an alternative design allowing increasing stiffness is the multi-bucket configuration, wherein loading response changes significantly with respect to a mono bucket. The following work is focused on loading of a multi-bucket foundation. The overturning bending moment is mainly transferred into vertical compression and tension loads in the buckets. For these reasons, it is important to understand the behaviour under tensile loading and improve the stiffness of the foundation so more correct design methods can be established. Experimental results of vertical axial loading cyclic tests of bucket foundation are conducted. The drained cyclic response was examined by simulating the long-term cyclic loading conditions for an offshore structure under the normal serviceability performance. Cyclic degradation was tested applying post-cyclic pull-out loads on the bucket foundation model.

Innovations of tool development for floating wind turbines

Different simulation tools for floating wind turbines with diverse complexity levels have been developed within the project. These tools can be applied at different stages of the design process, from conceptual design to a detailed analysis. The new features developed include coupled aeroelastic models considering the platform flexibility or advanced aerodynamic approaches such as the free vortex method. CFD codes have been also developed, including movable meshes that allow for the capturing of non-linear interaction between the fluid and the structure. This has particular importance in the analysis of cases with rough sea states. Other non-linear effects included in the existing integrated tools are mooring dynamics or fully non-linear

wave models. These effects have particular importance in the analysis of TLP platform concepts.

The simulation tools developed in this project have been validated against experimental data. This leads the tools to a TRL of 6 and increases the reliability of the simulation codes, providing a unique set of tools that can accurately capture the coupled dynamics of real floating wind turbines. The experimental data are publicly available for researchers and code simulators, which is an important contribution for the offshore wind turbine modeller community.

The measured data were obtained in two test campaigns: one was performed at EHEEA Nantes, France on a semi-submersible concept and the second one was carried out at DHI, Denmark on a TLP. The use of these two concepts with different dynamics improves the quality of the validation. Two types of codes for performing coupled analysis of a floating wind turbine have been validated, namely aero-hydro-elastic integrated tools and high fidelity aerodynamic and hydrodynamic CFD. It is worth noticing that CFD is not dependent on prior calibration and measurements where accurately predicted. This kind of code has a high computational cost, but can be used for the tuning of lower complexity codes when no measured data are available.

An additional test campaign focused on submerged chain dynamics where performed for the validation of the dynamic model of the floating platform mooring system. The code showed a good prediction of the measurements even in highly dynamic situations.

The resulting tools are a comprehensive set of codes with very advanced capabilities for the analysis of the coupled dynamics of floating wind turbines and for the optimization of the design. These codes are also unique because they have been extensively validated against experimental measurements.

Innovations of integrated methods for floating wind turbine control design

A methodology to optimize the main platform dimensions together with the control parameters has been developed. This is an innovative method, because it considers the control design from the very first steps of the design, improving the design process. Reduced models for the

design of floating wind turbines have been created, including the main parameters of the floating wind turbine and a PI controller for the pitch and the rotor speed. The optimization of the system is done with adapted static and dynamic models through a stepwise narrowing of the design space according to the requirements of floating wind turbines. The integrated design results have been verified with detailed full FEM simulations in connection to critical load cases for controller testing, reaching a TRL 3. The designs (platform and controller) delivered by the integrated methodologies show improvements in platform stabilization and load alleviation. In addition, the integrated method for the design and optimization of the platform + controller system is applicable independently on the size of the WT, its class or conception: both horizontal and vertical axes WT can be analysed.

Innovations of scaled testing methodologies for floating wind turbines

The correct design of experimental floating wind turbine models is a difficult procedure due to the interaction of the regarded system with two different environments – wind and waves – which require counteracting scaling procedures. While the hydrodynamic interactions can be correctly scaled using a constant ratio of the gravitational and inertial forces, aerodynamic interactions are usually scaled using a constant Reynolds number and thus maintaining the ratio between viscous and inertial forces. Both scaling methods cannot be satisfied in one and the same system.

For the scaling of aerodynamic loading during combined wave and wind scaled tests, a new methodology has been presented. The introduced method uses a ducted fan governed by a real time computation of the full rotor, coupled with the platform motions during the test. The so-called “Software-in-the-Loop” (SIL) approach enables the application of varying rotor thrust at the tower top of the floating model. Turbine control strategy, turbulent wind or wind gust can be modelled. This approach allows for time and cost savings in the preparation of the test campaign and is easily adaptable to changes in the scaled model.

Another approach for modelling aerodynamic forces and coupled rotor dynamic effects during the scaled tests has been applied and verified. The method consists of the redesign of the scaled rotor for low Reynolds numbers

which keeps roughly the tip-speed ratio and the Froude number, so that the dynamic response of the rotor is scaled adequately.

These methods have been applied to a semi-submersible and a TLP floating wind turbines design in scaled wave tank tests to verify its performance. The experimental results have been compared with computations and deliver a good correspondence. The methods are currently being used in several test campaigns within commercial projects and can now be considered a mature technology, with a TRL of 9.

4.3.3 DESIGNS FOR 10 MW WIND TURBINE CLASS

Jacket designs

Different jacket concepts have been developed to support the INNWIND.EU 10 MW reference wind turbine in a water depth of 50m. Designs are based on conceptual design level using a reduced number of (governing) integrated design load calculations in order to assess the fatigue limit state and ultimate limit state. The developed solutions are compared with an initially designed reference jacket considering the structural mass and associated manufacturing costs. The reference jacket is a classical 4-leg steel jacket concept with pre-piled foundation and is developed in the beginning of the INNWIND.EU project. In parallel, automated design optimization procedures have been developed and successfully applied, connecting the design changes with the design and cost assessment in a loop. The following jacket solutions are addressed and a sketch of each concept is given in Figure 4.44:

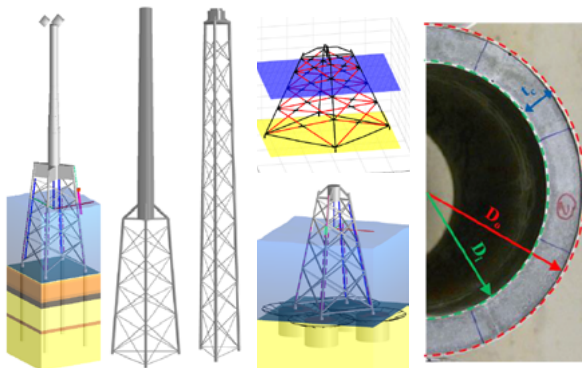
1. Modular 4-leg and 3-leg jackets with classical pre-piled foundation and tubular tower;
2. Full-lattice tower concept;
3. Hybrid jacket using sandwich materials;
4. 4-leg jacket variant with suction buckets to substitute the piled foundation.

A central core of the research is the analysis of cost reduction potential considering either innovative support structure concepts or innovations on component level as

well as optimized state of the art solutions, such as the application of new materials and load mitigation concepts. At the beginning of the project, a target cost reduction value of 20% was defined. The final cost calculations show a reduction potential between 12%-43%. It should be noted that the technology-readiness level and the level of development differ significantly between the different proposed concepts. Consequently, a direct comparison is rather difficult and the resulting cost estimates of novel concepts still have high uncertainty.

FIGURE 4.44

Bottom-fixed support structure concepts analysed. From left to right: 4-leg jacket, 3-leg jacket, full-lattice tower, hybrid jacket using sandwich material and a jacket with suction buckets.



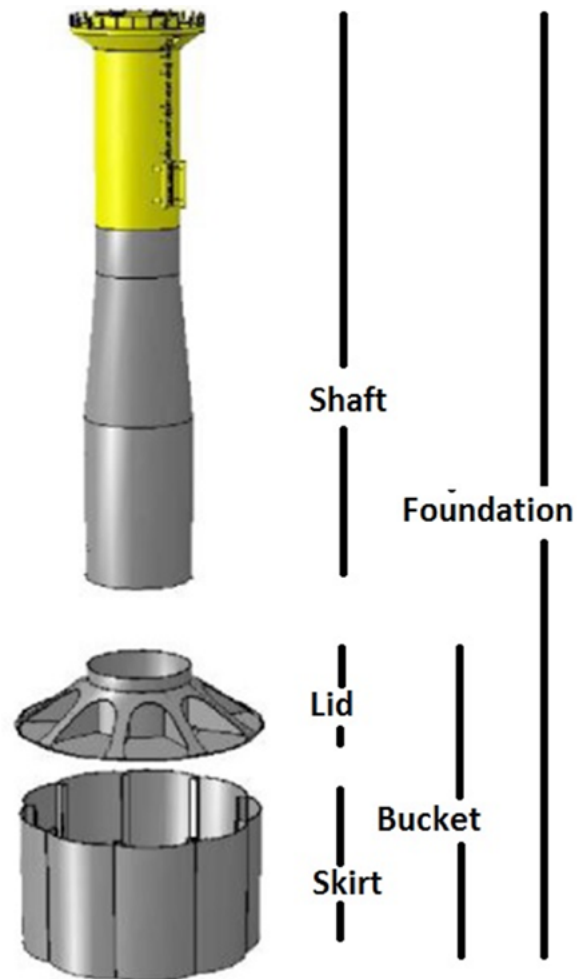
Mono-bucket design

The mono-bucket foundation is a novel foundation concept that is potentially capable of delivering significant cost reduction to offshore wind farms. The bucket foundation is a cylindrical pre-buckled steel structure which is installed in the seabed by suction-assisted penetration. Control of the verticality and the penetration process is ensured by using several pressure chambers inside the bucket which can be controlled individually using pumps. The installed steel bucket acts as a combination of a large diameter monopile and a gravitation-based foundation. The structure consists of the skirt, lid, shaft and the top flange which connects the mono-bucket foundation with the tower. A separate transition piece or grouted connections are not required due to the reduced overall height of the structure compared with a monopile, which should simplify and shorten the installation procedure. Additionally the noise emission from suction bucket installation is

much lower than using hydraulic hammers to drive a piled foundation. The most complex part of the mono-bucket concept is the lid construction which needs to transfer the loads from the shaft to the large diameter of the bucket. A sketch of the concept from Universal Foundation A/S is given in Figure 4.45

FIGURE 4.45

Mono-bucket design concept



Preliminary floater concepts: Torus, Semi-floater, concrete floater, semi-submersible

Four different innovative floating concepts supporting the INNWIND.EU 10 MW reference wind turbine have been designed at a conceptual level to evaluate the advantages and disadvantages of the different designs. A sketch of these concepts is shown in Figure 4.46.

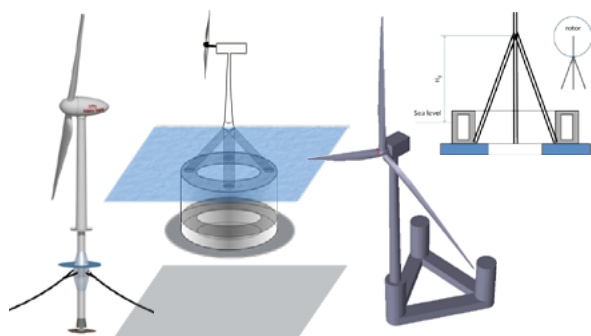
A semi-floater design is proposed combining the strengths of floating structures with those of bottom-fixed ones. This is a solution well suited for intermediate water depths (50-70m) where fixed sub structures may be too expensive and floating sub structures may not be used.

Two different torus-shape structures in concrete have been developed. The torus has the advantage of a reduced draft for an increased flexibility to the water depth and it significantly reduces the wave excitation due to the “moonpool” feature and the steel construction around water level, where wave forces are high. One of the designs has two dynamically linked floating bodies to reduce excitation from waves. The use of concrete as material can drastically reduce the cost of these designs.

Finally, there is an asymmetric semi-submersible floater which aims at reducing the need of lattice construction elements. The substructure is composed of three cylinders, connected by pontoons to form a geometrically simple shape. The function of the pontoons is not only structural, but also hydrodynamic: the pontoons work as heave plates to damp the motion of the offshore wind turbine. In addition, the wind turbine is mounted on one of the cylinders, instead of building a central structure to hold it in the platform centre. This allows for the simplification of the structure and reduction in manufacturing costs.

The analysis of these concepts indicates that the semisubmersible design has good dynamic behaviour, together with manufacturing and installation advantages. On the other hand, the use of concrete can potentially reduce the cost of the platforms.

FIGURE 4.46
Conceptual designs analysed. From left to right: semi-floater, concrete torus, semisubmersible and concrete torus linked with floating bodies



“Triple Spar” reference floater design

From the analysis of the different concepts, it was concluded that concrete material has a great potential to decrease the cost of the platform and that the semisubmersible configuration has several advantages in terms of dynamics, transport and installation. Based on this, a hybrid concrete semi-submersible platform, called “Triple Spar” was designed: this combines a low-cost steel transition piece, a low draft for flexible deployment and a simple assembly and installation. An artistic representation of the “Triple Spar” is presented in Figure 4.47, giving an impression of its dimensions.

FIGURE 4.47
“Triple Spar” reference platform supporting the 10 MW INNWIND.EU wind turbine



The platform is semisubmersible and composed of three concrete cylinders. Heave plates, also in concrete, are added at the column's base to increase the damping in heave. The columns are connected by a steel tripod (Figure 4.48) which supports the tower of the 10 MW INNWIND.EU reference wind turbine.

FIGURE 4.48
Structural mesh for the Finite Element analysis of the transition tripod



A solution has been designed for the connection between the steel transition tripod and the concrete columns. The connection is composed of twelve inclined steel radial rods with hollow cylindrical cross-sections. The system of the 12 rods distributes the transferred force to 12 different positions along the concrete wall. The inclination angle is 60 degrees in order to minimize the horizontal force transferred to the wall, since the axial force of each member is reduced. The rods are hinged at both ends, reducing the lateral buckling phenomena. Twelve horizontal ties, made of steel hollow cylindrical sections, are installed and pinned to the concrete shell. These ties will prevent any bulging failure of the concrete due to the force transmitted through the inclined members. The ties are connected to a steel ring on the transition piece.

4.3.4 DESIGNS FOR 20 MW WIND TURBINE CLASS

Assumptions of the 20 MW wind turbine

The INNWIND.EU 20 MW reference wind turbine is developed by directly upscaling from the 10 MW RWT design. Similar to the 10 MW design, the water depth is 50m. However, only one concept is considered for this design which includes a modular 4-leg jacket with classical pre-piled foundation, transition piece and a tubular tower. At the early stage of the design, a reduced model of the complex jacket structure is considered which is called the superelement. This replaces the jacket structure and hydrodynamic loads with mass, stiffness and wave-load matrices. The interface loads and moments according to the DLC 1.2 and 6.4 are obtained at the tower bottom and used to update and optimize the jacket dimensions. The cost reduction potential resulted by the load mitigation concepts are addressed. The key design parameters of the reference wind turbine are listed in Table 4.6.

TABLE 4.6
Design parameter of the 20 MW reference wind turbine design

PARAMETERS	VALUES
Rotor type, orientation	3 bladed - Clockwise rotation – Upwind
Control	Variable speed – Collective pitch

Cut-in, rated, cut-out wind speed	4 m/s, 11.4 m/s, 25 m/s
Rated power	20 MW
Rotor, hub diameter	252.2 m, 7.9 m
Hub height	167.9 m
Drivetrain	Medium speed, Multiple-stage Gearbox
Minimum, maximum rotor speed	4.45 rpm, 7.13 rpm
Maximum generator speed	339.4 rpm
Gearbox ratio	47.6
Maximum tip speed	90.0 m/s
Hub overhang	10.0 m
Shaft tilt, coning angle	5.0°, -2.5°
Blade prebend	4.7 m
Rotor mass including hub	632,016 kg
Nacelle mass	1,098,270 kg

Integrated Jacket Design for 20 MW

A state of the art jacket concept for large wind turbines having a rated electrical power output of 20 MW was developed in the final phase of the INNWIND.EU project. A 4-leg jacket with pre-piled foundations was selected. Large diameters of the brace ends (also using brace end cones in the lowest sections) are required to achieve sufficient stability, which makes a design with only three legs not realistic at present due to the risk of overlapping elements at the tubular joints. The starting point for the design was the up-scaled INNWIND.EU reference wind turbine with rated power of 20 MW. Initially, a so-called land-version of the wind turbine was developed and design loads were calculated for a range of first natural frequencies in the soft-stiff design region. Consequently, the initial jacket design was carried out on a conceptual level based on static extreme loads and simplified load cases for fatigue analysis with isolated wind- and wave- fatigue damage calculations. In a second phase, the integrated model of the offshore wind turbine with the jacket was assembled and advanced control for load mitigation were implemented for the 20 MW wind turbine. The advanced control concepts are based on the findings from the innovation on the 10 MW scale and were adapted accordingly for the large wind turbine. The design load calculations are based on the methodology shown in Figure 4.42 using

the same met-ocean parameters as for the 10 MW jacket designs. The resulting main properties of the 20 MW reference jacket are given in Table 4.7.

TABLE 4.7
20 MW reference jacket design

JACKET MAIN PROPERTIES	UNIT	VALUE
Base Width	[m]	38
Top Width	[m]	20
Interface elevation	[mMSL]	26
Jacket legs outer diameter	[mm]	1829 - 2642
Brace outer diameter	[mm]	914 – 1168*
Pile diameter	[mm]	3500
Mass of TP (estimated)	[t]	450
Mass of jacket	[t]	1670
Mass of one pile	[t]	230
First natural frequency of the full model	[Hz]	0.163

4.3.5 MAIN SCIENTIFIC AND TECHNOLOGICAL ACCOMPLISHMENTS

Major progress has been made on small- and medium-scale laboratory experiments. This concerns material testing, testing of installation methods of piles and buckets and a sophisticated wave tank experiment. The results and experiences from these analyses have been successfully transferred to improve the methodologies and led to their validation. Finally, various support structure design

solutions for the 10 MW (bottom-fixed and floating) and 20 MW (bottom-fixed) wind turbine class have been developed. The findings are summarized in Figure 4.49 and Figure 4.50.

The main scientific and technological achievements on floating wind turbine design are as follows:

- A comprehensive set of codes has been developed with very advanced features for the analysis of the coupled dynamics of floating wind turbines at different stages of the design process, allowing for platform optimization. These codes are unique because they have been extensively validated against experimental measurements.
- Design methodologies for floating wind turbines have been created, integrating, since the first dimensioning, the control design. This allows a better optimization of the system in the first design steps.
- New methodologies for scaled wave tank tests have been developed. These methods allow for combined wave and wind testing, sorting the conflict of the scaling laws and have proved to be very efficient.
- A database with experimental data from several test campaigns has been publicly setup as a contribution to the floating wind turbine modeller's community.
- An innovative hybrid floating platform has been designed for a 10 MW wind turbine, combining steel and concrete to reduce the cost.

FIGURE 4.49

Scientific and technological accomplishments for bottom-fixed structures

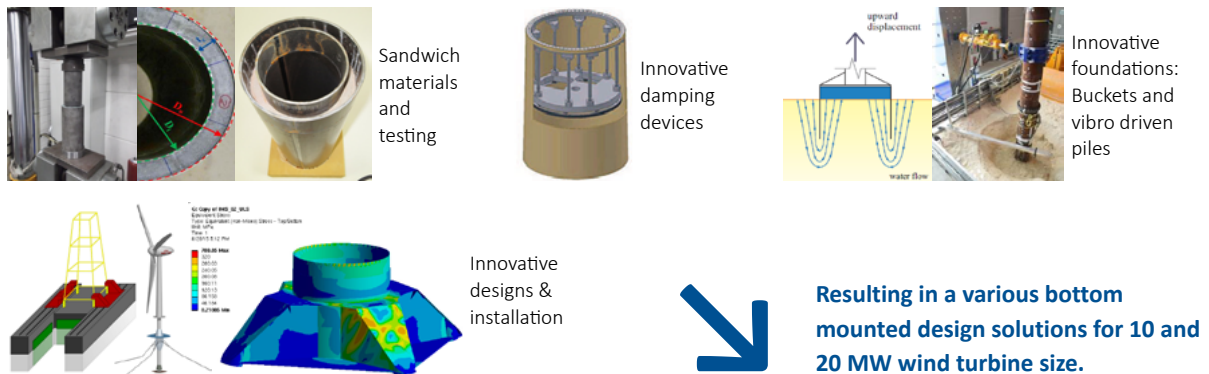


FIGURE 4.50

Scientific and technological accomplishments for floating structures

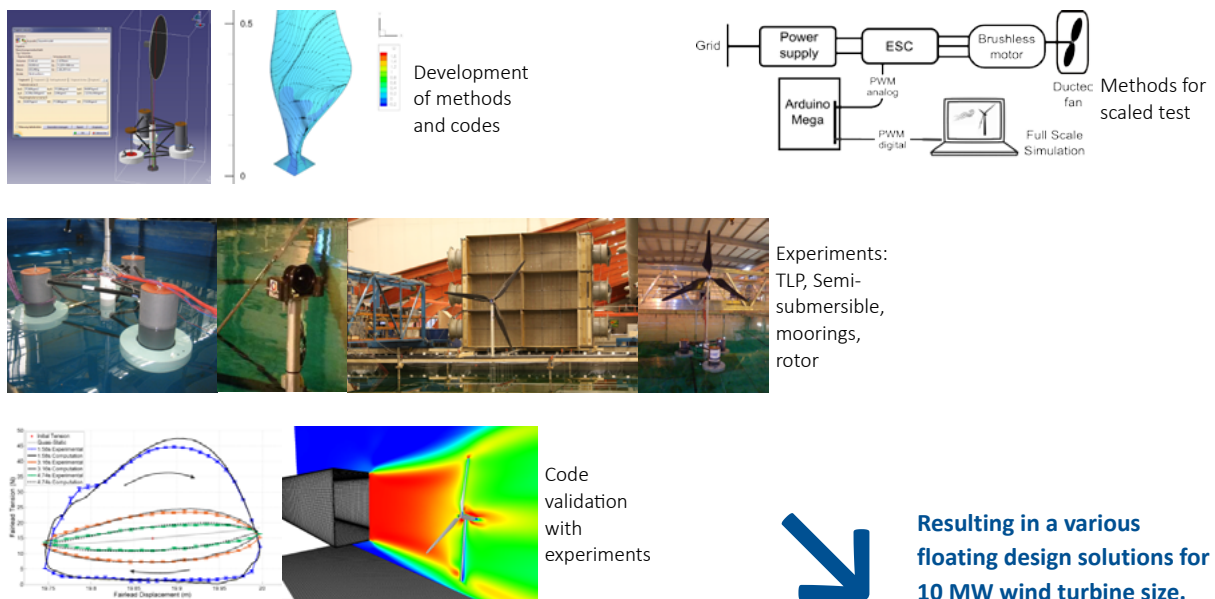


FIGURE 4.51Technology Readiness Levels²⁵ vs wind turbine development phases

TRL LEVEL	DESCRIPTION ²⁵	WIND TURBINE DEVELOPMENT PHASE
9	Actual system proven in operational environment (competitive manufacturing in the case of key enabling technologies; or in space)	Commercial turbine (0 series)
8	System complete and qualified	Prototype according to certification requirements
7	System prototype demonstration in operational environment	Pre-production prototype
6	Technology demonstrated in relevant environment (industrially relevant environment in the case of key enabling technologies)	Functional prototype
5	Technology validated in relevant environment (industrially relevant environment in the case of key enabling technologies)	Key aspects environment
4	Technology validated in lab	Integration of components
3	Experimental proof of concept	Feasibility / concept design
2	Technology concept formulated	
1	Basic principles observed	

4.4 ROAD TO MARKET

4.4.1 TECHNOLOGY ROADMAPS – OVERALL PRINCIPLE

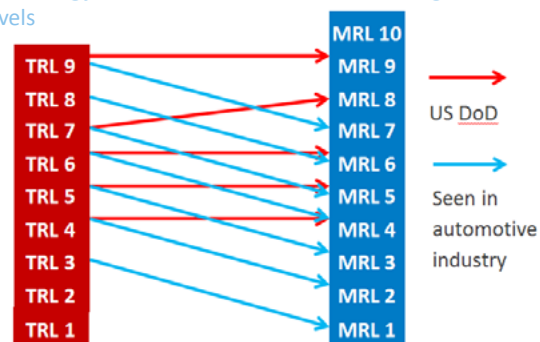
Technology Roadmaps have been developed for the innovations in the INNWIND.EU project. The technology Roadmap document²⁵ is available from <http://www.innwind.eu/publications/deliverable-reports> (deliverable 5.13). The technology roadmap uses Technology Readiness Levels (TRL) and Manufacturing Readiness levels (MRL).

The time-to-market of an innovation will be driven by TRLs or MRLs depending on aspects such as: application, quantity to be produced, market sector, supply chain, how difficult it is to produce it in terms of size, equipment or technology required, whether it is a state-of-the-art technology or a technology transfer. Figure 4.52 below depicts how these two levels relate for two different industries: the USA Department of Defence (DOD) and the automotive industry. These two industries have different objec-

tives: while the DOD aims to accomplish highly innovative functions with state of the art technology of a limited quantity, the automotive industry focuses on accomplishing high technological functions aiming at mass production and therefore, at lowering manufacturing costs. For the wind energy industry, the relation between TRLs and MRLs is expected to be somewhere in the middle of these two industries. Here, see Figure 4.52.

FIGURE 4.52

Technology Readiness Levels vs manufacturing readiness levels



²⁵ “Horizon 2020 Work Programme 2016-2017”. ‘Secure, Clean and Efficient Energy’. European Commission, 2016”

4.4.2 TECHNOLOGY ROADMAPS – EXAMPLE

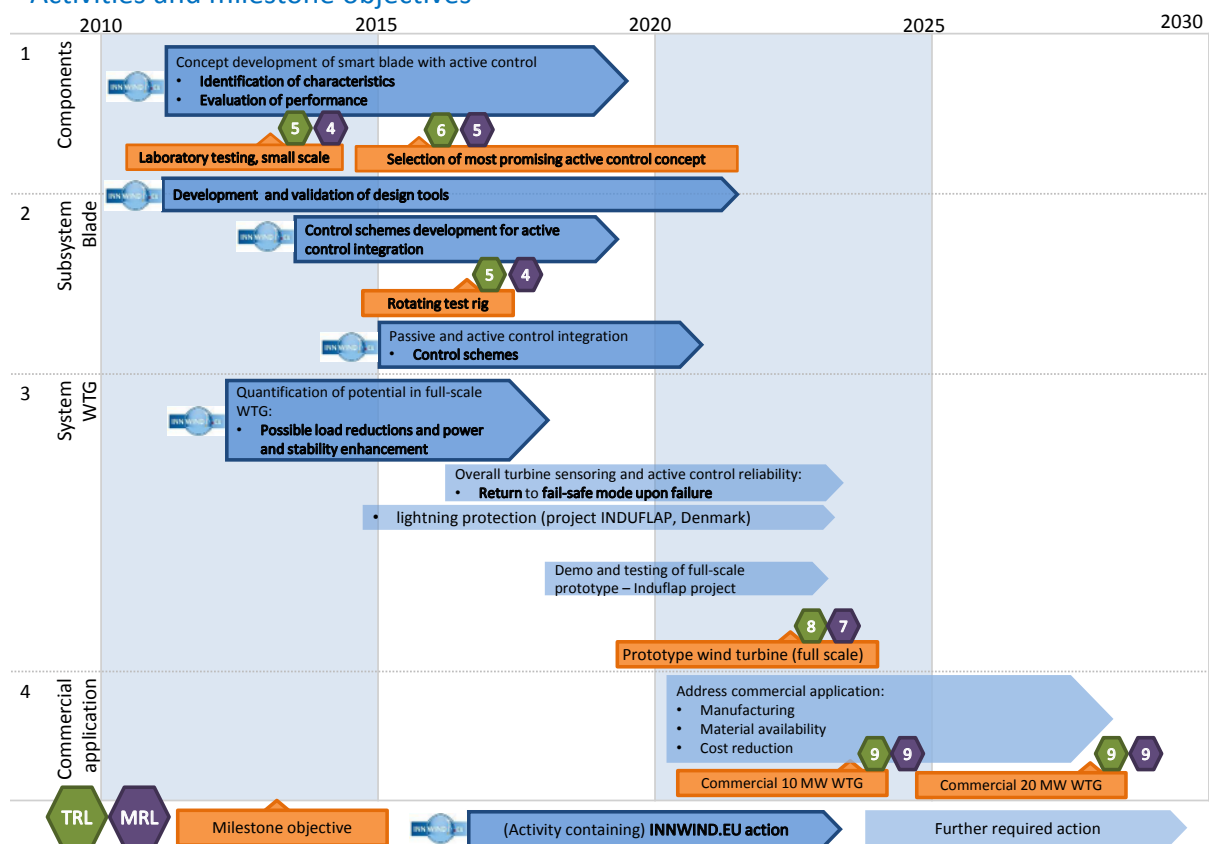
The technology roadmap presented below indicates the TRL and MRL at different levels, ranging from component level (e.g. trailing edge flaps), right up to wind turbine system level and commercial application. The objective of the technology roadmap is to inform future decisions that

will enable the technology to develop, with the required next steps and expected timeline clearly illustrated. Refer to the key at the bottom of the Technology Roadmap (Figure 4.53); in particular, further required actions are indicated by light blue shaded actions. The dark blue shaded actions contain INNWIND.EU action, but are not limited solely to INNWIND.EU action, and thus can continue after the project ends in 2017.

FIGURE 4.53

Example technology roadmap (one of eleven presented²⁶) – Smart Blades

TECHNOLOGY ROADMAP – ACTIVE CONTROLS FOR SMART BLADES (Trailing edge flaps) Activities and milestone objectives



26 Innwind Technology Roadmap, DNV GL (UK), 2017

5.

CONTROLS AND INTEGRATIONS OF INNOVATIONS AT THE SYSTEM LEVEL

5.1.1 INTRODUCTION OF THE STATE OF THE ART IN CONTROLLERS FOR LARGE OFFSHORE TURBINES

Beyond the basic need to regulate rotor speed and power output, the turbine controller has an important role in managing mechanical loading. Essentially, it does this by changing blade pitch angles dynamically to control thrust-related loads, and adjusting generator torque to damp out vibrations. The generator speed signal, which generally has high resolution and a fast sampling rate, is used effectively for the latter task, although further improvement can be obtained if suitable measurements of shaft torque or in-plane blade root loads are available, or if the rotational speed of the hub or low speed shaft is measured to sufficient accuracy to allow for the calculation of the twist velocity.

The control of thrust-related loads using blade pitch is the subject of many different control enhancements, usually requiring additional load sensors, such as blade root loads, tower top loads, main shaft loads etc. in terms of strains, position or acceleration. Such pitch control is often termed Individual Pitch Control (IPC) since each blade

can, in principle, be rotated to a different pitch angle to satisfy a minimum load objective. However, in practice, usually only the blade root loads or tower top loads can be effectively mitigated, because it is often difficult to mitigate the loads at the tower base and further below for offshore sub structures using IPC. Collective Pitch Control (CPC) does not usually involve load-based sensors, but does use several filters effectively to reduce resonant excitation of different wind turbine structures and provide control-based damping. A pitch control strategy in-between is termed cyclic pitch control, which is a form of IPC that essentially aims to cancel out the effect of wind shear over the rotor, but this may be further enhanced using wind observers.

The wind turbine is conventionally unable to measure the instantaneous incoming wind speed, since the nacelle based anemometer and wind vane provide only point measurements of the highly disturbed flow behind the rotor, although they can be filtered to provide inputs representing, for example, 10-minute averaged wind speed and direction. The wind turbine loads depend on wind speed, but are also influenced by other wind parameters such as the wind turbulence, length scales, spatial coherence in the wind field, as well as spatial variations in wind direction (veer) or speed (shear). Such measured wind quan-

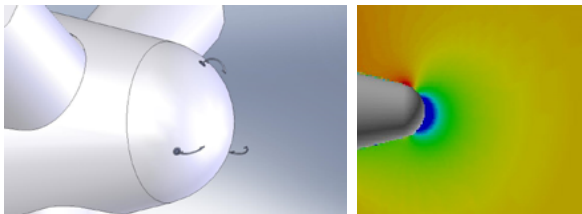
tities, if fed to the controller in advance of the turbine experiencing the wind field, can enable significant load reduction. Such a concept is termed ‘feed-forward control’ and is based on measured wind field sensors. LiDARS are laser-based devices that transform the back scatter from aerosols in the incoming wind to wind velocity measurements. Nacelle- or spinner-mounted LiDAR can be used to measure the incoming wind speed to improve CPC and potentially to measure the asymmetry of the wind field as an alternative input for IPC. The load reductions should be made possible without detriment to energy capture, and will even facilitate a small increase in energy by avoiding compromises which might have otherwise been needed.

5.1.2 NEW SENSORS FOR TURBINE CONTROL

The main innovation required in terms of sensors is the development of wind sensors that can be used to mitigate loading without compromising on energy production. Two new sensors are investigated here: the Spinner anemometer and the Spinner LiDAR. The spinner anemometer comprises 3 sonics (ultrasonic anemometers) which measure the instantaneous directional wind velocity at three positions on the spinner, as shown in Fig. 5.1. The spinner anemometer also has a built-in rotor azimuth sensor: each sonic wind speed sensor has a built-in accelerometer in the sensor foot which is used to determine the rotor azimuth angle of the rotor. Flow speeds around a spinner are shown in Figure 5.1. The sonic sensors are normally positioned on the spinner where the flow speed is approximately the same as that of the free wind speed when the flow is normal to the rotor.

FIGURE 5.1

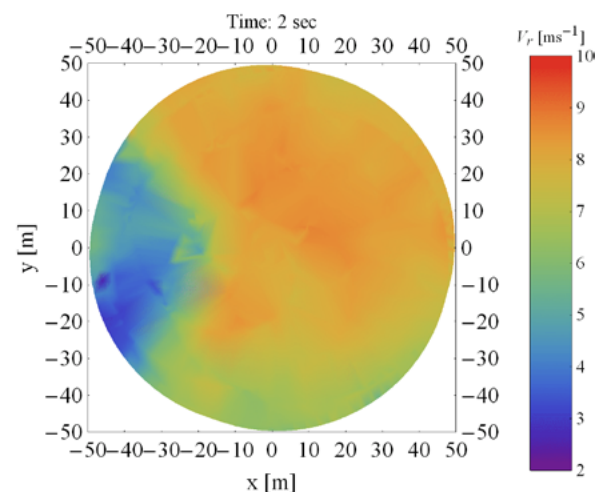
Spinner anemometer consisting of a spinner mounted with three sonic sensors, with an accelerometer mounted at the foot of each sonic sensor. Flow speed contours around a spinner with wind from the right, at a flow inclination angle of -10° , which means flow is coming from below.



The Spinner LiDAR is a remote-sensing instrument for scanning the wind inflow at several points in a plane ahead of the wind turbine as shown in Figure 5.2. It is installed in the spinner of a wind turbine hub. Nacelle-mounted LiDARS could also be used for this purpose but, being downwind of the rotor, they have to take account of blockage of the LiDAR beam whenever a blade passes in front. A Spinner LiDAR using a continuous wave, coherent doppler system manufactured by ZephIR LTD (UK) and adapted for spinner-based inflow measurements was used successfully in the project. An integer number (between 4000 and 5000) of Doppler spectra continuously sampled are averaged, such that the output averaged spectra for further processing are available at rates between 48 Hz and 390 Hz. These Doppler spectra are processed for providing line-of-sight wind speed and the integrated spectral power. The use of a LiDAR device allows the control system to adapt the rotor speed and pitch angle to the inflow conditions. The controller receives the LiDAR measurement, allowing it to anticipate the incoming wind speed, and therefore adjust the blade pitch and generator torque demand trajectories to match the wind speeds expected at the rotor in a few seconds' time. For example, if a high wind gust approaches, the set-points could be changed to protect the turbine; but, more importantly, by continuously anticipating oncoming turbulence during normal operation, the control action can be adjusted to minimise fatigue loading.

FIGURE 5.2

Measured Line of sight wind speeds at a plane in front of the wind turbine using Spinner Lidar



5.2 INNOVATIVE WIND TURBINE CONTROL CONCEPTS

For long slender blades which extend from 89 m for 10 MW wind turbines to more than 175 m for the 20 MW wind turbine, it is highly challenging to alleviate loads by only pitching the entire wind turbine blades. In the INN-WIND.EU project, several types of blade flaps have been developed for installation on the blades, to achieve finer control of the loads along the blade based on various objectives. These flaps have also been tested for their performance in the wind tunnel, on a rotary test rig in turbulent wind conditions and on a high-fidelity simulation of a commercial Suzlon turbine.

5.2.1 INDIVIDUAL PITCH AND FLAP CONTROL

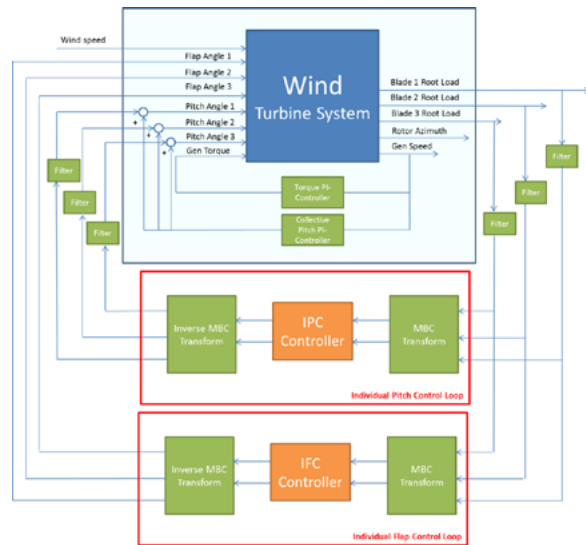
A conventional collective-pitch controller is not capable of reducing the periodic loads on the turbine blades and other components that occur at frequencies of 1P (rotor speed), and its harmonics: 2P, 3P, and so on. These loads arise out of wind shear, tower shadow effects, yaw misalignments and the rotational sampling of turbulence, and form a dominant component of the turbine load spectrum. These loads can be alleviated by pitching the three blades individually. This is known as Individual Pitch Control (IPC).

Fundamentally, the objective of the IPC controller is to minimise the measured blade root bending moments by issuing the correct individual pitch commands to the three blades. However, since the coupling between rotating blades and the non-rotating parts of the turbine is azimuth-dependent, a Multi-Blade Coordinate transformation (MBC) is used to represent the rotor in an equivalent non-rotating frame of reference. This transformation decomposes the three measured rotating blade loads into two orthogonal loads in the fixed frame of reference, which may be physically interpreted as the yaw and tilt loads on the hub of the turbine. Depending on the load peak to be attenuated (i.e., 1P, 2P and so on), the corresponding MBC transform is used, which shifts the load peak to a simple DC offset that can be reduced using a pair of simple diagonal integral or PI controllers, one for each of the two orthogonal loads. This controller is designed using industry-standard PI tuning rules, and the generat-

ed pitch control actions are shifted back into the rotating frame of reference using the corresponding inverse MBC transform. (The MBC transform is also known as ‘the Coleman transform,’ as used in helicopters, or as ‘Park’s transformation,’ as used for three-phase electrical circuits.)

FIGURE 5.3

Flap controller block diagram – relation to main controller, sensors and actuators.



Pitching larger, longer and heavier blades at frequencies and amplitudes required for load reduction can impose substantial loading requirements for the pitch actuation system and lead to significant wear in those same systems. In addition, pitching the entire blade could prove inefficient if localised aerodynamic profiles of the blades can be changed.

Distributed aerodynamic surfaces or other flow control devices present a method of achieving this localised control to improve blade-load reduction performance and to reduce the duty of pitch actuator systems. Trailing-edge flaps (TEFs) have shown the highest TRL in terms of flow control devices and have been field tested. TEFs (like ailerons on aircraft) require small motions to achieve large impacts on the localised aerodynamics of the blade and so have potential for lower power requirements than full-span pitch systems; they can also be deployed at higher frequencies.

Individual Flap Control (IFC) is the use of TEFs to reduce the loading peaks 1P, 2P and so on, using flap activity to

replace or augment the blade pitch activity from IPC. The basic implementation of IFC follows the same controller logic as IPC, described in Figure 5.3. Essentially, as in IPC, the blade root bending moments measured from the three blades are transformed to two load signals in the stationary frame of reference. These signals are fed to an IFC controller, which is typically also an orthogonal pair of integral or PI controllers, and the commanded control inputs are then inverse-transformed and used to actuate a trailing-edge flap located one on each blade. The IFC controller can operate both below and above the rated wind

speed in order to maximise the reduction of fatigue loads, although if used below-rated there may be a trade off against a small loss of energy production (just as with IPC).

For the INNWIND 10 MW reference turbine, some of the most important lifetime fatigue loads are compared in Figure 5.4, while the extreme maximum loads are compared in Figure 5.5. Looking at the Out-of-Plane Bending moments, the IPC controller shows load reductions of 3.5%, with the IFC controller showing load reductions of 6.5%.

FIGURE 5.4
Comparison of normalised fatigue loads for different controllers

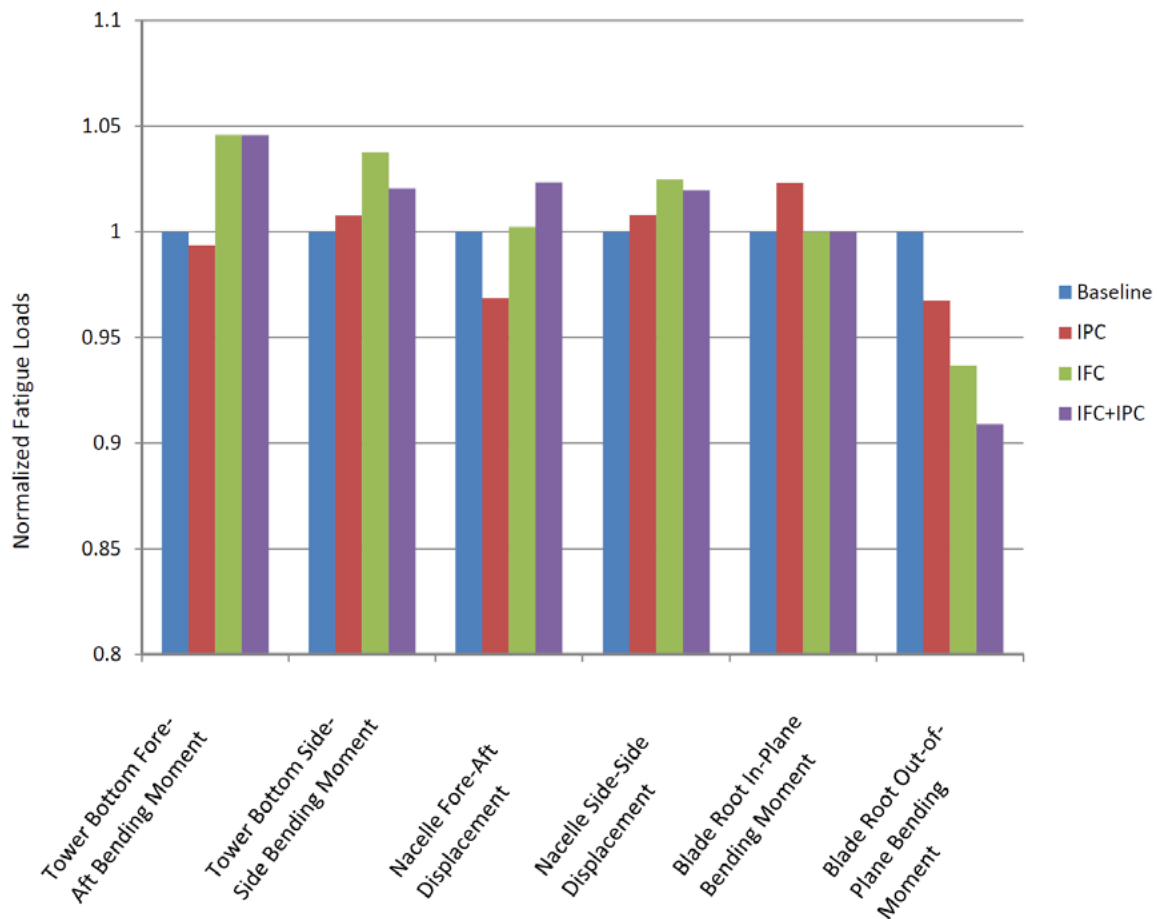
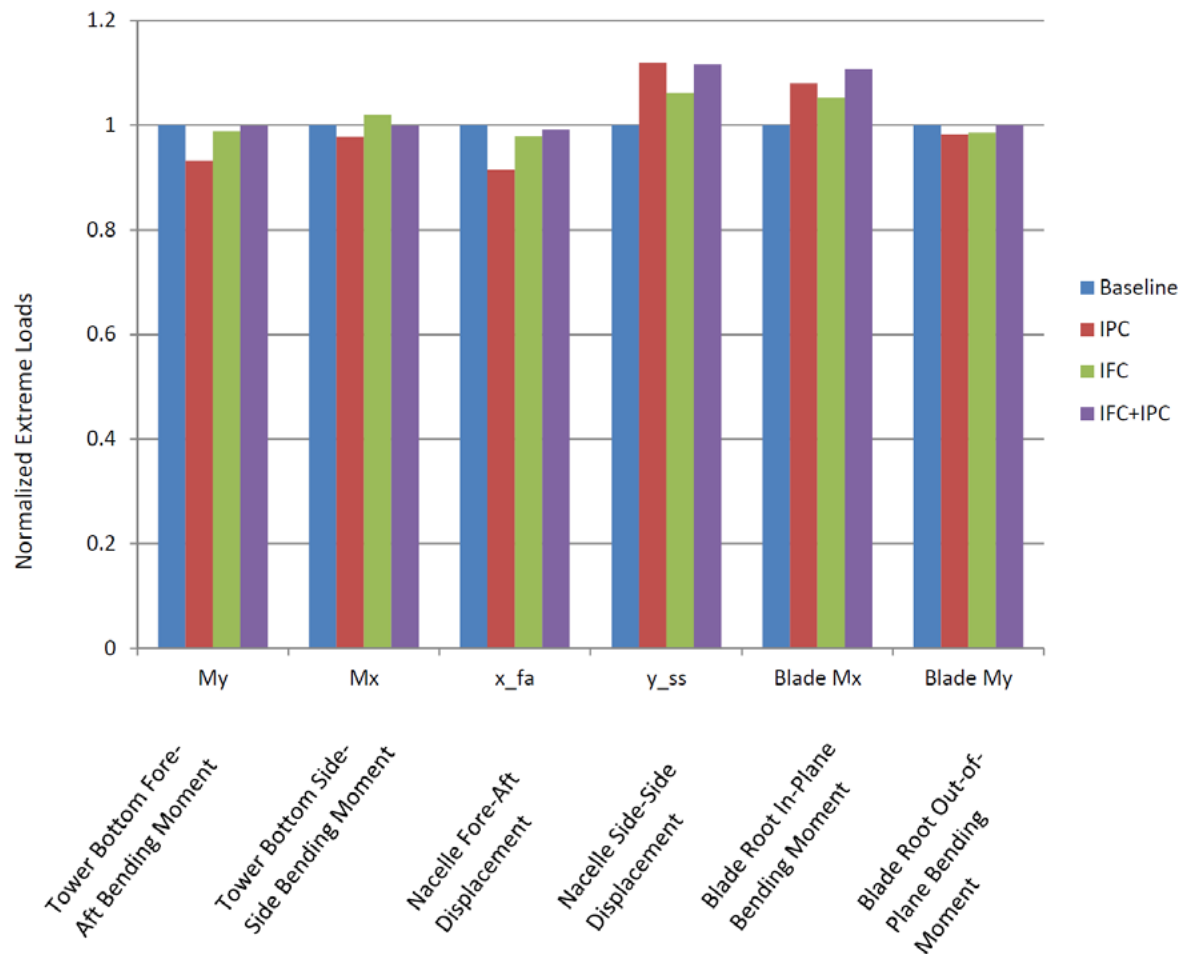


FIGURE 5.5

Comparison of extreme loads for different controllers



The combined controllers show increased load reduction up to 9.8%. The IPC controller increases pitch activity by 300%, while the IFC controller only causes a pitch activity increase of 45%. The flap controller leads to an increase in tower loads, and a smaller increase in nacelle motion. The trade-off between increased tower loads and reduced Out-of-Plane bending moments heavily depend on the controller gains and can be optimized for the worst-case scenario. The controller as described above is an extension of traditional IPC. Within the project several other advanced controllers have also been developed.

- Subspace Repetitive control – a fully adaptive control methodology that learns an internal model and corresponding optimal control law
- Iterative Feedback Tuning – a data-driven technology to simultaneously find the optimal gains of the IPC and IFC.
- Linear Individual Pitch Control – for 2-bladed wind turbines a dedicated MBC transformation is developed which enables fixed-structure control design

All these concepts and approaches have been tested using high-fidelity simulations and experiments and show high potential.

5.2.2 BLADE INDEPENDENT ACTIVE FLAP CONTROL

The blade-independent, feedback-active flap controller is a simple implementation of a blade-independent, feedback action on the high-pass-filtered blade root flapwise bending moment. Only the dynamic part of the controller is de-

scribed herein, with no supervisory functions (wind speed range of operation, transition in power regions, faults etc.).

The block diagram of the flap controller is shown, in relation to the main controller, sensors and actuators in Figure 5.6 and the internal flow of inputs, gains and outputs is shown in Figure 5.7.

FIGURE 5.6

Flap controller block diagram – relation to main controller, sensors and actuators.

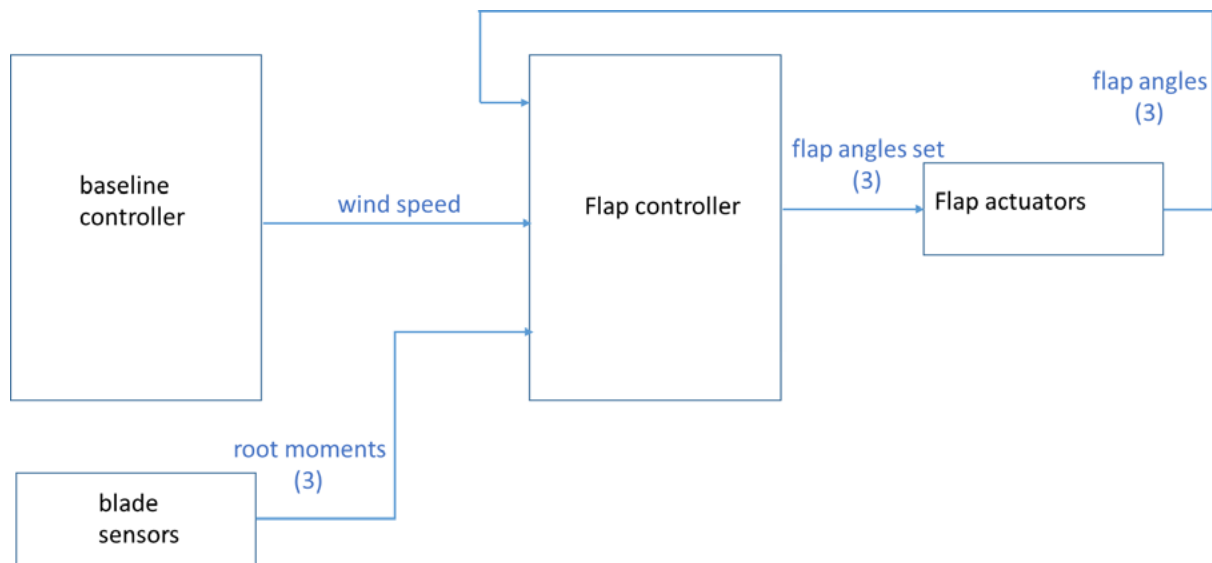
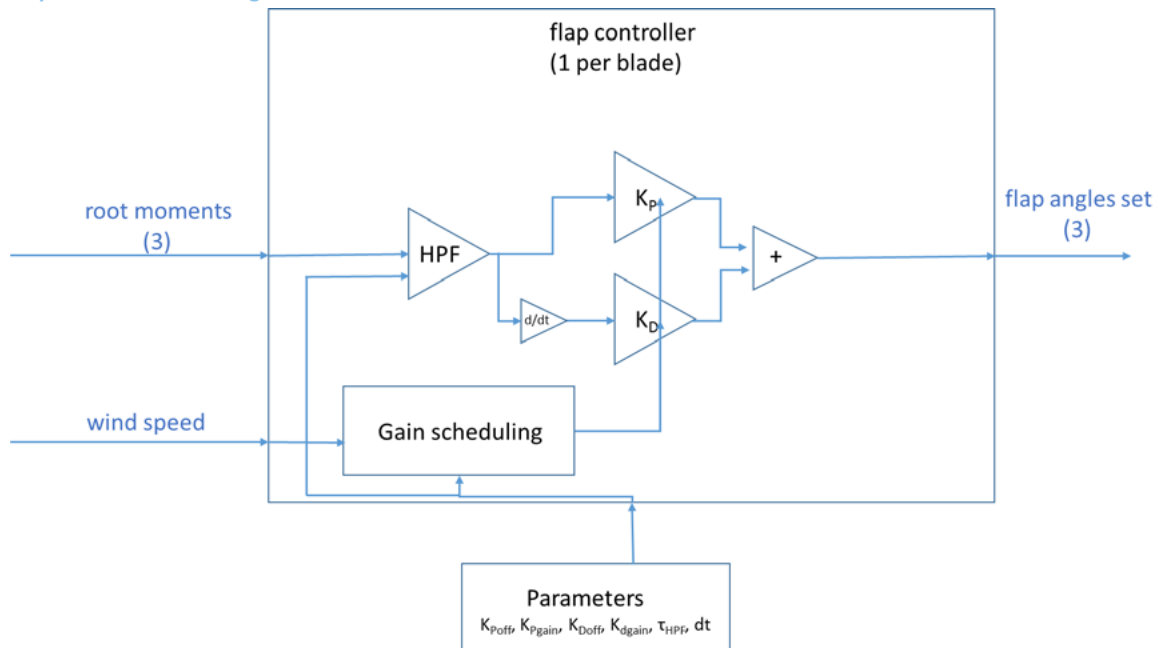


FIGURE 5.7

Flap controller block diagram – Controls flow chart



Inputs & outputs

The flap controller uses the input signals of the blade root bending moments from the three blades and prescribes three flap angles as output, one for each blade respectively, as shown in Figure 5.7.

At every time step, the flap controller reads the measured blade flapwise root-bending moments and applies a high-pass filter (HPF) with a lower cut-off frequency of the order of 0.05 Hz. in order to remove the steady-state part. A proportional gain (P) is applied on the HPF moments and a derivative gain (D) on the derivatives of the HPF moments, and signals are summed. The actual P and D gains are calculated in every time step, based on the average wind speed. The resulting flap angle command signals are then sent to the flap servos, modelled in our case with a first-order low-pass filter simulating the flap actuator response.

Another implementation of blade independent flap control, which is based on wind speed measurements obtained with a spinner anemometer, is described below. This controller uses flap actuators with the aim of removing any deterministic source of blade-load variation (concentrated on multiples of the rotational frequency) associated with the characteristics of the inflow (e.g. wind-yaw misalignment, within the range that yaw control is not activated, and/or wind shear and inclination). The aim of the controller is to assist operation of the conventional feedback individual pitch controller (IPC) and thereby reduce its control duty. IPC control is only then employed with the aim of removing 1P excitation due to the rotational sampling of turbulence.

From the three components of the wind speed measured by the spinner anemometer the inflow yaw and inclination (combination of tilt and upflow) angles are calculated. Information about the wind characteristics (an estimate of the wind shear exponent) is also obtained through cross correlation characteristics of the axial and vertical wind components. The instantaneous yaw and tilt angles are low pass filtered with the aim of removing the high frequency/low energy turbulent content. Filtered yaw and tilt angle and shear exponent input characteristics are then translated into periodic variations (1P and 2P) of the flap angle of the three blades. The amplitude of the flap angle variation must be proportional to the load amplitude (gain scheduling is applied based on the low-pass-filtered wind

speed) caused by the asymmetry of the flow, while an out-of-phase variation of the flap angle must be imposed to counteract the load variation. Look-up tables for the amplitude and phase of the flap angle variations have been created through a tuning process based on deterministic runs over the whole range of operational wind speeds and combinations of yaw, tilt angles and shear exponents.

Figure 5.8 compares deterministic simulation results with and without flap control. The plot presents the results of blade root flapwise bending moment at the wind speed of 8 m/s for different yaw angles ranging between 0°-45°. It is seen that 1P variation of the bending moment due to the effect of the yaw misalignment of the flow is substantially reduced when flap control is applied.

FIGURE 5.8

Effect of flap controller on M_{flap} variation at the wind speed of 8 m/s and for different yaw misalignment angles (dashed lines: no control, solid lines: flap control).

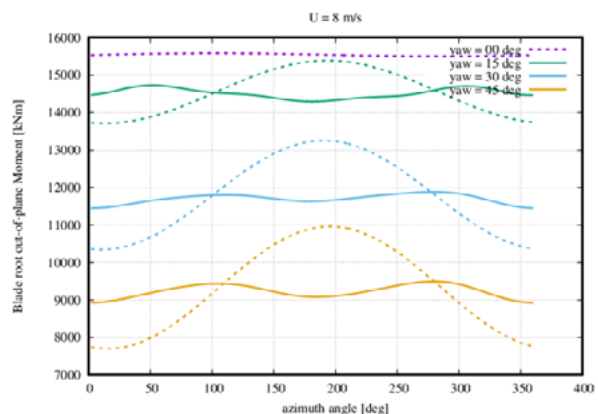
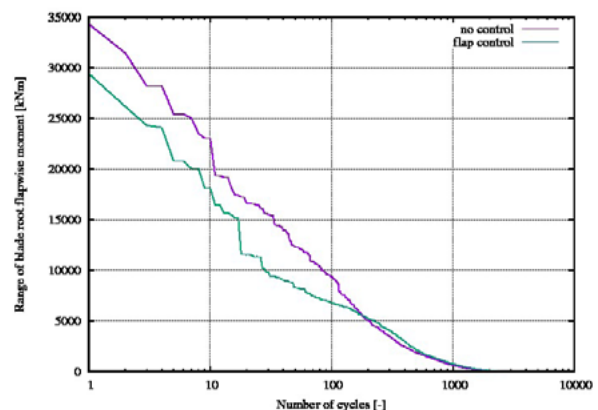


FIGURE 5.9

Rainflow counting of the M_{flap} at the wind speed of 8 m/s and a mean yaw angle of 15 degrees



Results from the application of the control scheme in a turbulent wind case are shown in Figure 5.9. Overall, a 15% reduction of the fatigue load is foreseen as a result of the application of the method, which can be directly translated to reduced pitch activity of the IPC control.

5.3 INNOVATIVE TURBINES WITH ADVANCED CONTROL- APPRECIATION OF LCOE REDUCTION POTENTIAL

The Individual Flap control is applied on the 2-bladed 10 MW rotor mounted on a semi-floater with and without Spinner anemometer based wind measurement input-based feed-forward control. Figure 5.10 describes the reduction in principal fatigue damage equivalent moments obtained using IFC and compared with the same turbine using standard control and with a land-based 2-bladed turbine. Other than blade root torsion (M_{zBR}) and blade root edge (M_{yBR}) moments, all other fatigue load components are seen to be reduced with IFC. The blade root flap moment (M_{xBR}) is seen to be reduced with IFC to nearly 70% (0.7) of the onshore value and the tower top bending moments (M_{zTT} , M_{yTT}) are greatly reduced. The reduction in design loads will reduce CAPEX and can also lower OPEX costs due to reduced fatigue damage.

A scheduled quasi-steady active flap controller utilizing only spinner anemometer inflow signals is also implemented to reduce fatigue loads by sensing the turbulence from Spinner anemometer-based measurements. If the turbulence level is more than a threshold value, the flaps are pitched to alleviate fatigue loads. Below rated wind speed, the wind speed measured is used in feed-forward control to increase the annual energy production by up to 0.5%. The controller comprises a flap scheduling for below-rated operating, targeting at increasing power output, and an on-off flap target for increased turbulence operation above-rated. The block diagram of the flap controller with Spinner anemometer based wind measurements for below-rated and above-rated action is shown in Figure 5.11, in relation to the main controller, sensors and actuators.

FIGURE 5.10
Reduction in fatigue damage equivalent Loads (TT - tower top, TB - tower base, MB- main bearing, BR- Blade root)

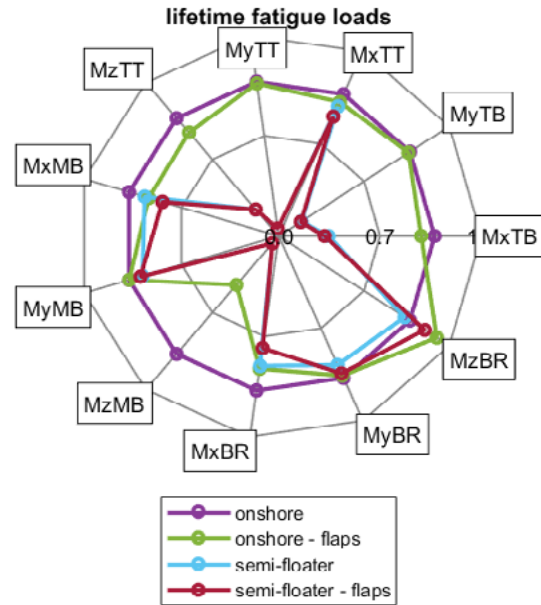
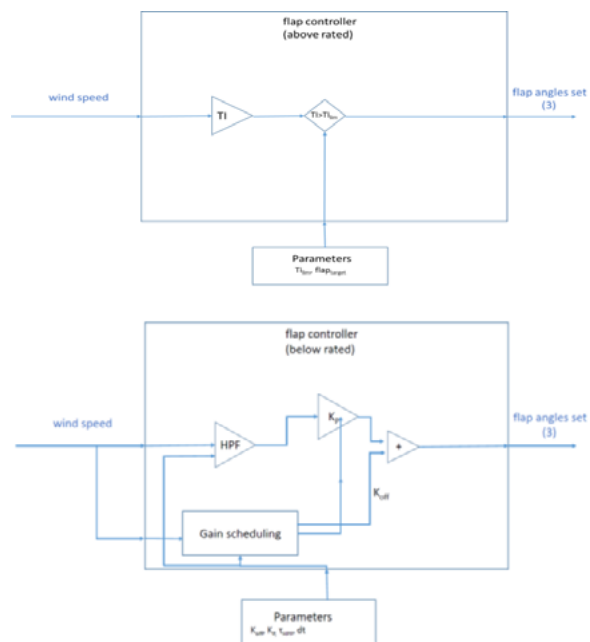


FIGURE 5.11
Spinner Anemometer measured Inflow-based flap controller block diagram



Normal power production DLC1.2 cases are simulated with no wind or wave misalignment, incorporating the derived turbulence characteristics from the spinner anemometer data, for the case of the two-bladed DTU 10 MW RWT on the semi-floater. The effect of the below-rated part of the controller is shown in Figure 5.12 and Figure 5.13, where it is seen that the (collective) flap control targets optimal settings, increasing with wind speed and resulting in increased power capture. This results in a gain of +0.5% in AEP for class IA wind conditions.

The technology roadmaps to market of the smart blade with flap based control and the Spinner LiDAR are available from the Deliverable D5.13 report downloadable from <http://www.innwind.eu/publications/deliverable-reports>

FIGURE 5.12

Comparison of power curves – baseline vs flaps (semi-floater).

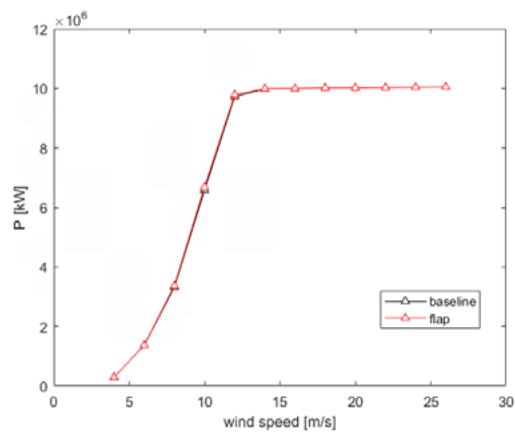
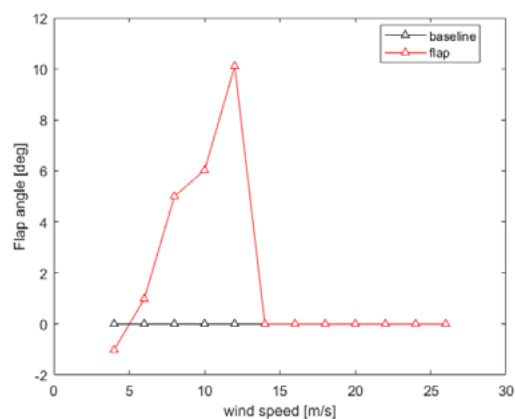


FIGURE 5.13

Comparison of average flap angle – baseline vs flaps (semi-floater).



6.

REVOLUTIONARY PLATFORMS

Two very different, but potentially beneficial turbine architectures: a multi-rotor system at 20 MW and a vertical axis floating turbine at 10 MW are presented in the following sections.

6.1 A 20 MW MULTIROTOR SYSTEM

6.1.1 WHY MULTIROTOR?

Very large generating units, per installed megawatt, can minimise offshore infrastructure costs and benefit from having fewer maintenance sites. The dominant solution considered is to upscale the established 3 bladed single rotor design. This poses challenges in developing unusually large turbine components and is adverse for turbine CAPEX (see Section 2). The multirotor concept of having many rotors on a single support structure avoids the up-scaling disadvantages of the unit turbine and facilitates the benefits of large unit capacity (potentially much larger than will be economically feasible for the single turbine) at a single location. Rotor nacelle systems mass reduction and CAPEX savings at 20 MW scale compared to a single rotor turbine can approach 80%. The multirotor idea is an

old one revitalized by consideration of scaling and logistical benefits. It poses some new challenges for engineering and logistical modelling and for integrated system design but requires no significant innovation in turbine technology and with unique potential benefits in standardization, quantity production and turbine reliability.

6.1.2 THE INNWIND.EU 20 MW MULTIROTOR

The project reference wind turbine was an advanced 10 MW design considered to be the most economic size for future offshore single turbines in wind farm deployment. Nevertheless, the multirotor system was developed (Figure 6.1) at 20 MW scale as a key advantage of multirotor systems lies in the relative facility for very large unit capacity. A number of key design challenges were foreseen in:

- Validation of aerodynamic performance of an array of turbines at close lateral spacing;
- Providing a support structure of satisfactory weight, cost and integrity;

- Providing an effective and economic solution to yawing of the complete system;
- Evaluating O & M and associated availability and reliability impacts.

Both inviscid vortex modelling of blade aerodynamics and CFD modelling representing the rotors as actuator discs, confirmed previous work (experimental and theoretical) on smaller arrays that, compared to the equivalent single rotor, there was no penalty to net power in close spacing of the rotors (2.5% of diameter).

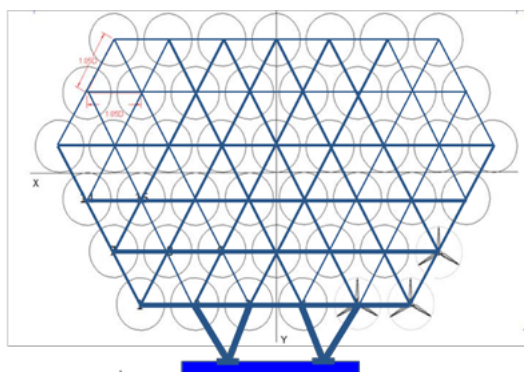
DNV GL undertook a crucial but demanding preliminary task to develop single turbine aerodynamic and loads modelling (Bladed software tool) to deal with turbulent wind input over an array of 45 turbines. A restricted number of critical load cases were then selected for analysis and time series of 6 load components at each rotor centre, along with an in-house optimization tool to select tubular mem-

bers of the space frame structure so as to meet critical extreme and fatigue loads embodying a robustness criterion to have structural integrity in event of failure of the most highly stressed member. The 45 turbines were operated independently at variable speeds and hence at slightly different frequencies in general turbulence. This introduced averaging effects leading to some very substantial reductions in varying rotor loads fed into the structure.

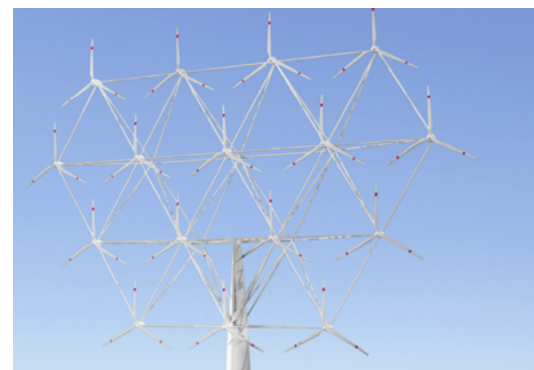
The yawing solution adopted a design of the Hamburg University of Applied Sciences to carry the rotor support structure on twin bearings around a tubular tower which extended from the sub-sea jacket structure above the water level. After considering the added mass of tower and structure for bearing connection, hanging the support frame on twin bearings put more tubular elements into tension. With this benefit, the complete system with yawing capability was only a little larger than one rigidly connected at base level. Yaw bearings selected by Rothe Erde were not of problematic size or duty.

FIGURE 6.1

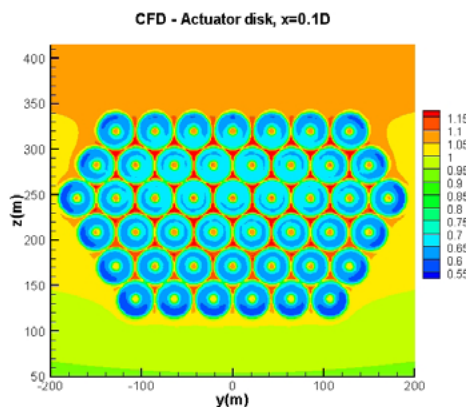
The 20 MW multirotor system of INNWIND.EU.EU



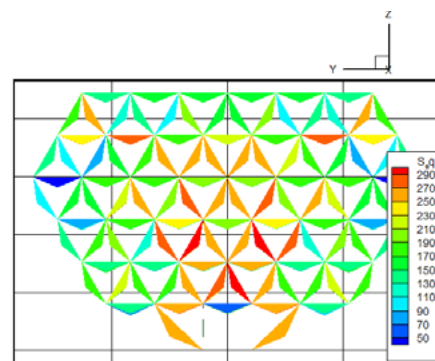
20MW system, 45 rotors of 41m dia. 450kW rating



Visualization of a section of the MRS



CFD results - 8% power gain



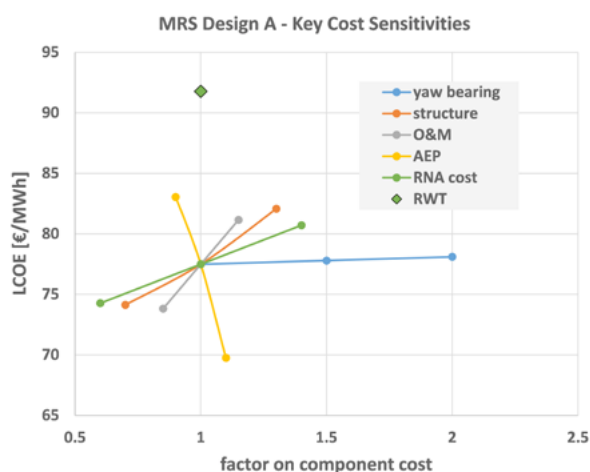
Stress analysis

The University of Strathclyde adapted a detailed existing offshore wind farm O & M cost model to deal with the 20 MW multirotor system. This was supported by an evaluation of availability and reliability. The assembly and maintenance concepts for the multirotor system avoided any requirement for a jack-up vessel. Overall savings in O & M cost $\sim 13\%$ were predicted. To secure this advantage, the study showed it is vital to have efficient systems for dealing with minor faults.

6.1.3 LCOE EVALUATION

An LCOE analysis using the cost model developed in the project compared 20 MW multirotor systems to 10 MW reference turbines in a specified 500 MW wind farm showing major benefit for the multirotor concept. For the INNWIND.EU project, the reference values of LCOE for offshore wind and the DTU reference wind turbine were 107 €/MWh and 92 €/MWh. The multirotor system achieved 77 €/MWh in a baseline case (Figure 6.2) without credit for power gains suggested 13% O&M benefit and 72 €/MWh with such credits – a cost reduction $\sim 33\%$ relative to the reference offshore LCOE and $\sim 22\%$ compared to the DTU reference turbine.

FIGURE 6.2
LCOE evaluation of the 20 MW multirotor system of INNWIND.EU



6.1.4 LESSONS LEARNT

A future multirotor system will pose few problems for turbine manufacturers and may not be fundamentally challenging for manufacturers of large offshore structures. However, as a complete innovative system design in its early stages, it certainly stretches modelling capability. It is demanding both quantitatively and qualitatively to extend single machine design tools for performance and load prediction. In any further development of the multirotor concept, with reasonable comfort now achieved in areas of aerodynamics and structures, the most critical focus will be on design of logistical procedures and engineering systems for maintenance.

6.2 A 10 MW FLOATING VERTICAL AXIS WIND TURBINE

The main advantage of VAWT is the lower position of the centre of gravity (estimated $\sim 20\%$ compared to a similar HAWT) which, in the case of a floating system, may have implications on the design and cost of the support structure. Also in favour to VAWT is that there is no need for a yawing mechanism which, towards an upscaling beyond 10 MW, may simplify the design of the support structure. The third point to mention is that research on VAWT over the last years was limited in comparison to HAWT. Most of the available information on VAWT comes from old studies which are regarded as being outdated, especially at multi-MW scale, where the only recent research project is the 5 MW DeepWind concept developed at DTU (<http://www.deepwind.eu/>). In order to also cover this option, it was decided to investigate the characteristics of a floating VAWT being aware of that results will not reflecting an optimized concept.

The rotor is 2-bladed of Darrieus type, the floater is a typical spar buoy which houses the generator at its lower end and is equipped with catenary mooring lines.

The floater is made of steel and has five sections:

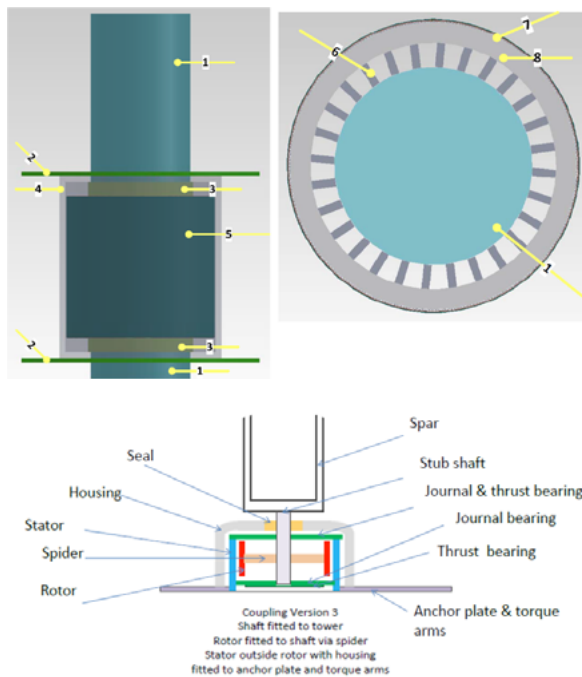
- A slender section near the water line.
- A transition section connecting the water line section to the main hull section.

- The upper main hull section is a voluminous section, mainly providing buoyancy.
- The lower main hull section contains the solid ballast. The ballast material is un-compact, water-saturated Olivine with a density of 2600 kg/m³.
- A bottom part which contains the generator.

The system is equipped with 3 or with 6 mooring lines (spaced at 60 degrees) for which the latter, besides providing adequate redundancy, also have enough horizontal stiffness and resistance to yawing by means of pretension. The generator module is made of the principal components sketched in Figure 6.3.

FIGURE 6.3

Left: Front -and top view section of generator and bearings
Right: Sketch showing the components



1-Foater	5-Generator
2-Axial Bearing	6-Support Spider Leg
3-Radial Bearing	7-airgap-active part of the generator
4-Generator Box	8-Rotor Core

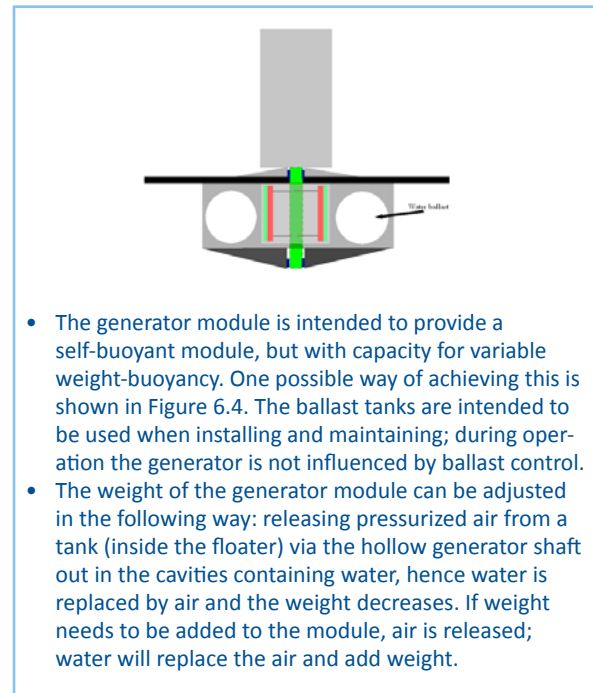
A direct-drive radial flux generator has been chosen with permanent magnets and iron lamination core on the ro-

tor and double-layer concentrated windings-copper and iron lamination core for the stator. The system is equipped with magnetic bearings: one (upper)radial -bearing with a single copper layer windings and with iron core, one (lower)radial -copper single layer windings and with iron core, and (upper and lower)a pair of axial -copper single layer windings with iron core.

The generator is supported by a radial set of elements connecting the generator rotor to the floater. The generator box containing the electrical generator has two radial magnetic bearings and four bearing enclosures (two for the axial and two for the radial bearings)

FIGURE 6.4

Conceptual view of generator module, torque absorption and variable ballast section.



- The generator module is intended to provide a self-buoyant module, but with capacity for variable weight-buoyancy. One possible way of achieving this is shown in Figure 6.4. The ballast tanks are intended to be used when installing and maintaining; during operation the generator is not influenced by ballast control.
- The weight of the generator module can be adjusted in the following way: releasing pressurized air from a tank (inside the floater) via the hollow generator shaft out in the cavities containing water, hence water is replaced by air and the weight decreases. If weight needs to be added to the module, air is released; water will replace the air and add weight.

The original 5 MW rotor has been re-investigated for parametric sensitivity analysis of instabilities leading to an increase of the torsional stiffness of the superstructure as a whole. The 10 MW system was then obtained using geometrical similarity. For the components lying above SWL, S.F SQRT (2) was used. For the underwater part, Froude scaling of 1.22 was applied.

The following table presents a summary of the gross properties of the reference and upscaled wind turbine using

the scale factor (S.F.) equal to SQRT (2), powered by its correspondent exponent according to size dependency (see also Table 6.1 for details on how scaling affects the

design parameters). Finally, in Figure 6.5 the dimensioning of the rotor is given.

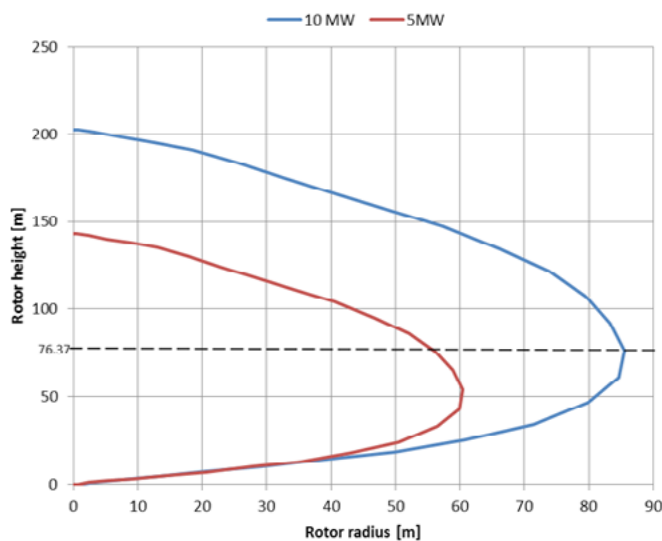
TABLE 6.1

Cross properties of the reference 5 MW and the upscaled 10 MW DeepWind VAWT

Property	REFERENCE WIND TURBINE		UPSCALED WIND TURBINE	
	Dimension	Value	Scaling Factor (S.F.^num)	Value
Rating power	MW	5.00	2	10.00
Rated rotational speed	rpm	6	-1	4.24
Rated wind speed	m/s	14	0	14
Cut in wind speed	m/s	4	0	4
Cut out wind speed	m/s	25	0	25
Rotor radius	m	60.49	1	85.55
Rotor height	m	143.00	1	202
Blade chord	m	5.00	1	7.07
Solidity	[-]	0.1653	0	0.1653
Swept area	m ²	11996	2	23992
Blade mass (1 blade)	tn	48.03	3	129.2
Tower mass	tn	382	3	1079
Floater mass(hull)	tn	567	3	1030
Ballast mass	tn	3003	3	5453
Generator core mass	tn	50	3	91

FIGURE 6.5

Rotor dimensions comparison between the reference 5 MW and the upscaled 10 MW DeepWind VAWT, with indication of height at maximum radius.



The floater design allows to substitute steel of 3 €/kg(2012 price level) with reinforced concrete at a cost of roughly 1.25 €/kg(2012). Blades are pultruded at a cost of blade manufacturing of 6 €/kg. Olivine as ballast material costs in the range of 19-50 €/kg(2012). The 5 MW DeepWind study dealt with special VAWT - and NACA00 airfoils -however these improvements in airfoil design for increasing aerodynamic performance could not be examined further in this upscaling exercise. The 5 MW generator and bearings cost was estimated to be 435 €/kW. With a mean annual wind of 9.2 m/s ($A=10.38$, $k=2$), AEP for 10 MW would correspond to 43 GWh.

A major difference in cost structure compared to conventional concepts is supposed to be in O&M, where this design allows simple and easy erection and O&M, with the help of small ships and underwater/ROV technology at reduced cost of what might be ~20-40%. The estimated 5 MW turbine cost was 1800 €/kW, and LCOE at ~ 65 €/MWh. Additional use of different materials replacing steel and large scale production assumptions brings LCOE around 20 €/MWh.

7.

IMPACT OF INNOVATION ON LCOE AT COMPONENT AND PLATFORM LEVEL

The comparison of the studied concepts in terms of the Performance Indicators (PIs) set for the INNWIND.EU project is presented in Table 7.1 and Table 7.2. The first table presents dimensional values of the PIs while the second shows percentage changes in comparison to the PI values of the 20 MW Reference Wind Turbine. Some promising combinations of the rotor/drive train/support structure concepts are also included in the tables.

Although the tables refer to 20 MW designs we have included for comparison the relevant PI values of the 10 MW RWT. Moving from 10 to 20 MW, it is noteworthy that there is a slight increase of the wind farm capacity factor due to less wake effects for the same installed capacity. There is also a significant reduction of O & M cost, from nearly €35/MWh to €28/MWh.

LIR concept. The new hybrid (glass-carbon) blade is lighter (16%) than the full-glass classically up-scaled 20 MW RWT blade, but it is also more expensive (7.3%). This is due to its longer span and the use of expensive carbon. Nevertheless, the overall increase in turbine CAPEX is 3.4% because in offshore wind the blades represent a small fraction of the turbine and support structure cost. Despite the higher CAPEX the larger, less loaded rotor, increases the turbine yield (capacity factor CF) by 7.5%. As

stated earlier, a 4.5% comes from the LIR platform and another 3% from the dedicated low lift profiles. Even more important is the increase of the wind farm capacity factor by 9.7% due to the lower wake losses of LIR rotors. This is the highest value achieved among the different rotor concepts. Overall, LIR promises a 3.9% reduction of LCOE compared to the 20 MW RWT.

Bend-Twist Coupled Rotor. The conclusions here regarding the impact of the BTC concept on LCOE are similar to those extracted for 10 MW designs. No significant reduction in the cost of energy is expected maintaining the reference rotor diameter. Such designs may reduce the fatigue and the ultimate loading of the blade itself and, also, of the support structure having an indirect effect on CAPEX reduction which, however, is not taken into account here. The BTC blade is highly loaded (high C_p max design) and 8.5% lighter and cheaper than the RWT blade. The overall CAPEX and LCOE improvement is small (1%) leading to an LCOE reduction of 0.6%. Due to the assumptions made, we can consider that BTC improvements can be superimposed to LIR summing up their individual impacts to all PIs.

TABLE 7.1

Performance Indicators of the innovative concepts studied at 20MW Scale

ROTOR	Component Mass (tn)	Component Cost (k€)	Overall CAPEX (k€)	Turbine CF	Wind Farm CF	O&M (€/MWh)	LCOE (€/MWh)
RWT - 10MW	42	448	30,650	0.507	0.425	34.81	98.56
RWT - 20MW	118	1,274	64,550	0.508	0.437	28.08	93.22
Low Induction Rotor (LIR) 20MW	99	1,367	66,750	0.546	0.480	28.08	89.58
BTC Rotor 20MW ($D=D^{RWT}$)	108	1,163	64,000	0.508	0.438	28.08	92.67
DRIVE TRAIN & NACELLE	Component Mass (tn)	Component Cost (k€)	Overall CAPEX (k€)	Turbine CF	Wind Farm CF	O&M (€/MWh)	LCOE (€/MWh)
RWT - 10MW	338	4,515	30,650	0.507	0.425	34.81	98.56
RWT - 20MW	914	11,300	64,550	0.508	0.437	28.08	93.22
PDD Generator 20MW	950	10,500	63,200	0.513	0.442	28.08	91.35
OFFSHORE SUPPORT STRUCT	Component Mass (tn)	Component Cost (k€)	Overall CAPEX (k€)	Turbine CF	Wind Farm CF	O&M (€/MWh)	LCOE (€/MWh)
RWT - 10MW	1,920	9,497	30,650	0.507	0.425	34.81	98.56
RWT - 20MW	3,090	13,950	64,550	0.508	0.437	28.08	93.22
Advanced Jacket (AJ) 20MW		11,160	61,800	0.508	0.437	28.08	90.53
ADVANCED CONTROL	Component Mass (tn)	Component Cost (k€)	Overall CAPEX (k€)	Turbine CF	Wind Farm CF	O&M (€/MWh)	LCOE (€/MWh)
RWT - 10MW			30,650	0.507	0.425	34.81	98.56
RWT - 20MW			64,550	0.508	0.437	28.08	93.22
Advanced Control (AC) 20MW							89.49
COMBINATIONS			Overall CAPEX (k€)	Turbine CF	Wind Farm CF	O&M (€/MWh)	LCOE (€/MWh)
RWT - 10MW			30,650	0.507	0.425	34.81	98.56
RWT - 20MW			64,550	0.508	0.437	28.08	93.22
LIR + BTC + PDD + AJ + AC (20MW)			62,100	0.551	0.485	28.08	80.74

TABLE 7.2

Percentage improvement of PIs in comparison to the 20 MW RWT

ROTOR	Component Mass ($\Delta\%$)	Component Cost ($\Delta\%$)	Overall CAPEX ($\Delta\%$)	Turbine CF ($\Delta\%$)	Wind Farm CF ($\Delta\%$)	O&M ($\Delta\%$)	LCOE ($\Delta\%$)
Low Induction Rotor (LIR) 20MW	-16.1%	7.3%	3.4%	7.5%	9.7%	0.0%	-3.9%
BTC Rotor 20MW ($D=D^{RWT}$)	-8.5%	-8.7%	-0.9%	0.1%	0.1%	0.0%	-0.6%
DRIVE TRAIN & NACELLE	Component Mass ($\Delta\%$)	Component Cost ($\Delta\%$)	Overall CAPEX ($\Delta\%$)	Turbine CF ($\Delta\%$)	Wind Farm CF ($\Delta\%$)	O&M ($\Delta\%$)	LCOE ($\Delta\%$)
PDD Generator 20MW	3.9%	-7.1%	-2.1%	1.0%	1.1%	0.0%	-2.0%
OFFSHORE SUPPORT STRUCT	Component Mass ($\Delta\%$)	Component Cost ($\Delta\%$)	Overall CAPEX ($\Delta\%$)	Turbine CF ($\Delta\%$)	Wind Farm CF ($\Delta\%$)	O&M ($\Delta\%$)	LCOE ($\Delta\%$)
Advanced Jacket (AJ) 20MW		-20.0%	-4.3%	0.0%	0.0%	0.0%	-2.9%
ADVANCED CONTROL	Component Mass ($\Delta\%$)	Component Cost ($\Delta\%$)	Overall CAPEX ($\Delta\%$)	Turbine CF ($\Delta\%$)	Wind Farm CF ($\Delta\%$)	O&M ($\Delta\%$)	LCOE ($\Delta\%$)
Advanced Control (AC) 20MW							-4.0%
COMBINATIONS			Overall CAPEX ($\Delta\%$)	Turbine CF ($\Delta\%$)	Wind Farm CF ($\Delta\%$)	O&M ($\Delta\%$)	LCOE ($\Delta\%$)
RWT - 10MW			-5.0%	-0.2%	-2.8%	24.0%	5.7%
LIR + BTC + PDD + AJ + AC (20MW)			-3.8%	8.6%	10.9%	0.0%	-13.4%

Magnetic Pseudo Direct Drive (PDD). The PDD generator with highly efficient power electronics promises a good LCOE performance (2 % lower than the reference) combined with a significant nacelle/drive train cost reduction of 7%. The nacelle mass is slightly increased by 4% while the capacity factor increases by 1.1 % which, along with the reduced CAPEX, is the reason of LCOE improvement. The improved capacity factor comes as a combination of the highly efficient 20 MW PDD generator (~ 98.5% at full load) and the highly efficient power electronics.

Bottom Mounted Offshore Support Structure. An advanced design/manufacturing of the 20 MW RWT jacket is expected to reduce the original cost of ~14 M€ by 20%. Such a reduction would decrease the overall CAPEX by 4.3% translated to 3% reduction of the LCOE.

Advanced Control in 20 MW. An LCOE drop of 4% can be expected due to the mitigation of design loads of the turbine and its support structure offered by advanced control. In the present context advanced control was mainly

targeted in reducing blade than support structure loads. Such a reduction can be used for increasing the rotor diameter and improve LCOE through better energy capturing. Alternatively, one can target on the reduction of the support structure fatigue loads which are the design drivers of the jacket. For jacket structures load reduction is nearly proportional to mass reduction. Since the offshore turbine support structure has a significant contribution to CAPEX, the reduction of the jacket fatigue loads through advanced control can also lead to an LCOE reduction of order 4% without increasing rotor diameter.

A simplified methodology for estimating the combined performance of the researched concepts would sum-up the percentage gains of the individual innovations as soon as they can be considered independently from each other. Some examples of such combinations are given in the lower parts of the PI Tables.

For bottom-mounted designs at INNWIND.EU's 20 MW RWT conditions, the following expectations regarding LCOE reduction from new technology are presented:

• Low induction rotors with conventional inner structure	4.0%
• Aeroelastically tailored rotors	0.5%
• Drive train (reduced CAPEX, increased efficiency)	2.5%
• Advanced Jacket	3.0%
• Advanced control	4.0%
Expected Overall LCOE reduction	14.0%

Starting from the EWII LCOE value of €106.93/MWh corresponding to 5 MW turbine sizes, and considering more realistic O & M costs, this number dropped at €98.56/MWh (8.5% reduction) for the 10 MW RWT and €93.22/MWh (14.7% reduction) for the 20 MW RWT. These reductions were due to the larger turbine sizes, along with the use of a lightweight rotor with thick profiles, and the shift from traditional three-stage geared drive trains to medium speed drive while employing state of the art designed and manufactured jackets. An additional 14% reduction of LCOE can be expected for both 10 and 20 MW designs, thanks to the advanced concepts researched in INNWIND.EU, getting LCOE close to €80/MWh for 20 MW turbines (and €85/MWh for 10 MW turbines).

8.

CONCLUSIONS

The project has investigated offshore wind turbines between 10 MW – 20 MW capacity with the development of several component innovations and demonstrations of some of the key technologies. Over the period of its 5-year progress, it has satisfactorily addressed all objectives that were targeted. Several of the results can be directly used by the industry. A summary of key scientific findings is given below.

ROTORS

- Large, high-tip speed rotors of moderate power density show a significant potential for LCOE reduction. This is partially due to the small contribution of the rotor CAPEX in offshore wind LCOE, but also facilitated by advanced control technology that mitigates higher loads from larger rotors.
- Special thick airfoil families optimized for the high Reynolds numbers of the MW machines can further improve turbine efficiency.
- Aero-elastically tailored blades with innovative inner structure, active aerodynamic control devices such as distributed flaps, combined with advanced wind

measurement sensors (spinner anemometer or LiDAR for instance) and control strategies may significantly reduce turbine loading and therefore the weight and CAPEX of the load carrying components.

DRIVETRAIN

- Reduction of tower top mass is not a significant factor in reducing the LCOE of bottom fixed large offshore wind turbines of 10 MW-20 MW capacities.
- Direct drive generators may improve the reliability and availability of offshore turbines. Superconducting generators may be an option for lightweight RNAs (when desired) with small dependence on rare earth materials, but appear to be extremely costly in present times (require to reduce the SC wire cost by 4 and increase its capacity by 4 to be competitive).
- Magnetic pseudo direct drives are competitive in terms of cost and performance, but vulnerable to magnetic material prices.

SUBSTRUCTURE

- Jackets have a large cost reduction potential through design optimisation, use of cost-effective materials and improved –automated- manufacturing and installation practices.
- At 50 m water depth, for 3-bladed 10 MW turbines, 3P excitation of the support structure may compromise the turbine performance and fatigue life of the substructure, when jackets are used; to keep the support structure frequency low enough results in a jacket with a smaller footprint and higher mass and this is compounded if there are tower top mass reductions.
- For larger turbines nearing 20 MW scale, there is no 3P excitation of the substructure due to the reduction in support structure frequencies at this size, hence savings in tower top mass are not penalized by rising support structure costs and the support structure design can be better optimized owing to less frequency constraint.
- Avoiding rotor-support structure resonance is rather impossible for efficient two-bladed rotors. Such rotors may only be combined with flexible substructures, such as the semi-floater at 50 m - 70 m water depths.
- The optimal size of floating turbines is not yet mastered. A cost effective semi-submersible tripod floater has been designed and assessed for a 10 MW turbine.

Overall the LCOE of the 20 MW offshore wind turbine was reduced by more than 30% as compared to the 2012 EWII basis of the 5 MW wind turbine. This evaluation of LCOE was primarily based on direct CAPEX savings and increase in AEP from the innovations combined with the larger capacities. Further savings in the LCOE due to OPEX reduction from lower fatigue loading and ease of maintenance is also expected.

The findings encourage the continued development of the 20 MW offshore wind turbine with more research on efficient design and manufacturing of RNA components, along with fundamental investigations on large rotor interactions with tall atmospheric conditions.

9.

FURTHER READING

All reports from this project are available at <http://www.innwind.eu/>



www.innwind.eu

INN WIND.EU

The overall objectives of the INN WIND.EU project are the high performance innovative design of a beyond-state-of-the-art 10-20MW offshore wind turbine and hardware demonstrators of some of the critical components.